

**POWER Release 8.0.1 (with GIS Applications) Methodology  
(Data Parameters, Sources, & Validation)**  
**Documentation Date December 12, 2018**  
**(All previous versions are obsolete)**  
**(Data Version 8.0.1; Web Site Version 1.1.0)**

**Paul W. Stackhouse, Jr<sup>1</sup>, Taiping Zhang<sup>2</sup>,  
David Westberg<sup>2</sup>, A. Jason Barnett<sup>3</sup>, Tyler Bristow<sup>3</sup>,  
Bradley Macpherson<sup>3</sup>, James M. Hoell<sup>2</sup>**

**<sup>1</sup>NASA Langley Research Center; <sup>2</sup>SSAI/NASA Langley Research Center;  
<sup>3</sup>Booz Allen Hamilton, Norfolk, VA**

<b>1. Introduction .....</b>	<b>3</b>
<b>2. Parameters &amp; Data Sources .....</b>	<b>4</b>
<b>2.1 Underlying data solar and meteorological data .....</b>	<b>4</b>
<b>2.2 Surface meteorology and Solar Energy (SSE) Parameters .....</b>	<b>6</b>
<b>2.2.1 SSE Climatologically Averaged Parameters .....</b>	<b>6</b>
<b>2.2.2 SSE Interannually Averaged Parameters .....</b>	<b>8</b>
<b>2.3 SSE Daily Mean Time Series .....</b>	<b>9</b>
<b>2.3.1 Sustainable Building Inter-Annual Variability .....</b>	<b>10</b>
<b>2.3.2 Sustainable Building Daily Mean Time Series .....</b>	<b>10</b>
<b>2.3.3 Sustainable Building DOE/ASHRAE Climate Building parameters .....</b>	<b>11</b>
<b>2.3.4 Sustainable Building Monthly Averaged Parameters .....</b>	<b>11</b>
<b>2.4 Agroclimatology Parameters .....</b>	<b>13</b>
<b>3. Parameter Accuracy -Summary .....</b>	<b>13</b>
<b>3.1 Solar Insolation .....</b>	<b>13</b>
<b>3.2 Meteorology .....</b>	<b>17</b>
<b>4. Global Short Wave (SW) Solar Insolation &amp; Long Wave (LW) Radiative Flux .....</b>	<b>17</b>
<b>4.1 GEWEX SRB 3.0 SW &amp; LW Radiative Transfer Models .....</b>	<b>18</b>
<b>4.2 FLASHFLUX SW &amp; LW Radiative Transfer Models .....</b>	<b>20</b>
<b>4.3 Validation of SW Solar Insolation &amp; LW Radiative Flux (All Sky Conditions) .....</b>	<b>21</b>
<b>4.3.1 SRB 3.0 Daily Mean SW Solar Insolation .....</b>	<b>23</b>
<b>4.3.2 SRB 3.0 Daily Mean LW Radiative Flux .....</b>	<b>24</b>
<b>4.3.3 FLASHFLUX Daily Mean SW Solar Insolation .....</b>	<b>26</b>
<b>4.3.4 FLASHFLUX Daily Mean LW Radiative Flux .....</b>	<b>28</b>
<b>4.4 Validation of SW Solar Insolation (Clear Sky Conditions) .....</b>	<b>31</b>
<b>4.4.1 SRB 3.0 Daily Mean SW Solar Insolation .....</b>	<b>32</b>
<b>4.4.2 FLASHFLUX Daily Mean SW Solar Insolation .....</b>	<b>33</b>
<b>5. Diffuse and Direct Normal Radiation on a Horizontal Surface .....</b>	<b>36</b>
<b>5.1 SSE Method .....</b>	<b>37</b>
<b>5.2 Validation .....</b>	<b>38</b>
<b>5.2.1 Monthly Mean Diffuse (All Sky Conditions) .....</b>	<b>39</b>
<b>5.2.2 Monthly Mean Direct Normal (All Sly Conditions) .....</b>	<b>40</b>
<b>5.2.3 Monthly Mean Diffuse (Clear Sky Conditions) .....</b>	<b>41</b>
<b>5.2.4 Monthly Mean Direct Normal (Clear Sky Conditions) .....</b>	<b>42</b>
<b>6. Irradiance on a Tilted Surface .....</b>	<b>43</b>
<b>6.1 Overview of RETScreen Method .....</b>	<b>43</b>
<b>6.2.0 Old SSE Monthly Tilted Solar Irradiances Tables .....</b>	<b>45</b>
<b>6.2.1 Update to SSE Tilted Solar Irradiances .....</b>	<b>45</b>
<b>6.3 Validation: Monthly Mean Irradiance (All Sky Conditions) .....</b>	<b>46</b>
<b>6.3.1 SSE vs RETScreen .....</b>	<b>46</b>
<b>6.3.2 SSE vs Direct Measurements of Tilted Surface Irradiance .....</b>	<b>47</b>
<b>6.3.3 SSE vs BSRN Based Tilted Surface Irradiance .....</b>	<b>48</b>
<b>7.0 Parameters for Sizing Battery or Other Energy -Storage Systems .....</b>	<b>48</b>
<b>7.1 Minimum insolation as % of average values over consecutive-day period .....</b>	<b>49</b>
<b>7.2 Solar Insolation deficits below expected values over consecutive-day period .....</b>	<b>50</b>

7.3 <a href="#"><u>Equivalent number of NO-SUN days over consecutive-day period</u></a> .....	50
7.4 <a href="#"><u>Available Surplus Insolation Over Consecutive -day period</u></a> .....	51
<b>8.0 <a href="#"><u>Solar Geometry</u></a> .....</b>	<b>51</b>
<b>9.0 <a href="#"><u>Overview of Meteorological Data</u></a> .....</b>	<b>52</b>
9.1 <a href="#"><u>Validation Methodology</u></a> .....	54
9.2 <a href="#"><u>Temperature</u></a> .....	55
9.3 <a href="#"><u>Precipitation</u></a> .....	57
9.4 <a href="#"><u>Specific Humidity</u></a> .....	61
9.5 <a href="#"><u>Relative Humidity</u></a> .....	62
9.6 <a href="#"><u>Surface Pressure</u></a> .....	65
9.7 <a href="#"><u>Wind Speed</u></a> .....	66
9.8 <a href="#"><u>Dew Point</u></a> .....	68
9.9 <a href="#"><u>Heating/Cooling Degree Days</u></a> .....	69
9.10 <a href="#"><u>Cloud Cover</u></a> .....	72
<b>10.0. <a href="#"><u>References</u></a> .....</b>	<b>73</b>
<b>APPENDIX A: <a href="#"><u>Validation Methodology</u></a></b> .....	<b>77</b>
<b>APPENDIX B: <a href="#"><u>Averaging Methodology</u></a></b> .....	<b>79</b>
<b>APPENDIX C: <a href="#"><u>Solar Geometry</u></a></b> .....	<b>80</b>
<b>APPENDIX D: <a href="#"><u>Solar Radiation on a Tilted Surface: Old SSE vs New POWER</u></a></b> .....	<b>90</b>

**1. Introduction:** NASA, through its Earth science research program has long supported satellite systems and research providing data important to the study of climate and climate processes. These data include long-term climatologically averaged estimates of meteorological quantities and surface solar energy fluxes. Additionally, mean daily values of the based meteorological and solar data are provided in a time series format. These satellite and model-based products have been shown to be accurate enough to provide reliable solar and meteorological resource data over regions where surface measurements are sparse or nonexistent. The products offer two unique features – the data is global and, in general, contiguous in time. These two important characteristics, however, tend to generate very large data archives which can be intimidating for users, particularly those with little experience or resources to explore these large data sets. Moreover, the data products contained in the various NASA archives are often in formats that present challenges to new users. To foster the usage of the global solar and meteorological data, NASA's Earth Science Division Applied Sciences Program supported, and continues to support, the development of user-friendly data sets formulated specifically for designated user communities and access to these data via a user friendly web based mapping portal.

The Surface meteorology and Solar Energy (SSE) project is one of the earlier activities funded by the Applied Science Program to foster use of NASA's data holdings. The SSE data-delivery website is focused on providing easy access to parameters valued in the renewable energy industry (e.g. solar and wind energy) and was initially released in 1997. The solar and meteorological data contained in this first release was based on the 1993 NASA/World Climate Research Program Version 1.1 Surface Radiation Budget (SRB) science data and TIROS Operational Vertical Sounder (TOVS) data from the International Satellite Cloud Climatology Project (ISCCP). Release 2 of SSE was made public in 1999 with parameters specifically tailored to the needs of the renewable energy community. Subsequent releases of SSE - SSE-Release 3.0 in 2000, SSE-Release 4.0 in 2003, SSE-Release 5.0 in 2005, and SSE-Release 6.0 in 2008 – have continued to build upon an interactive dialog with potential customers resulting in updated parameters using the most recent NASA data as well as inclusion of new parameters that have been requested by the user community.

The POWER project was initiated in 2003 as an outgrowth of the Surface meteorology and Solar Energy (SSE - [https://eosweb.larc.nasa.gov/project/sse/sse\\_table](https://eosweb.larc.nasa.gov/project/sse/sse_table)) project. The initial POWER project encompassed the SSE component and added two new datasets with applicability to the architectural (e.g. Sustainable Buildings) and agricultural (e.g. Agro-climatology) industries, with the continuing objective of improvements to and expansion of the focused parameters included in each section of POWER.

Recent upgrades to the SSE component of POWER were initiated to include Geographic Information System (GIS) functionality as an option to the data ordering/access process. SSE-GIS constituted the Release 7.0 version, but did provide updated data sets. The POWER Release-8 encompasses the three focused data components of POWER - SSE, Sustainable Building, and Agroclimatology- in a new responsive data portal built on upgrades to the underlying based metrological data, and is designed to fit on desktop, tablet and smart phone platforms, and adds geospatially enabled online tools to facilitate data ordering and viewing as well as analysis of the solar and meteorological data.

The meteorological data/parameters in POWER Release-8 are based upon a single assimilation model from Goddard's Global Modeling and Assimilation Office (GMAO). The updated meteorological data are derived from the GMAO Modern Era Retrospective-Analysis for Research and Applications (MERRA-2) assimilation model products and GMAO Forward Processing – Instrument Teams (FP-IT) GEOS 5.12.4 near-real time products. The MERRA-2 data spans the time period from 1981 to within several months of real time; the GEOS 5.12.4 data span the time period from the end of the MERRA-2 data stream to within several days of real time. The MERRA-2 and GEOS 5.12.4 versions are essentially the same and thus discontinuities that are often apparent between different assimilation models are minimized.

The solar based data/parameters in POWER Release-8 will continue to be based upon satellite observations with subsequent inversion to surface solar insolation by NASA's Global Energy and Water Exchange Project /Surface Radiation Budget (SRB) and NASA's Fast Longwave And SHortwave Radiative project (FLASHFlux).

The data/parameters in POWER Release-8 are provided on a global grid with a spatial resolution of  $0.5^{\circ}$  latitude by  $0.5^{\circ}$  longitude. Thus, this POWER Release 8.0 consolidates the SSE, Sustainable Building, and Agroclimatology components in a single data portal with updated and low latency solar and meteorological data products, and provides GIS compatible data formats and GIS-enabled web applications.

The purpose of this documentation is to describe the underlying solar and meteorological data sources, to provide estimates of the accuracy associated with the underlying data and resulting parameters, and to enumerate the data/parameters in each component of POWER Release-8.

[\(Return to Content\)](#)

**2. Parameters & Data Sources:** The parameters contained in the POWER Release-8 archive are based upon solar radiation derived from satellite observations and meteorological data from assimilation models. The parameters in the three sections of POWER, while tailored to the respective user communities – solar and renewable energy, energy-efficient and sustainable buildings, and agricultural - are calculated from the same underlying solar and/or meteorological values. Additionally, the respective parameters are given in units that are commonly employed in each user community.

**2.1 Underlying data solar and meteorological data:** Table 2.1 lists the underlying solar and meteorological data sources and their respective temporal coverage.

For a discussion of the solar values based upon the various versions FLASHFlux see [https://eosweb.larc.nasa.gov/sites/default/files/project/ceres/quality\\_summaries/FFv3\\_TISA\\_DQ\\_S.pdf](https://eosweb.larc.nasa.gov/sites/default/files/project/ceres/quality_summaries/FFv3_TISA_DQ_S.pdf). We note here that the solar data from these primary sources are produced on a global  $1^{\circ}$  latitude/ longitude grid and remapped to a  $0.5^{\circ}$  spatial grid via replication of the  $1^{\circ}$  values to the four  $0.5^{\circ}$  grid cells within the respective  $1^{\circ}$  cell. *Note that the time series of daily surface insolation may include multiple data sources; accordingly, it is not recommended for use in assessing climate trends that encompass a source data change.*

Meteorological parameters are taken from NASA's Modern Era Retro-analysis for Research and Applications – (MERRA-2) assimilation model (<https://gmao.gsfc.nasa.gov/reanalysis/MERRA-2/>), and from the GEOS version 5.12.4 assimilation model. MERRA-2 is a new version of NASA's Goddard Earth Observing System Data Assimilation System (Bosilovich, M. G., et al 2016). The GEOS version 5.12.4 has the same grid resolution as MERRA-2 (and the same model physics less selected observations and surface rain gauge normalized precipitation). The GEOS 5.12.4 ([https://gmao.gsfc.nasa.gov/news/geos\\_system\\_news/2016/FP-IT\\_NRT\\_G5.12.4.php](https://gmao.gsfc.nasa.gov/news/geos_system_news/2016/FP-IT_NRT_G5.12.4.php)) data are processed by the POWER project team on a daily basis and appended to the end of the MERRA-2 daily time series to provide low latency products which are generally ready within about 4 days of real-time. The MERRA-2 values in the resulting daily time series are typically updated every several months.

Values from MERRA-2 and GEOS 5.12.4 models are initially produced on a 1/2-degree by 2/3-degree global grid and then bi-linearly interpolated by the POWER project to a global 0.5° grid. The data are also transformed from Universal Time (UT) to solar local time (i.e., noon is defined to be solar noon without local time zone definitions taken into account).

Table 2.1 This table summarizes the base solar and meteorological data underlying all the POWER Release-8 parameters. The base data and subsequent parameters are available globally on a user specified 0.5° latitude/longitude grids. Tables 2.2, 2.3, and 2.4 list the specific parameters available in the SSE, Sustainable Building and Agroclimatology sections of POWER Release-8.

<b>Base Data</b>	<b>Temporal Coverage</b>	<b>Source (see notes below)</b>
<ul style="list-style-type: none"> <li>• All Sky &amp; Clear Sky Insolation on Horizontal Surface;</li> <li>• All Sky Downward Longwave Radiative Flux;</li> <li>• Top-of-atmosphere Insolation</li> </ul>	July 1, 1983 through Dec. 31, 2007	GEWEX SRB 3.0
	Jan. 1, 2008 through Dec. 31, 2012	FLASHFlux Version 2(D,E,G,H)
	Jan. 1, 2013 through near real time	FLASHFlux Version 3 (A,B,C)
<ul style="list-style-type: none"> <li>• Average Air Temperature at 2 m</li> <li>• Minimum/Maximum Air Temperature at 2 m</li> <li>• Relative Humidity at 2m</li> <li>• Specific Humidity at 2m</li> <li>• Dew/Frost Point Temperature at 2 m</li> <li>• Wind Speed at 2 m, 10 m, and 50 m</li> <li>• Precipitation</li> </ul>	Jan, 1, 1981 – few months of real time	MERRA-2
	End of MERRA2 through near-real time	GEOS 5.12.4

Notes:

1. GEWEX SRB 3.0 → NASA's Global Energy and Water Exchange Project /Surface Radiation Budget (<http://gewex-srb.larc.nasa.gov/> & [https://eosweb.larc.nasa.gov/project/srb/srb\\_table](https://eosweb.larc.nasa.gov/project/srb/srb_table))
2. FLASHFlux → NASA's Fast Longwave And SHortwave Radiative Fluxes (<http://flashflux.larc.nasa.gov/> )
3. MERRA-2 → NASA's Modern Era Retro-analysis for Research and Applications –assimilation model (<https://gmao.gsfc.nasa.gov/reanalysis/MERRA-2/> )
4. GEOS 5.12.4 → [https://gmao.gsfc.nasa.gov/news/geos\\_system\\_news/2016/FP-IT\\_NRT\\_G5.12.4.php](https://gmao.gsfc.nasa.gov/news/geos_system_news/2016/FP-IT_NRT_G5.12.4.php)

[\(Return to Content\)](#)

**2.2 Solar and Renewable Energy Community (originally the Surface meteorology and Solar Energy or SSE users):** The solar and meteorological parameters are available as climatologically and inter-annual (monthly and annual) average values, as well in a daily time series format for user selected grids. All SSE parameters are provided on user specified  $0.5^{\circ}\times 0.5^{\circ}$  grids. The climatologically averaged parameters are calculated to support applications such as solar cooking, sizing solar panels, sizing battery backup systems, etc. The inter-annually averaged parameters are provided as monthly and annual averaged values by year for each of the base solar and meteorological data parameters. The daily time series include the basic solar and meteorology parameters as well as additional calculated parameters such as diffuse and direct normal radiation.

The following tables provide an explicit list of the parameters in each SSE data section.

- SSE Climatologically Averaged Parameters – [Table 2.2.1](#):
- SSE Inter-annually (Monthly, Annually) Averaged Parameters – [Table 2.2.2](#):
- SSE Daily Mean Time Series – [Table 2.2.3](#):

**Table 2.2.1 Overview of the SSE climatologically averaged parameters**

- All parameters are available on  $0.5^{\circ}\times 0.5^{\circ}$  latitude, longitude global grids.
- All solar related parameters are derived from data taken from the NASA GEWEX/SRB release 3.0 archive (<http://gewex-srb.larc.nasa.gov>) over the time period July 1, 1983 - June 30, 2005 (22 years) and available as a 22-year average for each month and as a 22-year annual average.
- Temperature, moisture, and wind related parameters are derived from data taken from the NASA's GMAO (<http://gmao.gsfc.nasa.gov>) MERRA-2 assimilation model over the time period January 1, 1984 – December 31, 2013 (30 years) and available as a 30-year monthly average for each month and as a 30-year average.

([APPENDIX B](#) describes methodology for calculating monthly, annual & climatologically averaged parameters

#### 1. Parameters for Solar Cooking:

- Average Insolation
- Midday Insolation
- Clear sky Insolation
- Clear sky days

#### 2. Parameters for Sizing and Pointing of Solar Panels and for Solar Thermal Applications:

- Insolation on horizontal surface (Average, Min, Max)
- Diffuse radiation on horizontal surface (Average, Min, Max)
- Direct normal radiation (Average, Min, Max)
- Insolation at 3-hourly intervals
- Insolation clearness index, K (Average, Min, Max)
- Insolation normalized clearness index
- Clear sky Insolation
- Clear sky Insolation clearness index
- Clear sky Insolation normalized clearness index
- Downward Longwave Radiative Flux

**Table 2.2.1 Overview of the SSE climatologically averaged parameters  
(cont'd)**

**3. Solar Geometry:**

- Solar Noon
- Daylight Hours
- Daylight average of hourly cosine solar zenith angles
- Cosine solar zenith angle at mid-time between sunrise and solar noon
- Declination
- Sunset Hour Angle
- Maximum solar angle relative to the horizon
- Hourly solar angles relative to the horizon
- Hourly solar azimuth angles

**4. Parameters for Tilted Solar Panels:**

- Radiation on equator-pointed tilted surfaces
- Minimum radiation for equator-pointed tilted surfaces
- Maximum radiation for equator-pointed tilted surfaces

**5. Parameters for Sizing Battery or other Energy-storage Systems:**

- Minimum available Insolation as % of average values over consecutive-day period
- Horizontal surface deficits below expected values over consecutive-day period
- Equivalent number of NO-SUN days over consecutive-day period

**6. Parameters for Sizing Surplus-product Storage Systems:**

- Available surplus as % of average values over consecutive-day period

**7. Diurnal Cloud Information:**

- Daylight cloud amount
- Cloud amount at 3-hourly intervals
- Frequency of cloud amount at 3-hourly intervals

**8. Meteorology (Temperature):**

- Air Temperature at 2 m
- Daily Temperature Range at 2 m
- Cooling Degree Days above 18 °C
- Heating Degree Days below 18 °C
- Arctic Heating Degree Days below 10 °C
- Arctic Heating Degree Days below 0 °C
- Earth Skin Temperature
- Daily Mean Earth Temperature (Min, Max, Amplitude)
- Frost Days
- Dew/Frost Point Temperature at 2 m
- Air Temperature at 3-hourly intervals

**9. Meteorology (Wind):**

- Wind Speed at 50 m (Average, Min, Max)
- Percent of time for ranges of Wind Speed at 50 m
- Wind Speed at 50 m for 3-hourly intervals
- Wind Direction at 50 m
- Wind Direction at 50 m for 3-hourly intervals
- Wind Speed at 10 m for terrain similar to airports

**10. Meteorology (Moisture, pressure):**

- Relative Humidity
- Humidity Ratio (i.e. Specific Humidity)
- Surface Pressure
- Total Column Perceptible Water
- Precipitation

**Table 2.2.1 Overview of the SSE climatologically averaged parameters  
(cont'd)**

**11. Supporting Information**

- Top of Atmosphere Insolation
- Surface Albedo

**12. Global Radiation Data Files of Monthly and Annual Averages by Year**

- Insolation on Horizontal Surface
- Insolation Clearness Index
- Clear Sky Insolation
- Diffuse Radiation
- Minimum Diffuse Radiation
- Maximum Diffuse Radiation
- Direct Normal Radiation
- Minimum Direct Radiation
- Maximum Direct Radiation
- Clear Sky Insolation Clearness Index
- Downward Longwave Radiative Flux
- Top-of-atmosphere Insolation
- Maximum NO\_SUN of BLACK Days

**13. Global Metrological Data Files of Monthly and Annual Averages by Year**

- Surface Air Pressure
- Earth Skin Temperature
- Average Air Temperature at 2 m
- Minimum Air Temperature at 2 m
- Maximum Air Temperature at 2 m
- Specific Humidity at 2 m
- Relative Humidity at 2 m
- Dew/Frost Point Temperature at 2 m
- Heating Degree-Days Below 18.3C°
- Cooling Degree-Days above 18.3C°
- Cooling Degree-Days above 10C°

**14. Global Solar Geometry Data for the “Monthly Average Day”**

[\(Return to Content\)](#)

**Table 2.2.2. SSE: Inter-Annual Variability**

- All parameters are available on a 0.5° x 0.5° latitude, longitude global grid.
- 24-year monthly & annual solar climatologies (January 1984 - December 2007) are based upon solar insolation pulled from NASA GEWEX/SRB (<https://gewex-srb.larc.nasa.gov/>) release 3.0.
- 30-year monthly & annual meteorological climatology (January 1984 - December 2013) are based upon data pulled from NASA's Modern Era Retro-analysis for Research and Applications –assimilation model (MERRA-2; <http://gmao.gsfc.nasa.gov/merra/> ).

**1. Solar Parameters**

- All sky shortwave insolation of a horizontal surface
- Shortwave top-of-atmosphere
- Clear sky shortwave insolation of a horizontal surface
- Insolation Clearness Index
- Clear Sky Insolation Clearness Index
- All sky longwave insolation of a horizontal surface

**Table 2.2.2. SSE: Inter-Annual Variability (cont'd)**

- |  |
|--|
| <p><b>2. Meteorological Parameters</b></p> <ul style="list-style-type: none"> <li>• Earth Skin Temperature</li> <li>• Average Air Temperature at 2 m</li> <li>• Minimum Air Temperature at 2 m</li> <li>• Maximum Air Temperature at 2 m</li> <li>• Specific Humidity at 2m</li> <li>• Relative Humidity at 2m</li> <li>• Dew/Frost Point Temperature at 2m</li> <li>• Surface pressure</li> </ul> |
|--|

[\(Return to Content\)](#)

**Table 2.2.3. Overview of daily mean SSE parameters**

- |  |
|--|
| <ul style="list-style-type: none"> <li>• All parameters are available on a <math>0.5^{\circ}</math> x <math>0.5^{\circ}</math> latitude, longitude global grid</li> <li>• Daily mean solar related parameters are derived from data taken from the NASA GEWEX/SRB (<a href="http://gewex-srb.larc.nasa.gov/">http://gewex-srb.larc.nasa.gov/</a>) release 3.0 archive (July 1, 1983 – Dec. 31, 2007) and NASA's FLASHFlux project (<a href="http://flashflux.larc.nasa.gov/">http://flashflux.larc.nasa.gov/</a>; Jan. 1, 2008 – to within about 7-days of real time)</li> <li>• Meteorological related parameters are derived from data taken from the NASA GMAO (<a href="http://gmao.gsfc.nasa.gov/">http://gmao.gsfc.nasa.gov/</a>) MERRA-2 assimilation model (Jan. 1, 1981 to within a few months of real time) plus GEOS-5.12.4 FP-IT (End of MERRA-2 to within several days of real time)</li> </ul> |
|--|

#### **1. DAILY INSOLATION and RELATED PARAMETERS:**

- Shortwave Insolation on Horizontal Surface
- Insolation Clearness Index
- Clear Sky Insolation
- Clear Sky Diffuse Insolation
- Clear Sky Direct Normal Insolation
- Clear Sky Insolation Clearness Index
- Downward Longwave Radiative Flux
- Top-of-atmosphere Insolation

#### **2. DAILY METEOROLOGICAL:**

- Surface Air Pressure
- Earth Skin Temperature
- Average Air Temperature at 2 m
- Minimum Air Temperature at 2 m
- Maximum Air Temperature at 2 m
- Specific Humidity at 2 m
- Relative Humidity at 2 m
- Dew/Frost Point Temperature at 2 m

[\(Return to Content\)](#)

**2.3 Energy-Efficient (or Sustainable) Buildings Community:** The solar and meteorological parameters are available as climatologically and inter-annually average values, as well in a daily time series format. All parameters are provided on user specified  $0.5^{\circ}$ x $0.5^{\circ}$  grids. The climatologically averaged parameters are calculated to support the preliminary design and site selection for building projects. Inter-annually averaged parameters are provided as monthly and annual averaged values by year. The daily time series include a range of the basic solar and

meteorology parameters as well as additional calculated parameters such as diffuse and direct normal radiation, heating and cooling degree days, climate zones, etc.

The following tables provide an explicit list of the parameters in each sustainable building data sections.

<b>Table 2-3.1 Sustainable Building Inter-Annual Variability</b>	
	<ul style="list-style-type: none"> <li>• All parameters are available on a <math>0.5^{\circ}</math> x <math>0.5^{\circ}</math> latitude, longitude global grid</li> <li>• 24-year monthly &amp; annual solar climatologies (January 1984 - December 2007) are based upon solar insolation pulled from NASA GEWEX/SRB (<a href="https://gewex-srb.larc.nasa.gov/">https://gewex-srb.larc.nasa.gov/</a>) release 3.0.</li> <li>• 30-year monthly &amp; annual meteorological climatology (January 1984 - December 2013) are based upon data pulled from NASA's Modern Era Retro-analysis for Research and Applications –assimilation model (MERRA-2; <a href="http://gmao.gsfc.nasa.gov/merra/">http://gmao.gsfc.nasa.gov/merra/</a> )</li> </ul>
3. Solar Parameters	<ul style="list-style-type: none"> <li>• All sky shortwave insolation of a horizontal surface</li> <li>• Shortwave top-of-atmosphere</li> <li>• Clear sky shortwave insolation of a horizontal surface</li> <li>• Insolation Clearness Index</li> <li>• Clear Sky Insolation Clearness Index</li> <li>• All sky longwave insolation of a horizontal surface</li> </ul>
4. Meteorological Parameters	<ul style="list-style-type: none"> <li>• Earth Skin Temperature</li> <li>• Average, Minimum, &amp; Maximum Air Temperature at 2 m</li> <li>• Specific Humidity at 2m</li> <li>• Relative Humidity at 2m</li> <li>• Dew/Frost Point Temperature at 2m</li> <li>• Surface pressure</li> <li>• Heating Degree Days: Tbase = 18.3C, 10C, &amp; 0C</li> <li>• Cooling Degree Days: Tbase = 18.3C, 10C, &amp; 0C</li> </ul>

[\(Return to Content\)](#)

<b>Table 2.3.2. Daily mean Sustainable Building parameters</b>	
	<ul style="list-style-type: none"> <li>• All parameters are available on a <math>0.5^{\circ}</math> x <math>0.5^{\circ}</math> latitude, longitude global grid</li> <li>• Daily Mean solar related parameters are derived from data taken from the NASA GEWEX/SRB (<a href="http://gewex-srb.larc.nasa.gov/">http://gewex-srb.larc.nasa.gov/</a>) release 3.0 archive (July 1, 1983 – Dec. 31, 2007) and NASA's FLASHFlux project (<a href="http://flashflux.larc.nasa.gov/">http://flashflux.larc.nasa.gov/</a> ; Jan. 1, 2008 – to within about 7-days of real time)</li> <li>• Meteorological related parameters are derived from data taken from the NASA GMAO (<a href="http://gmao.gsfc.nasa.gov/">http://gmao.gsfc.nasa.gov/</a>) MERRA-2 assimilation model (Jan. 1, 1981 to within a few months of real time) plus GEOS-5.12.4 FP-IT (End of MERRA-2 to within several days of real time)</li> </ul>
1. DAILY INSOLATION and RELATED PARAMETERS:	<ul style="list-style-type: none"> <li>• Shortwave Insolation on Horizontal Surface</li> <li>• Downward Longwave Radiative Flux</li> <li>• Top-of-Atmosphere Insolation</li> <li>• Clear Sky Insolation</li> <li>• Clear Sky Insolation Clearness Index</li> </ul>
2. DAILY METEOROLOGICAL:	<ul style="list-style-type: none"> <li>• Surface Air Pressure</li> <li>• Earth Skin Temperature</li> <li>• Average, Minimum, &amp; Maximum Air Temperature at 2 m</li> <li>• Specific Humidity at 2m</li> </ul>

**Table 2.3.2. Daily mean Sustainable Building parameters (cont'd)**

- Relative Humidity at 2m
- Wind speed at 10m
- Dew/Frost Point Temperature at 2m
- Precipitation
- Heating Degree Days: Tbase = 18.3C, 10C, & 0C
- Cooling Degree Days: Tbase = 18.3C, 10C, & 0C

[\(Return to Content\)](#)

**Table 2.3.3. DOE/ASHRAE Climate Building parameters**

- All parameters are available on a 0.5° x 0.5° latitude, longitude global grid
- Selected parameters useful for design of residential and commercial buildings are available as monthly & yearly averaged values by year from Jan. 1, 1984 –Dec. 31, 2013
- Solar related parameters are based upon solar insolation data taken from the NASA GEWEX/SRB (<https://gewex-srb.larc.nasa.gov/>) release 3.0 archive (July 1, 1983 – Dec. 31, 2007) and the CERES Fast Longwave And Shortwave Radiation Fluxes (FLASHFlux) project (<https://flashflux.larc.nasa.gov/>; Jan. 1, 2008 – Dec. 31, . 2013)
- The meteorological parameters are based upon data pulled from NASA's Modern Era Retro-analysis for Research and Applications –assimilation model MERRA-2 ( <http://gmao.gsfc.nasa.gov/merra/> ; Jan. 1, 1984 – Dec. 31, 2013)
- Air Temperature @ 2m
- Precipitation
- Heating Degree Days: Tbase = 18.3C, 10C, & 0C
- Cooling Degree Days: Tbase = 18.3C, 10C, & 0C
- Climate Type
- Climate Zone

[\(Return to Content\)](#)

**Table 2.3.4. Sustainable Building Monthly Averaged Parameters**

- All parameters are available on a 0.5°x 0.5° latitude, longitude global grid.
- All solar related parameters are derived from data taken from the NASA GEWEX/SRB release 3.0 archive (<http://gewex-srb.larc.nasa.gov>) over the time period July 1, 1983 - June 30, 2005 (24 years) and available as a 24-year monthly average for each month and as a 23-year average.
- Temperature, moisture, and wind related parameters are derived from data taken from the NASA's GMAO (<http://gmao.gsfc.nasa.gov>) MERRA-2 assimilation model over the time period January 1, 1984 – December 31, 2013 (30 years) and available as a 30-year monthly average for each month and as a 30-year average.

#### 1. General Information:

- Latitude
- Longitude

#### 2. Solar Geometry:

- Solar Noon
- Daylight Hours
- Daylight average of hourly cosine solar zenith angles
- Cosine solar zenith angle at mid-time between sunrise and solar noon
- Declination
- Sunset Hour Angle
- Maximum solar angle relative to the horizon

**Table 2.3.4. Sustainable Building Monthly Averaged Parameters (cont'd)**

- Hourly solar angles relative to the horizon
- Hourly solar azimuth angles
- 3. Radiation**
  - All-sky Insolation (Average, Min, Max)
  - Diffuse horizontal radiation (Average, Min, Max)
  - Direct normal radiation (Average, Min, Max)
  - All-sky Insolation at available GMT times
  - Clear sky insolation
  - Clear sky diffuse
  - Clear sky direct normal
  - Radiation on tilted surfaces
- 4. Monthly Mean Illuminance**
  - Illuminance on tilted surfaces at available GMT times
  - Illuminance on tilted surfaces over a 24 hour period
- 5. Surface Albedo**
- 6. Monthly Clouds**
  - Daylight cloud amount
  - Cloud amount at available GMT times
  - Frequency of cloud amount at available GMT times
- 7. Parameters For Sizing Battery or Other -Storage Systems**
  - Minimum available insolation as % of average values over consecutive-day period
  - Horizontal surface deficits below expected values over consecutive-day period
  - Equivalent number of NO Sun days over consecutive day period
- 8. Meteorology (Wind):**
  - Percent of time for ranges of Wind Speed at 50 m
  - Wind Speed at 50 m for 3-hourly intervals
  - Wind Direction at 50 m
  - Wind Direction at 50 m for 3-hourly intervals
  - Wind Speed at 10 m for terrain similar to airports
  - Wind Speed at 50 m (Average, Min, Max)
- 9. Meteorology (Temperature):**
  - Air Temperature at 2 m
  - Daily Temperature Range at 2 m
  - Cooling Degree Days above 18 °C
  - Heating Degree Days below 18 °C
  - Arctic Heating Degree Days below 10 °C
  - Arctic Heating Degree Days below 0 °C
  - Earth Skin Temperature
  - Daily Mean Earth Temperature (Min, Max, Amplitude)
  - Frost Days
  - Dew/Frost Point Temperature at 10 m
  - Air Temperature at 3-hourly intervals

[\(Return to Content\)](#)

**2.4 Agroclimatology Community:** The agroclimatology solar and meteorological parameters are available daily mean time series formats. All parameters are provided on user specified  $0.5^\circ \times 0.5^\circ$  grids. The daily time series include the basic solar and meteorology parameters to

support agricultural decision support tools such as the Decision Support System for Agro-technology Transfer (DSSAT - <https://dssat.net/> ).

The following table provides an explicit list of the parameters in the agroclimatology archive

<b>Table 2.4. Agroclimatology: Daily Averaged Solar and Meteorological parameters</b>
<ul style="list-style-type: none"> <li>• All parameters are available on a 0.5° x 0.5° latitude, longitude global grid</li> <li>• Daily Mean solar related parameters are derived from data taken from the NASA GEWEX/SRB (<a href="http://gewex-srb.larc.nasa.gov/">http://gewex-srb.larc.nasa.gov/</a>) release 3.0 archive (July 1, 1983 – Dec. 31, 2007) and NASA's FLASHFlux project (<a href="http://flashflux.larc.nasa.gov/">http://flashflux.larc.nasa.gov/</a>; Jan. 1, 2008 – to within about 7-days of real time)</li> <li>• Meteorological related parameters are derived from data taken from the NASA GMAO (<a href="http://gmao.gsfc.nasa.gov/">http://gmao.gsfc.nasa.gov/</a>) MERRA-2 assimilation model (Jan. 1, 1981 to within a few months of real time) plus GEOS-5.12.4 FP-IT (End of MERRA-2 to within several days of real time)</li> </ul>

## 1. DAILY INSOLATION

- Shortwave Insolation on Horizontal Surface
- Downward Longwave Radiative Flux
- Top-of-Atmosphere Insolation

## 2. DAILY METEOROLOGICAL:

- Average Air Temperature at 2 m
- Minimum Air Temperature at 2 m
- Maximum Air Temperature at 2 m
- Relative Humidity at 2m
- Wind speed at 10m
- Dew/Frost Point Temperature at 2m
- Precipitation

[\(Return to Content\)](#)

**3. Summary of Parameters Accuracy:** As noted above, the POWER solar data are based upon satellite observations from which surface insolation values are inferred. The meteorological parameters are based upon the MERRA-2 assimilation model. This section provides a summary of the estimated uncertainty associated with the data underlying the solar and meteorological parameters available through POWER. The uncertainty estimates are based upon comparisons with surface measurements. A more detailed description of the parameters and the procedures used to estimate their uncertainties is given in the subsequent sections of this document.

Additional validation results have been reported by White, et al. (2008 and 2011) and by Bai, et al (2010).

**3.1 Solar Insolation:** We note that quality surface-measurements are generally considered more accurate than satellite-derived values. However, measurement uncertainties from instrument calibration drift, operational uncertainties, instrumental changes, or data gaps are often unknown or unreported for many surface data sets. In 1989, the World Climate Research Program estimated "end-to-end" uncertainties for most routinely-operation solar-radiation ground sites in the range from 6 to 12%. Specialized high quality research sites such as those in the Baseline Surface Radiation Network (BSRN - <http://bsrn.awi.de/> ) are estimated to be more accurate by a factor of two.

Note that the time series of daily solar data available from the POWER archive are taken from the GEWEX SRB project (July 1983 – December 31 2007) and for the time period January 1, 2008 to December 31, 2012 the solar parameters are based upon data from NASA’s Fast Longwave And SHortwave Radiative Fluxes (FLASHFlux - <http://flashflux.larc.nasa.gov/>) project version 2(D, E, G, H), and from January 1, 2013 through near real time the solar parameters are based upon data from FLASHFlux version 3 (A, B, C). ***Accordingly, it is not recommended to use these fluxes to assess climate trends that encompass changes in the source data without a careful assessment and analysis that accounts for discontinuities and uncertainties in the parameter values.***

The solar data from each source enumerated in the previous paragraph were initially produced on a  $1^{\circ}$  latitude/longitude grid and subsequently re-gridded via data replication to a  $0.5^{\circ}$  grid. Comparisons of the satellite based values to surface observations were performed using the  $1^{\circ}$  gridded values. However, since the re-gridding to  $0.5^{\circ}$  was performed via replication of the  $1^{\circ}$  values, the  $1^{\circ}$  comparison results are applicable to the  $0.5^{\circ}$  data.

Table 3.1.1 summarizes the results of comparing the NASA/GEWEX SRB 3.0 solar shortwave (SW) all sky and clear sky insolation, and longwave (LW) radiative flux on a horizontal surface to observations obtained at 47 [BSRN](#) surface sites.

Table 3.1.1 Comparisons of all sky and clear sky shortwave (SW) solar insolation and longwave (LW) radiative flux from NASA/GEWEX SRB 3.0 versus corresponding values from surface observations at NASA’s baseline surface radiation network [BSRN](#) for the time period January 1, 1992 - December 31, 2007. Clear-sky insolation validation is computed using comparisons between sites and satellite estimates when satellite give cloud fractions < 10% (see Section 5).

Parameter	Region:	Bias (%)	RMSE (%)
<a href="#">Daily Mean SW</a> <a href="#">All Sky Insolation</a> (NASA/GEWEX SRB 3.0)	All Sites	-1.72	20.47
	60° Poleward	-6.94	41.59
	60° Equatorward	-1.13	17.66
<a href="#">Daily Mean LW</a> <a href="#">All Sky Radiative Flux</a> (NASA/GEWEX SRB 3.0)	All Sites	0.16	7.0
	60° Poleward	1.27	13.44
	60° Equatorward	-0.03	5.73
<a href="#">Daily Mean SW</a> <a href="#">Clear Sky Insolation</a> (NASA/GEWEX SRB 3.0)	All Sites	-0.84	7.04

Tables 3.1.2 and 3.1.3 summarize respectively the comparison of the FLASHFLux solar SW insolation and LW Radiative flux to observational values from 59 [BSRN](#) surface sites.

Table 3.1.2: Comparison of all sky shortwave (SW) solar insolation from FLASHFlux version 2(D, E, G, H) and version 3(A, B) and for the ensemble of all versions of FLASHFlux from January 1, 2008 through December 31, 2016 with observational values from 59 [BSRN](#) surface sites.

Parameter	Region: All BSRN Sites	Bias (%)	RMSE (%)
<a href="#">Daily Mean All Sky SW Insolation</a> <a href="#">Jan.1, 2008 – Dec.31, 2012</a> (FLASHFlux Version 2(D, E, G, H))	All Sites	0.12	16.80
	60° Poleward	-5.57	33.86
	60° Equatorward	-0.74	14.19
<a href="#">Daily Mean All Sky SW Insolation</a> <a href="#">Jan.1, 2013 – Dec. 2016</a> (FLASHFlux Version 3(A, B))	All Sites	-3.11	17.45
	60° Poleward	-17.60	41.63
	60° Equatorward	-1.86	14.35
<a href="#">Daily Mean All Sky SW Insolation</a> <a href="#">Jan.1, 2008 – Dec. 31, 2016</a> (FLASHFlux Version 2+3)	All Sites	-1.18	17.06
	60° Poleward	-9.78	35.62
	60° Equatorward	-0.32	14.26

Table 3.1.3. Comparison of all sky longwave (LW) solar insolation from FLASHFlux version 2(D,E,G,H) and version 3(A, B) and for the ensemble of FLASHFLux versions 2 + 3 from January 1, 2008 through December 31, 2016 with observational values from 59 [BSRN](#) surface sites.

Parameter	Region: All BSRN Sites	Bias (%)	RMSE (%)
<a href="#">Daily Mean All Sky LW radiative flux</a> <a href="#">Jan. 1, 2008 – Dec. 31, 2012</a> FLASHFlux Version 2(D, E, G, H)	All Sites	0.01	5.55
	60° Poleward	0.98	12.39
	60° Equatorward	-0.13	4.34
<a href="#">Daily Mean All Sky LW radiative flux</a> <a href="#">Jan.1, 2013 – Dec. 31, 2016</a> FLASHFlux Version 3(A, B)	All Sites	-0.20	8.08
	60° Poleward	2.71	8.73
	60° Equatorward	-0.50	4.62
<a href="#">Daily Mean All Sky LW radiative flux</a> <a href="#">Jan. 1, 2008 – Dec. 31, 2016</a> FLASHFlux Version 2+3	All Sites	-0.08	5.38
	60° Poleward	1.45	11.16
	60° Equatorward	-0.28	4.46

Table 3.1.4 summarizes the comparison statistics for clear sky shortwave (SW) solar insolation from FLASHFlux versions 2(D, E, G, H), 3(A, B) and for the ensemble of versions 2 + 3 over the time period January 1, 2008 – December 31, 2016 with observational values from 27 [BSRN](#) clear sky surface sites.

Table 3.1.4: Comparison of clear sky shortwave (SW) solar insolation from FLASHFlux version-2(D,E,G,H) and version -3(A, B) and for the ensemble of FLASHFlux versions 2+3 from January 1, 2008 through December 31, 2016 with observational values from 27 [BSRN](#) surface observations.

Parameter	Region: All BSRN Sites	Bias (%)	RMSE (%)
<a href="#">Daily Mean Clear Sky SW Insolation Jan.1, 2008 – Dec 31, 2012</a> FLASHFlux Version 2(D, E, G, H)	All Sites	-3.42	5.44
	60° Poleward	0.21	5.36
	60° Equatorward	-3.65	5.45
<a href="#">Daily Mean Clear Sky SW Insolation Jan.1, 2013 – Dec. 31, 2016</a> FLASHFlux Version 3(A, B)	All Sites	-2.99	4.40
	60° Poleward	-4.53	7.08
	60° Equatorward	-2.94	4.31
<a href="#">Daily Mean Clear Sky SW Insolation Jan.1, 2008 – Dec. 31, 2016</a> FLASHFlux Version 2 + 3	All Sites	-3.25	5.07
	60° Poleward	-0.89	5.78
	60° Equatorward	-3.37	5.03

[\(Return to Content\)](#)

**3.2 Meteorology:** Table 3.2 summarizes the results of comparing the MERRA-2 parameters to surface observation reported in the National Center for Environmental Information (NCEI – formally National Climatic Data Center) Global Summary of the Day (GSOD) files. The slope, intercept, and R<sup>2</sup> listed in this table are associated with a linear least squares fit to a scatter plot of daily observations at each surface station to the corresponding MERRA-2 values for the overlapping grid cell for every 3<sup>rd</sup> year from 1981 – 2014 (e.g. 1981, 1984, 1987, etc.). The Mean Bias Error (MBE) and Root Mean Square Error (RMSE) represent mean values over the comparison years.

Table 3.2: Listed in this Table are the climatologically averaged statistics associated with comparisons of the daily meteorological parameters from the MERRA-2 assimilation model to corresponding surface observation in the National Center for Environmental Information (NCEI – formally National Climatic Data Center) GSOD files for every 3<sup>rd</sup> year for the time period January 1, 1981 through December 31, 2014 (e.g. 1981, 1984, 1987, etc.). The height above the surface over the entire grid box area is 2m for each parameter, except for the wind which is estimated at 10m.

Parameter	MBE	RMSE	Slope	Intercept	Rsqrd
<a href="#"><u>Tavg (°C)</u></a>	-0.52	2.29	1.00	-0.48	0.96
<a href="#"><u>Tmin (°C)</u></a>	0.50	3.05	0.97	0.73	0.93
<a href="#"><u>Tmax (°C)</u></a>	-1.38	3.16	0.98	-1.01	0.95
<a href="#"><u>Relative Humidity (%)</u></a>	4.44	12.06	0.78	19.88	0.61
<a href="#"><u>Dew Point (°C)</u></a>	0.37	2.53	0.95	0.69	0.95
<a href="#"><u>Daily Precipitation (mm/day)</u></a>	0.46	6.81	0.36	1.71	0.23
<a href="#"><u>Specific Humidity (g/kg)</u></a>	0.01	1.05	0.93	0.49	0.95
<a href="#"><u>Uncorrected Atmospheric Pressure (mb)</u></a>	-8.59	24.40	0.95	40.97	0.81
<a href="#"><u>Elevation Corrected Atmospheric Pressure (mb)</u></a>	0.03	2.82	1.00	1.08	1.00
<a href="#"><u>Wind Speed (m/s)</u></a>	0.37	1.65	0.73	1.36	0.55

[\(Return to Content\)](#)

**4.0 Global SW Solar Insolation & LW Radiative Flux:** The surface solar shortwave (SW) insolation and the longwave (LW) radiative flux available from the POWER data archives are based upon observational data from a variety of satellites. The basic observational data is the amount of radiative energy emerging from the earth's atmosphere at certain ranges of wavelengths from the solar through the thermal infrared. The amount of radiation measured is affected by atmospheric absorption, emission and scattering processes. Radiative transfer models and radiative transfer based parameterizations using the observations and information about the atmospheric constituents such as gaseous concentrations, aerosols and clouds are used for estimating the SW insolation and LW radiative flux.

The daily mean solar radiation data for the time period July 1, 1983 – December 31, 2007 are obtained from the NASA/Global Energy and Water Cycle Experiment - Surface Radiation Budget Project Release 3.0 archive (NASA/GEWEX SRB 3.0; see <https://gewex-srb.larc.nasa.gov/> & [https://eosweb.larc.nasa.gov/project/srb/srb\\_table](https://eosweb.larc.nasa.gov/project/srb/srb_table); Stackhouse et al., 2011)

Daily solar radiation data for the time period from January 1, 2008 to within 1-week of current time are taken from NASA's Fast Longwave And SHortwave Radiative Fluxes (FLASHFlux; see <https://flashflux.larc.nasa.gov/>) project. Specifically, from January 1, 2008 to December 31, 2012 FLASHFLux values are taken from version 2(D, E, G, H); from January 1, 2013 to within one week of real time values are taken from FLASHFlux version 3(A,B,C).

For a discussion of the differences between the various versions of FLASHFlux the User is referred to

[https://eosweb.larc.nasa.gov/sites/default/files/project/ceres/quality\\_summaries/FFv3\\_TISA\\_DQ\\_S.pdf](https://eosweb.larc.nasa.gov/sites/default/files/project/ceres/quality_summaries/FFv3_TISA_DQ_S.pdf), section “Data Sets within the Version3 family”

The solar data from these primary sources are initially produced on a global  $1^{\circ}$  latitude/ longitude grid and translated to a  $0.5^{\circ}$  spatial grid by the POWER project via replication of the  $1^{\circ}$  values to the four  $0.5^{\circ}$  grid cells within the respective  $1^{\circ}$  cell. Validation of the satellite based values was conducted via comparisons to surface observations using the 1-degree gridded values. However, since the re-gridding to  $0.5^{\circ}$  was based upon replication of values, the  $1^{\circ}$  comparison results are applicable to the  $0.5^{\circ}$  data.

We note here that the NASA/GEWEX SRB Project (<https://gewex-srb.larc.nasa.gov>) focuses on providing high quality estimates of the Earth's Top-of-atmosphere (TOA) and surface solar insolation in support of NASA's effort to quantify components of the Earth's radiation budget, while the focus of the FLASHFlux project is to provide solar data within one week of satellite observations with well validated estimates of its accuracy. The POWER data sets concurrently concatenate these data sets. However, *it is not recommended to use these fluxes to assess climate trends that encompass changes in the source data without a careful assessment and analysis that accounts for discontinuities and uncertainties in the parameter values.*

While it is not the intent or purpose of this document to provide a detailed description of the methodology for inferring solar data from satellite observations, a brief synopsis for each is provided in the following sections.

[\(Return to Content\)](#)

**4.1 GEWEX SRB 3.0 SW and LW Radiative Fluxes:** The GEWEX (Global Energy and Water Cycle Exchange program) Surface Radiation Budget (SRB) project has been supported by NASA and organized under the auspices of the World Climate Research Programme's (WCRP) GEWEX programme. The project endeavors to collaborate with other GEWEX organized projects to estimate the surface radiative components of the Earth's radiative energy budget. The latest version processes long-term estimates of global 3-hourly surface and cloud information and integrates this with ancillary information such as gaseous constituents of the atmosphere (water vapor, carbon dioxide and ozone) and aerosols to estimate the radiative fluxes at both the

surface and at the top-of-atmosphere for both the solar and thermal infrared. POWER data sets provide both the solar (shortwave) and thermal infrared (longwave) fluxes to users. An overview of the latest version of GEWEX SRB Release 3 data products is provided by Stackhouse et al., (2011). Here we briefly describe the algorithms and provide an overview of the data quality of these surface estimates.

The GEWEX Shortwave (SW) Algorithm uses a modified method of Pinker and Laszlo (1992) to solve the radiative transfer equation and provide the GEWEX SRB 3.0 estimates of surface SW solar insolation. This method involves the use of a radiative transfer model, along with cloud parameters derived from the DX data of the International Satellite Cloud Climatology Project (ISCCP; Rossow and Schiffer, 1999) and temperature and moisture profiles taken from 4-D data assimilation products provided by the Data Assimilation Office at NASA Goddard Space Flight Center (GSFC) and produced with the Goddard Earth Observing System model version 4 (GEOS-4) and ozone column amounts from satellite measurements. Three satellite visible radiances are used: the instantaneous clear sky radiance, the instantaneous cloudy sky radiance, and the clear sky composite radiance, which is a representation of a recent dark background value. The observed satellite radiances are converted into broadband shortwave TOA albedos, using Angular Distribution Models from the Earth Radiation Budget Experiment (Smith et al., 1986). The spectral shape of the surface albedo is fixed by surface type. The radiative transfer model (through the use of lookup tables) is then used to find the absolute value of the surface albedo which produces a TOA upward flux which matches the TOA flux from the conversion of the clear-sky composite radiance. For this step, a first guess of the aerosol amount is used. The aerosol used for this purpose was derived from six years (2000-2005) of daily output from the MATCH chemical transport model (Rasch *et al.*, 1997). A climatology of aerosol optical depth was developed for each of the twelve months by collecting the daily data for each grid cell, and finding the mode of the frequency distribution. The mode was used rather than the average so as to provide a typical background value of the aerosol, rather than an average which includes much higher episodic outbreak values. The surface albedo now being fixed, the aerosol optical depth is chosen within the radiative transfer model to produce a TOA flux which matches the TOA Flux from the conversion of the instantaneous clear sky radiance. Similarly, the cloud optical depth is chosen to match the TOA flux implied from the instantaneous cloudy sky radiance. With all parameters now fixed, the model outputs a range of parameters including surface and TOA fluxes. All NASA/GEWEX SRB 3.0 parameters are initially output on a  $1^{\circ}$  by  $1^{\circ}$  global grid at 3-hourly temporal resolution for each day of the month with subsequent re-gridding to a global  $0.5^{\circ}$  grid via replication.

The GEWEX Longwave (LW) Algorithm uses the Fu *et al.*, (1997) Thermal Infrared radiative transfer code with cloud and surface parameters requiring cloud, atmospheric profile information, and surface properties. Inputs to the algorithm were obtained from the following sources: The ISCCP DX cloud pixels were separated into categories of high, middle and low where middle and low clouds could be composed of ice or water. Cloud fractions and cloud optical depths were determined within these categories. Cloud particle sizes were assumed and cloud physical thicknesses were also designed based upon information from literature. Random overlap is used between the high, middle and low layers to better approximate under cast conditions.

[\(Return to Content\)](#)

**4.2. CERES FLASHFlux SW and LW Radiative Transfer Model:** The Fast Longwave and SHortwave radiative Flux (FLASHFlux; <https://flashflux.larc.nasa.gov>) project is based upon the algorithms developed for analysis and data collected by the Clouds and the Earth's Radiant Energy System (CERES - <http://ceres.larc.nasa.gov/> ) project. CERES is currently producing world-class climate data products derived from measurements taken aboard NASA's Terra and Aqua spacecrafts. While of exceptional fidelity, CERES data products require extensive calibration checks and validation to assure quality and verify accuracy and precision. The result is that CERES data are typically released more than six months after acquisition of the initial measurements. For climate studies, such delays are of little consequence especially considering the improved quality of the released data products.

There are, however, many uses for the CERES data products on a near real-time basis such as those referred to within the POWER project. To meet those needs, FLASHFlux has greatly sped up the processing by using the earliest stream of data coming from CERES instruments and using fast radiation algorithms to produce results within one week of satellite observations. This results in the loss of climate-quality accuracy due to bypassing some calibration checks, and some gaps in the earliest stream of satellite data. The result is that the FLASHFlux provides global estimates of daily solar (Shortwave) and thermal infrared (Longwave) radiation fluxes for the time period from January 1, 2008 to within 1-week of current time and these are made available through the POWER web services.

Both FLASHFlux and CERES rely on similar input data sets from the meteorological products and Moderate Resolution Imaging Spectroradiometer (MODIS). However, it is important to note that even though the FLASHFlux endeavor intends to incorporate the latest input data sets and improvements into its algorithms, there are no plans to reprocess the FLASHFlux data products once these modifications are in place. Thus, in contrast to the CERES data products, the FLASHFlux data products are **not** to be considered of climate quality. Users seeking climate quality should instead use the CERES data products.

For speedy retrieval of surface SW insolation, FLASHFlux uses the SW Model B that is also used in CERES processing (Kratz et al., 2010 & 2014). This model is named the Langley Parameterized SW Algorithm (LPSA) and described in detail in Gupta et al. (2001). It consists of physical parameterizations which account for the attenuation of solar radiation in simple terms separately for clear atmosphere and clouds. Surface insolation,  $F_{sd}$ , is computed as

$$F_{sd} = F_{toa} T_a T_c ,$$

where  $F_{toa}$  is the corresponding TOA insolation,  $T_a$  is the transmittance of the clear atmosphere, and  $T_c$  is the transmittance of the clouds.

The LW Radiative fluxes are produced via the Langley Parameterized Longwave algorithm (LPLA). Detailed descriptions of this algorithm can be found in Gupta et al. (1992; Gupta (1989) and Wilber et al. (1999) -

For a discussion of the differences between the various versions of FLASHFlux the User is referred to

[https://eosweb.larc.nasa.gov/sites/default/files/project/ceres/quality\\_summaries/FFv3\\_TISA\\_DQ\\_S.pdf](https://eosweb.larc.nasa.gov/sites/default/files/project/ceres/quality_summaries/FFv3_TISA_DQ_S.pdf), section “Data Sets within the Version3 family”

([Return to Content](#))

**4.3. Validation of SW Solar Insolation & LW Radiative Flux (All Sky Conditions):** The GEWEX SRB and FLASHFlux radiative transfer models described in the preceding sections produce estimates of the SW solar insolation and LW Radiative flux on a 1° latitude, longitude global grid. The validation of the SRB and FLASHFlux data is based on this 1° data. The 0.5° spatial solar data in the POWER archive has been generated from the 1° data via a straight replication process that assigns the 1° grid value to each of the four 0.5° grids contained in the respective 1° grid box. Consequently, the validation results reported here and by White et. al. (2011) for the 1° values are applicable to the 0.5° data.

Validation of both the SRB and FLASHFlux solar data is based upon comparisons against research quality observations from the Baseline Surface Radiation Network (BSRN; Ohmura *et al.*, 1998). Figure 4.4.1 shows the location of 47 ground stations within the BSRN network used for the GEWEX SRB 3.0 validation. Figure 4.4.2 shows the location of 59 ground stations within the BSRN network used for the FLASHFlux validation.

The validation time period for the SRB 3.0 shortwave (SW) insolation and longwave (LW) Radiative flux values is from July 1, 1983 – December 31, 2007. Specifically, from January 1, 2008 to December 31, 2012 FLASHFLux values are taken from version 2(D, E, G, H); from January 1, 2013 to within one week of real time values are taken from FLASHFlux version -3(A, B, C). For a discussion of the differences between the various versions of FLASHFlux see [https://eosweb.larc.nasa.gov/sites/default/files/project/ceres/quality\\_summaries/FFv3\\_TISA\\_DQ\\_S.pdf](https://eosweb.larc.nasa.gov/sites/default/files/project/ceres/quality_summaries/FFv3_TISA_DQ_S.pdf), section “Data Sets within the Version-3 family.” *Care should be taken when assessing climate trends that encompass changes in the solar source data.*

The solar data from these primary sources are initially produced on a global 1° latitude/ longitude grid and translated to a 0.5° spatial grid by the POWER project via replication of the 1° values to the four 0.5° grid cells within the respective 1° cell. Validation of the satellite based values was conducted via comparisons to surface observations using the 1-degree gridded values. However, since the re-gridding to 0.5° was based upon replication of values, the 1° comparison results are applicable to the 0.5° data.

See Appendix A, [Validation Methodology](#), for additional description of the validation methodology.

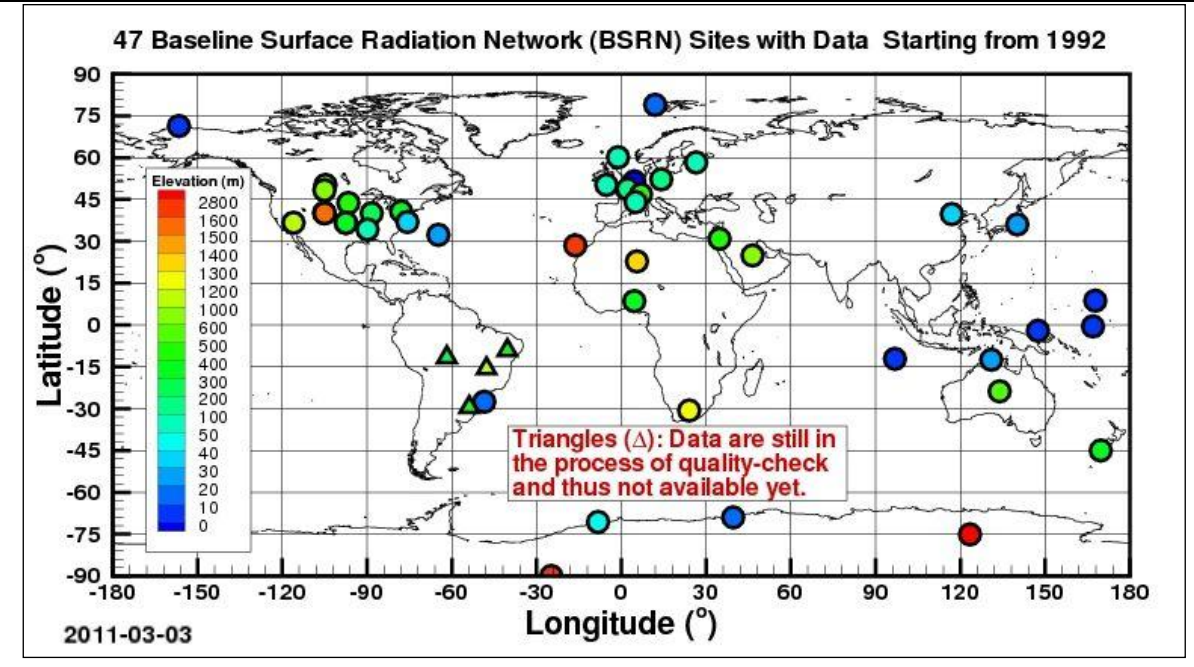


Figure 4.4.1. Location of ground stations in the Baseline Surface Radiation Network (BSRN) used for the validation of the SRB-3.0 SW solar insolation & LW radiative flux.

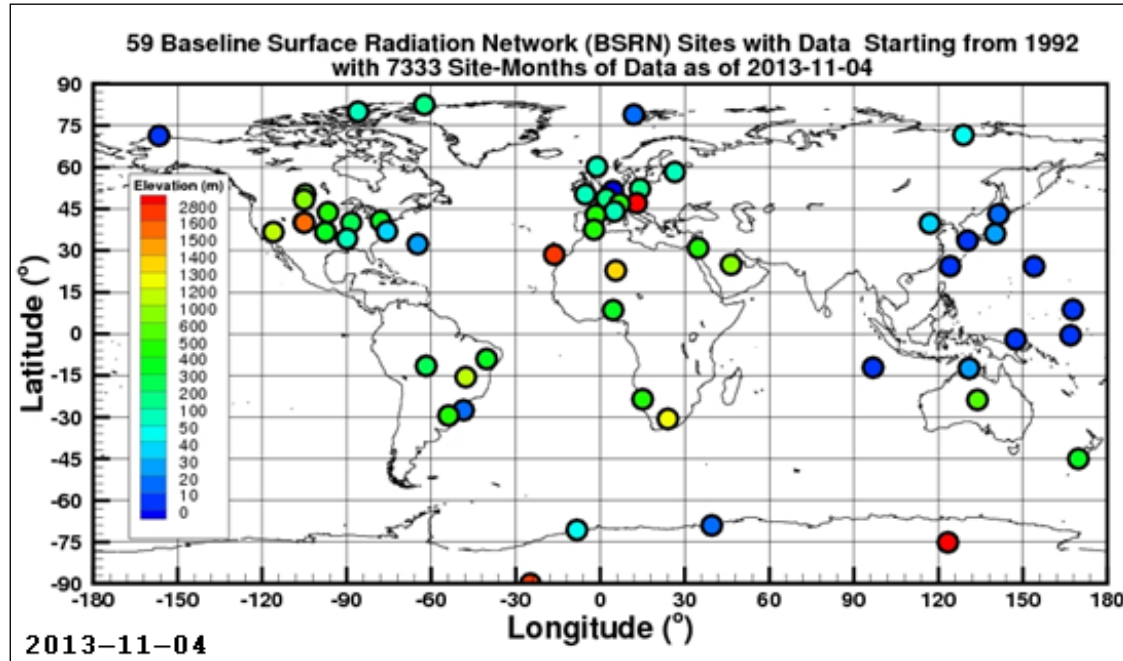


Figure 4.4.2. Location of ground stations in the Baseline Surface Radiation Network (BSRN) used to validation of the FLASHFlux SW solar insolation & LW radiative flux.

[\(Return to Content\)](#)

**4.3.1. SRB 3.0 Daily Mean SW Solar Insolation (All Sky Conditions);** A scatter plot of the total (i.e. diffuse plus direct) surface insolation observed at the BSRN ground sites versus the corresponding insolation values from the SRB release 3.0 archive is shown in Figure 4.4.1.1 for daily mean SW values. The comparison covers the time period January 1, 1992, the earliest that data from BSRN is available, through December 31, 2007.

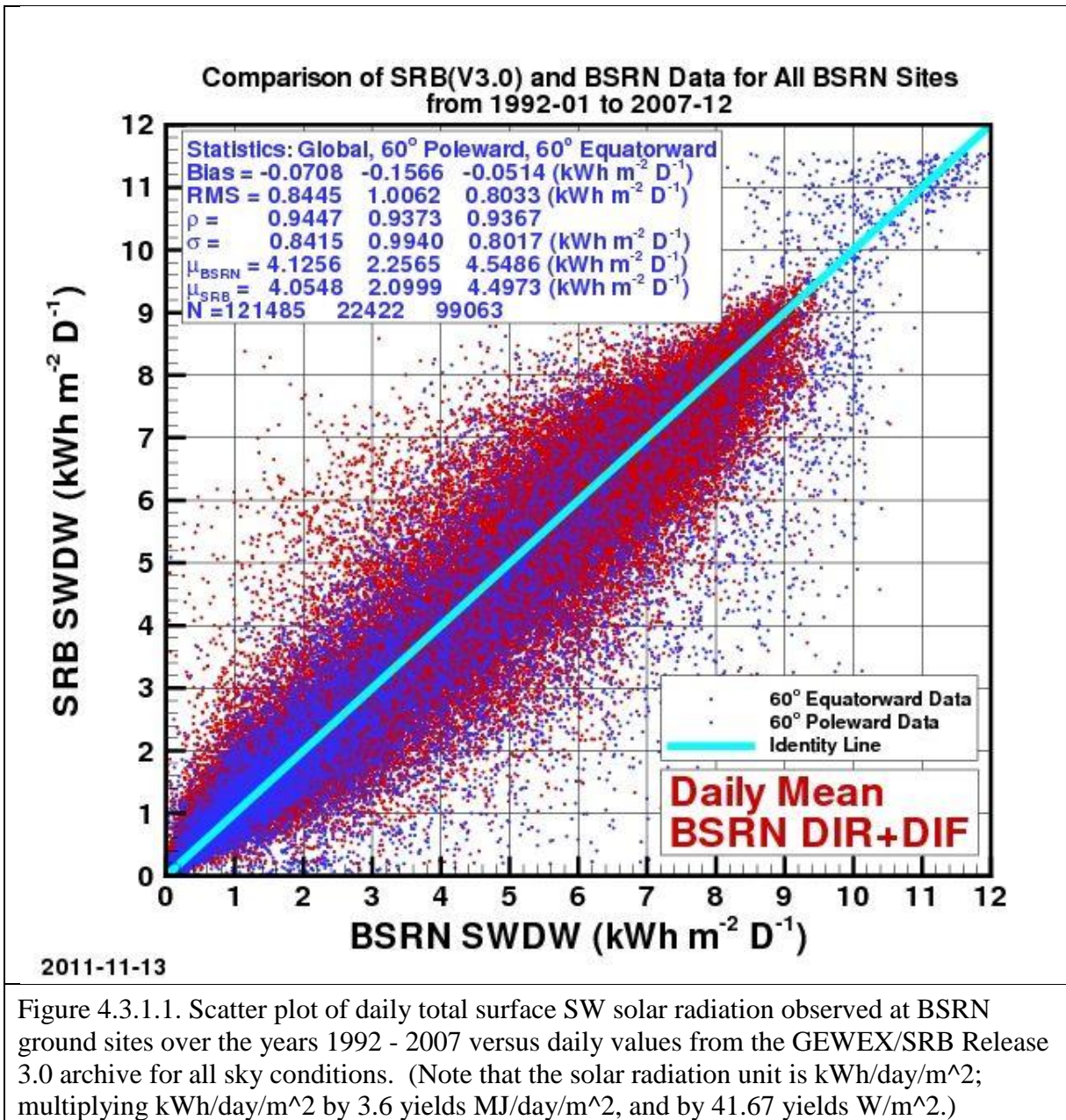


Figure 4.3.1.1. Scatter plot of daily total surface SW solar radiation observed at BSRN ground sites over the years 1992 - 2007 versus daily values from the GEWEX/SRB Release 3.0 archive for all sky conditions. (Note that the solar radiation unit is kWh/day/m<sup>2</sup>; multiplying kWh/day/m<sup>2</sup> by 3.6 yields MJ/day/m<sup>2</sup>, and by 41.67 yields W/m<sup>2</sup>.)

The statistics given in the upper left box are for all BSRN sites (Globally), those located 60-degree poleward, and for those located 60-degree equatorward. The Bias is the difference between the mean ( $\mu$ ) of the respective solar radiation values for SRB and BSRN. RMS is the root mean square difference between the respective SRB and BSRN values. The correlation

coefficient between the SRB and BSRN values is given by  $\rho$ , the variance in the SRB values is given by  $\sigma$ , and  $N$  is number of SRB:BSRN month pairs for each latitude region.

[\(Return to Content\)](#)

**4.3.2. SRB 3.0 Daily Mean LW Radiative Fluxes (All Sky Conditions):** The longwave (LW) radiative fluxes in the time period from July 1983 – December 2007 were taken from release 3 of the NASA/GEWEX Surface Radiation Budget project (GEWEX SRB 3.0 - <http://gewex-srb.larc.nasa.gov/> & [https://eosweb.larc.nasa.gov/project/srb/srb\\_table](https://eosweb.larc.nasa.gov/project/srb/srb_table)).

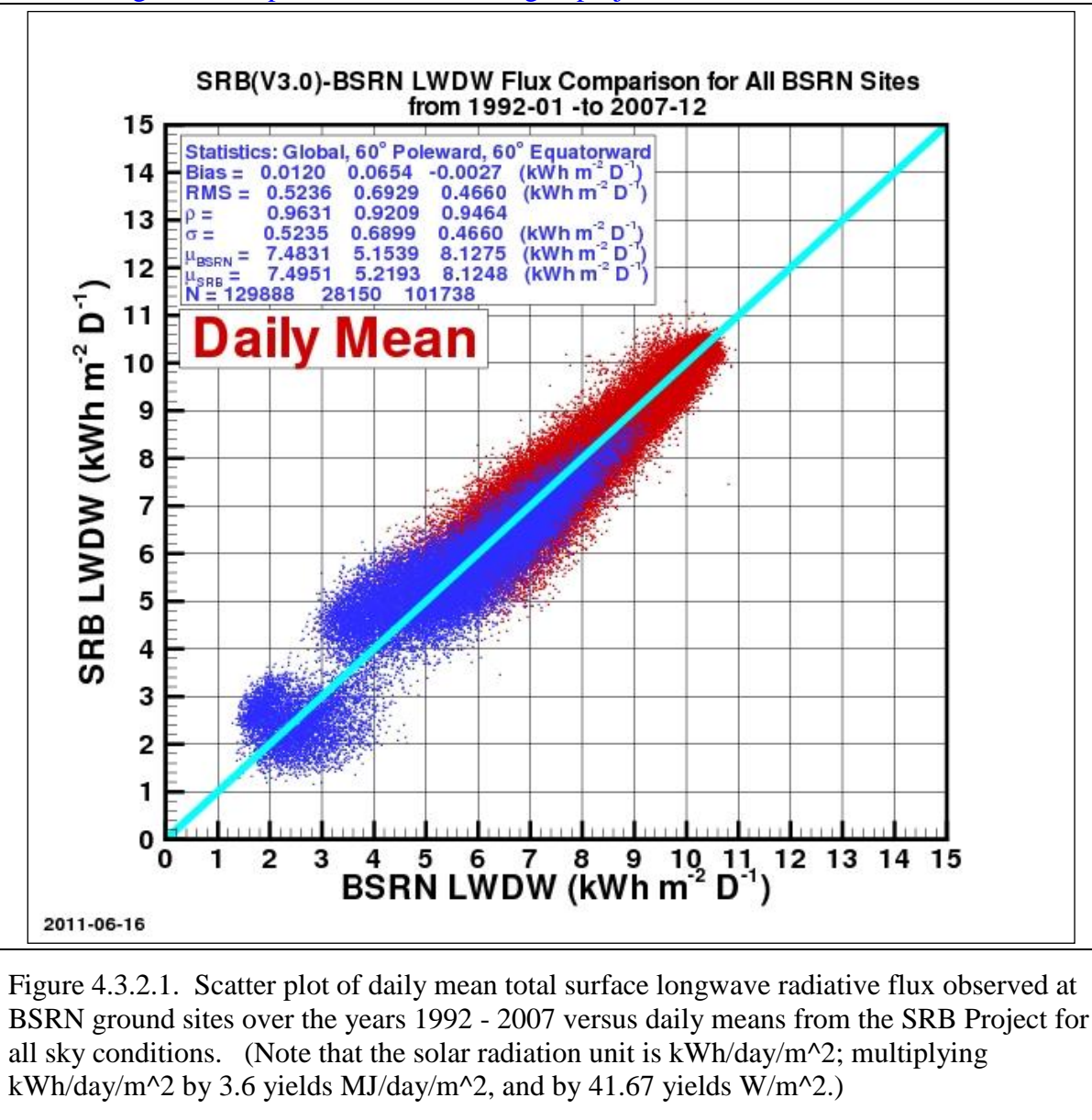


Figure 4.3.2.1. Scatter plot of daily mean total surface longwave radiative flux observed at BSRN ground sites over the years 1992 - 2007 versus daily means from the SRB Project for all sky conditions. (Note that the solar radiation unit is kWh/day/m<sup>2</sup>; multiplying kWh/day/m<sup>2</sup> by 3.6 yields MJ/day/m<sup>2</sup>, and by 41.67 yields W/m<sup>2</sup>.)

A scatter plot of the daily mean LW surface insolation observed at the BSRN ground sites versus corresponding values from the SRB release 3.0 archive is shown in Figure 4.3.2.1. The

comparisons cover the time period January 1, 1992, the earliest that data from BSRN is available, through December 31, 2007. The statistics given in the upper left box are for all BSRN sites (Globally), those located 60-degree poleward, and for those located 60-degree equatorward. The statistics given in the upper left box are for all BSRN sites (Globally), those located 60-degree poleward, and for those located 60-degree equatorward. The Bias is the difference between the mean ( $\mu$ ) of the respective solar radiation values for SRB and BSRN. RMS is the root mean square difference between the respective SRB and BSRN values. The correlation coefficient between the SRB and BSRN values is given by  $\rho$ , the variance in the SRB values is given by  $\sigma$ , and N is number of SRB:BSRN month pairs for each latitude region.

[\(Return to Content\)](#)

**4.3.3. FLASHFlux Daily Mean SW Solar Insolation (All Sky Conditions);** Scatter plots comparing the FLASHFlux SW solar data to the BSRN observations are shown in Figures 4.3.3.1, and 4.3.3.2 for FLASHFlux versions -2(D, E, G, H), -3(A, B) respectively and the ensemble of versions 2 + 3A in Figure 4.3.3.3.

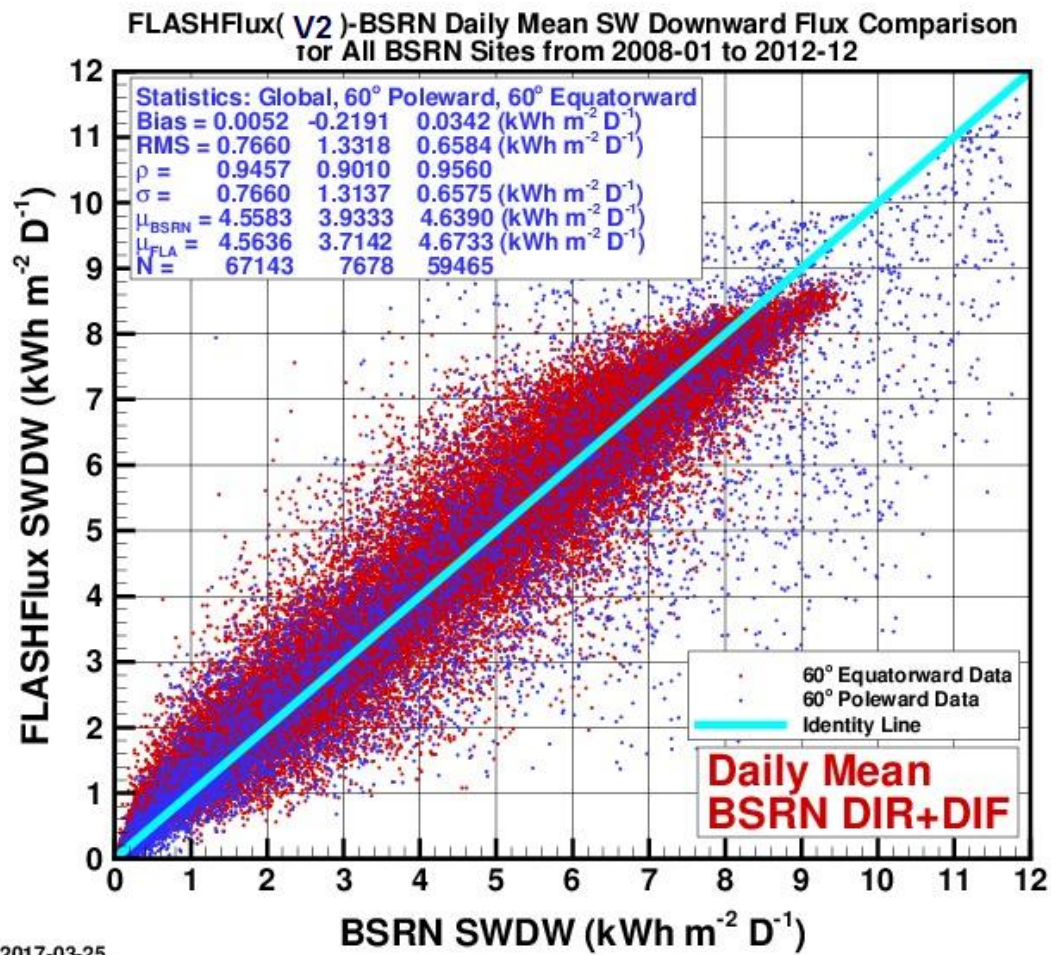


Figure 4.3.3.1. Scatter plot of daily total surface solar shortwave radiation observed at BSRN ground sites over the years January 1, 2008 – December 31, 2012 versus daily values from the FLASHFlux version-2(D, E, G, H). (Note that the solar radiation unit is kWh/day/m<sup>2</sup>; multiplying kWh/day/m<sup>2</sup> by 3.6 yields MJ/day/m<sup>2</sup>, and by 41.67 yields W/m<sup>2</sup>.)

The statistics given in the upper left box are for all BSRN sites (Globally), those located 60-degree poleward, and for those located 60-degree equatorward. The Bias is the difference between the mean ( $\mu$ ) of the respective solar radiation values for FLASHFlux and BSRN. RMS is the root mean square difference between the respective FLASHFlux and BSRN values. The correlation coefficient between the FLASHFlux and BSRN values is given by  $\rho$ , the variance in the FLASHFlux values is given by  $\sigma$ , and N is number of FLASHFlux:BSRN pairs for each latitude region.

[\(Return to Content\)](#)

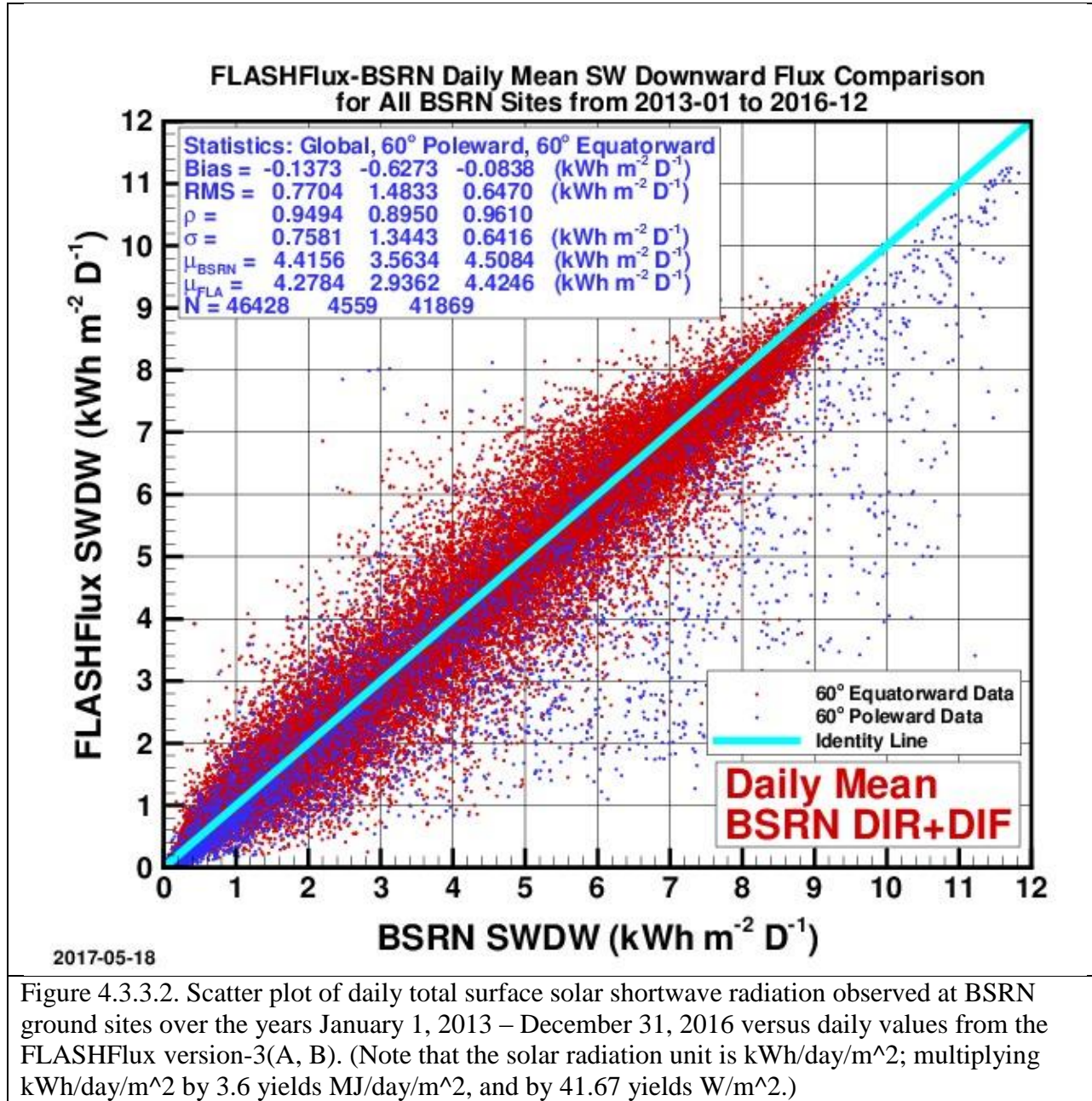


Figure 4.3.3.2. Scatter plot of daily total surface solar shortwave radiation observed at BSRN ground sites over the years January 1, 2013 – December 31, 2016 versus daily values from the FLASHFlux version-3(A, B). (Note that the solar radiation unit is kWh/day/m<sup>2</sup>; multiplying kWh/day/m<sup>2</sup> by 3.6 yields MJ/day/m<sup>2</sup>, and by 41.67 yields W/m<sup>2</sup>.)

[\(Return to Content\)](#)

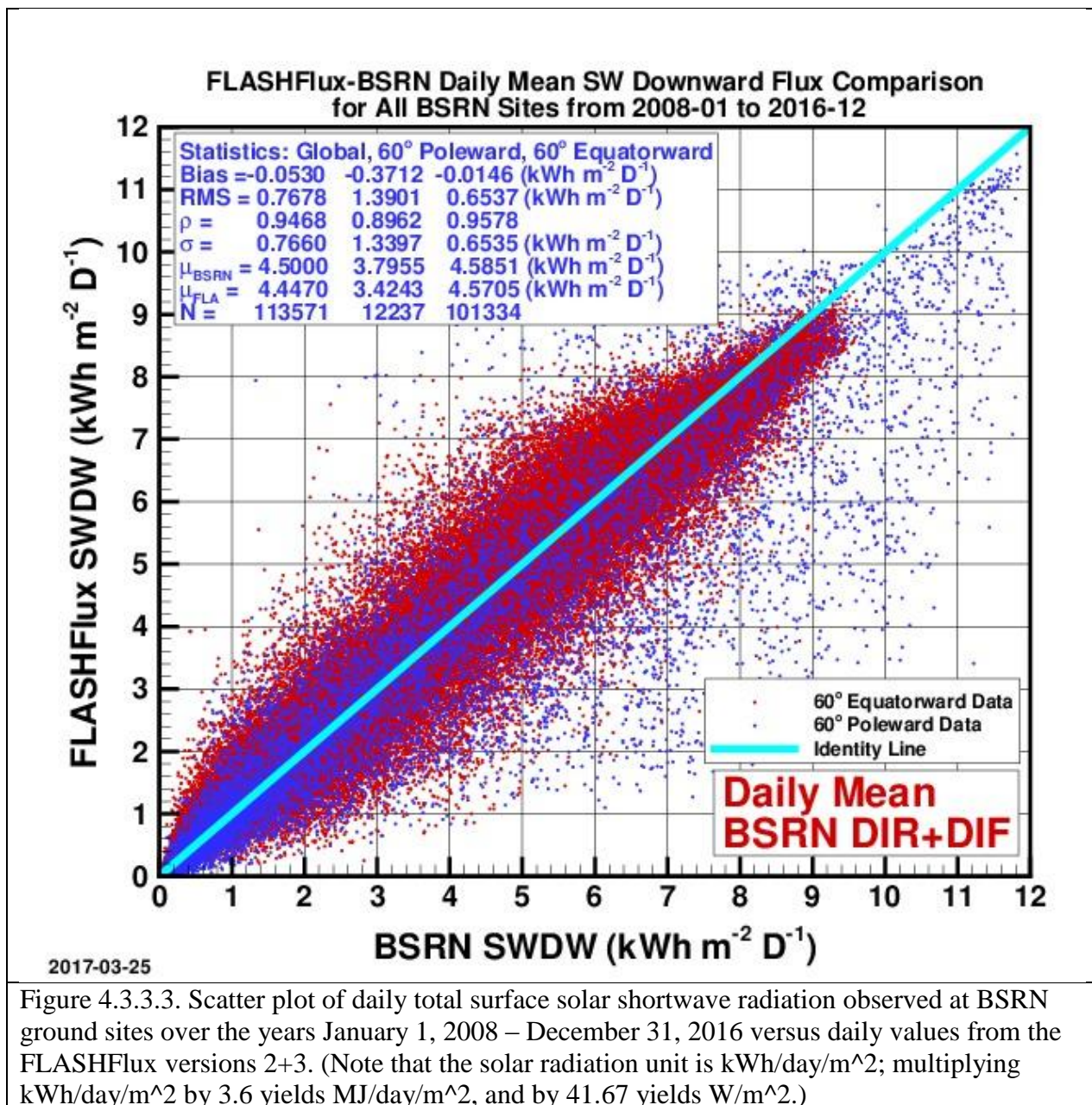


Figure 4.3.3.3. Scatter plot of daily total surface solar shortwave radiation observed at BSRN ground sites over the years January 1, 2008 – December 31, 2016 versus daily values from the FLASHFlux versions 2+3. (Note that the solar radiation unit is kWh/day/m<sup>2</sup>; multiplying kWh/day/m<sup>2</sup> by 3.6 yields MJ/day/m<sup>2</sup>, and by 41.67 yields W/m<sup>2</sup>.)

[\(Return to Content\)](#)

**4.3.4. FLASHFlux Daily Mean LW Radiative Flux (All Sky Conditions):** Scatter plots comparing the FLASHFlux LW solar data to the BSRN observations are shown in Figures 4.3.4.1, and 4.3.4.2 for FLASHFlux versions -2(D, E, G, H) and, versions -3(A, B) respectively and the ensemble of version 2 + 3 in Figure 4.3.4.3. The statistics given in the upper left box are for all BSRN sites (Globally), those located 60-degree poleward, and for those located 60-degree equatorward. The Bias is the difference between the mean ( $\mu$ ) of the respective solar radiation values for FLASHFlux and BSRN. RMS is the root mean square difference between the respective FLASHFlux and BSRN values. The correlation coefficient between the FLASHFlux

and BSRN values is given by  $\rho$ , the variance in the FLASHFlux values is given by  $\sigma$ , and  $N$  is number of FLASHFlux:BSRN pairs for each latitude region.

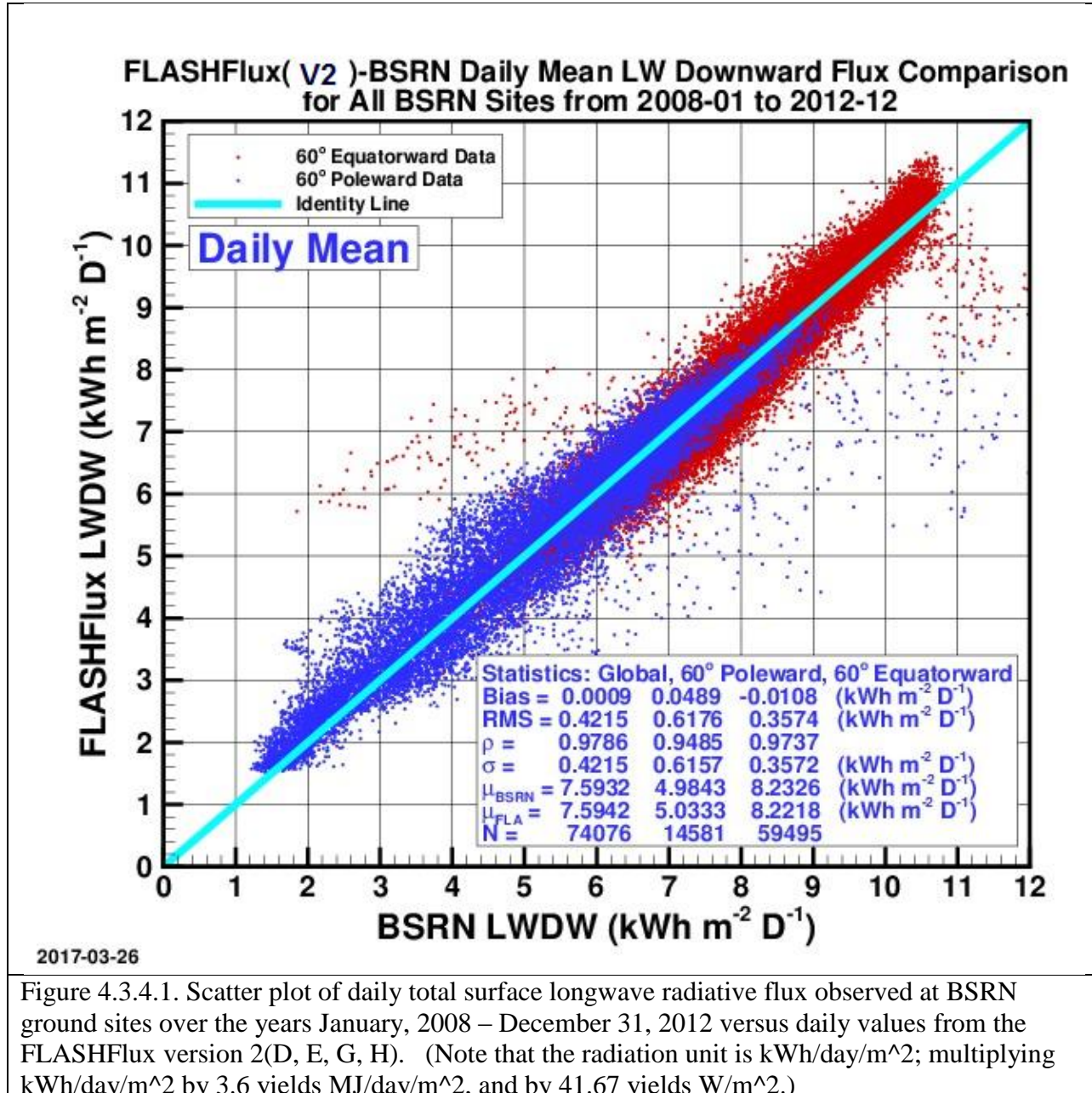
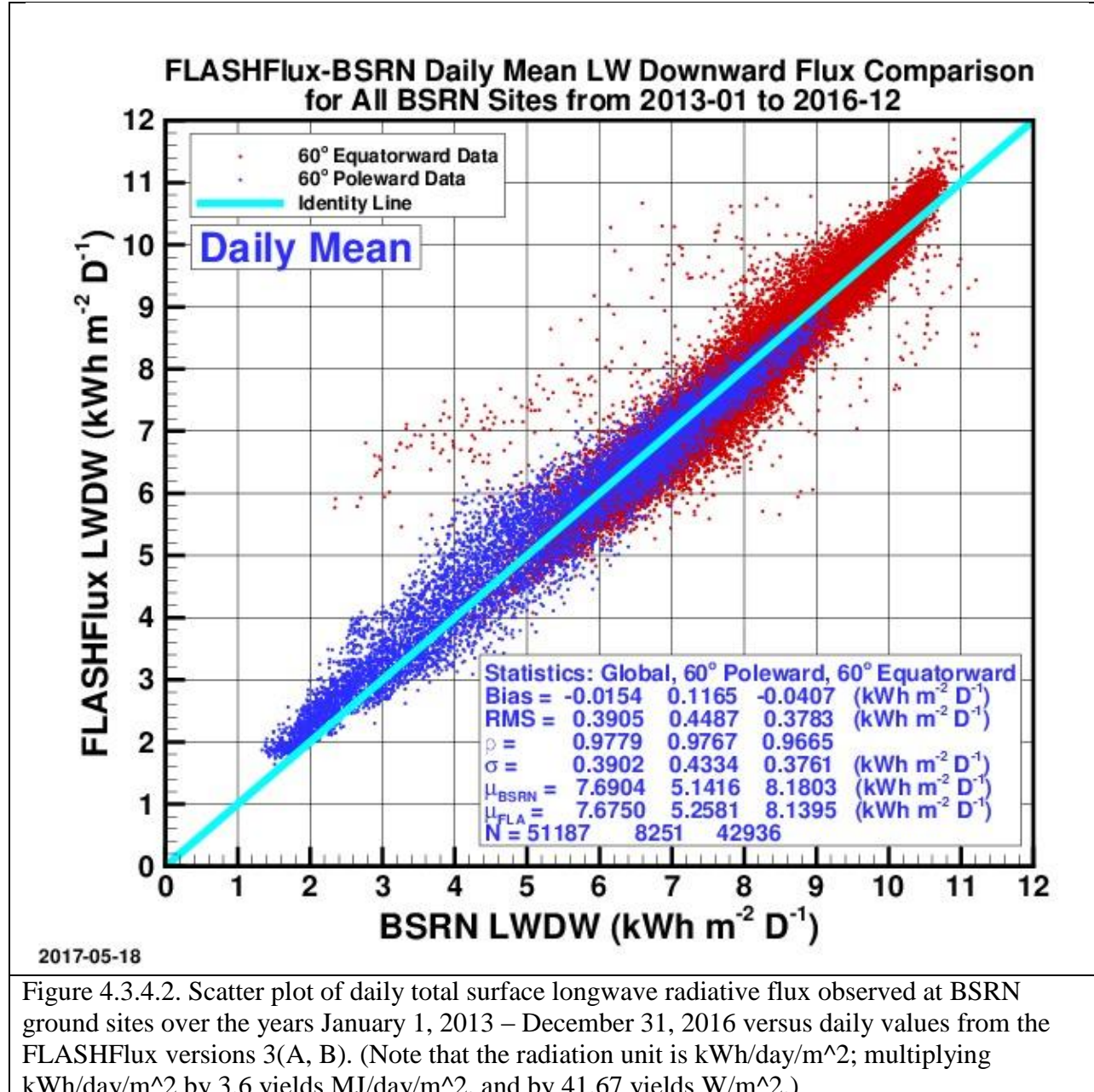
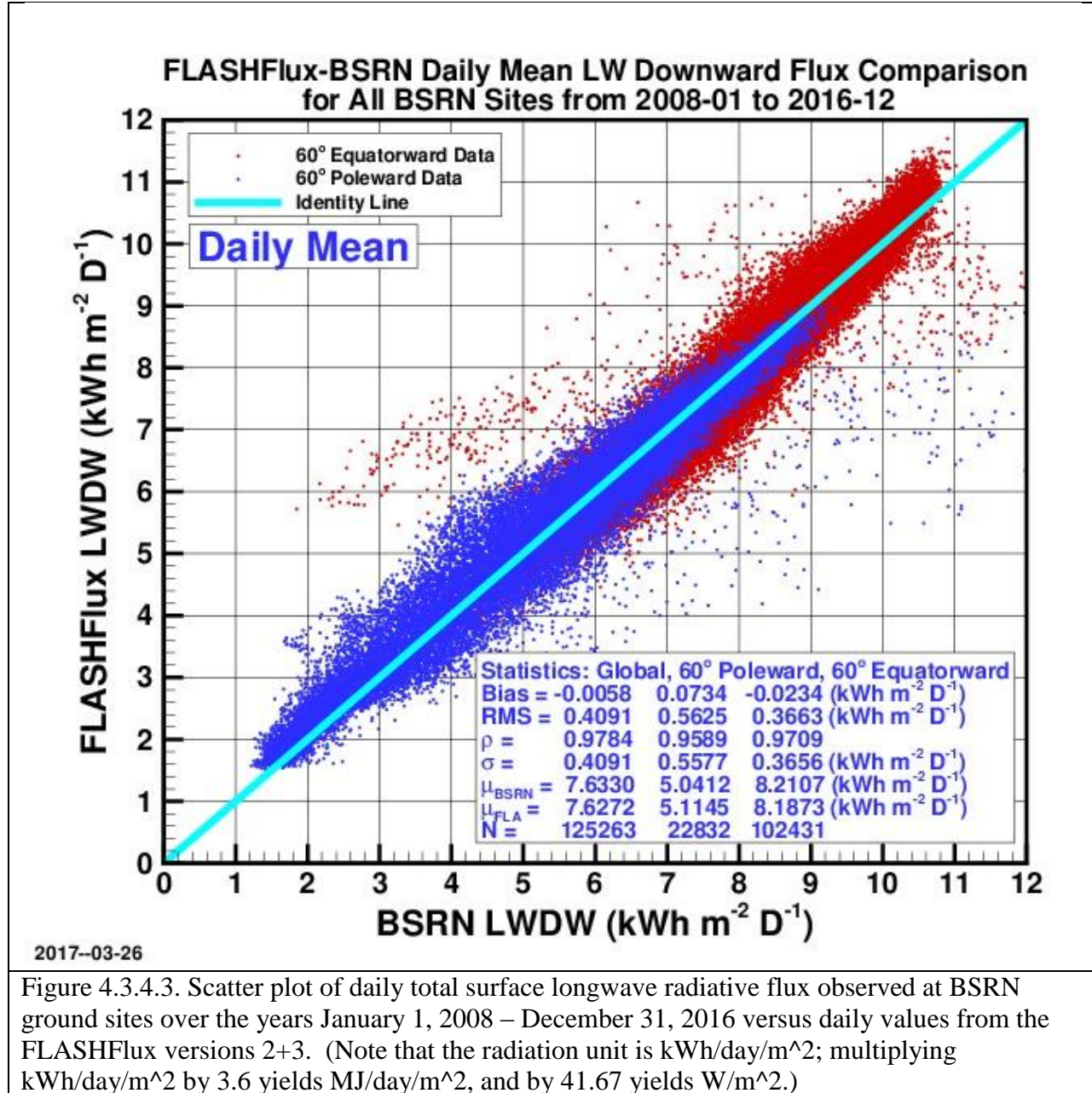


Figure 4.3.4.1. Scatter plot of daily total surface longwave radiative flux observed at BSRN ground sites over the years January, 2008 – December 31, 2012 versus daily values from the FLASHFlux version 2(D, E, G, H). (Note that the radiation unit is kWh/day/m<sup>2</sup>; multiplying kWh/day/m<sup>2</sup> by 3.6 yields MJ/day/m<sup>2</sup>, and by 41.67 yields W/m<sup>2</sup>.)

[\(Return to Content\)](#)



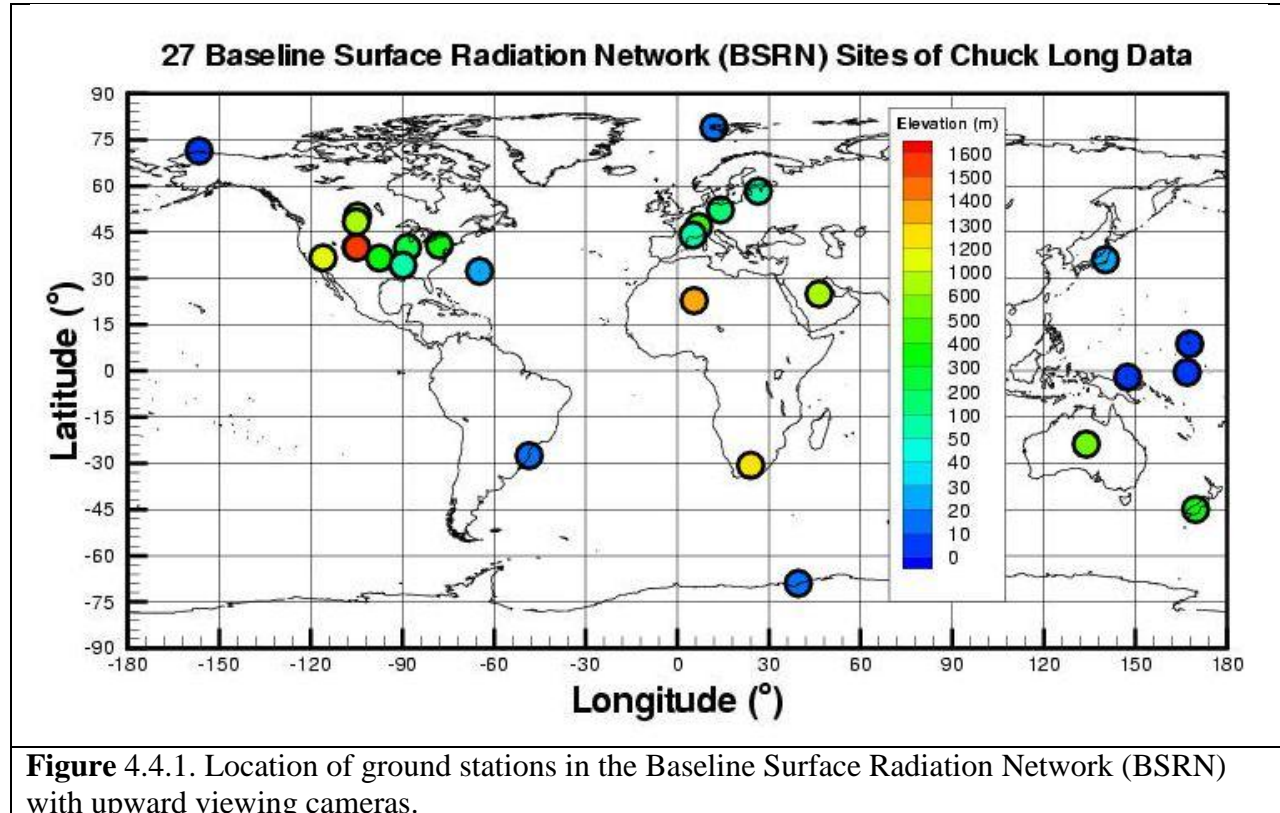
[\(Return to Content\)](#)



[\(Return to Content\)](#)

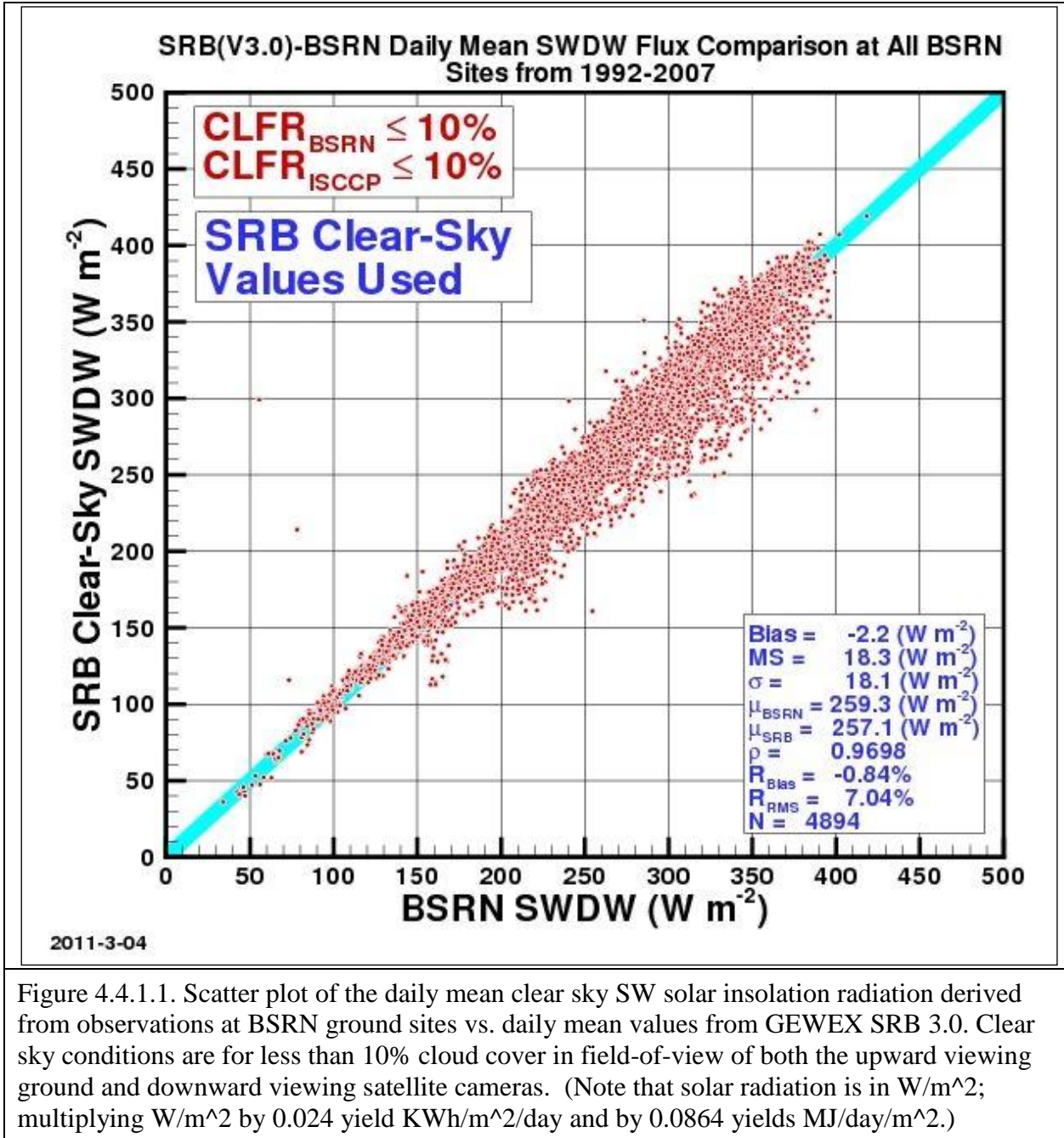
**4.4 Validation of SW Solar Insolation (Clear Sky Conditions):** For these comparisons it was necessary to ensure that the ground observations and the satellite derived solar radiation values are for equivalent clear sky conditions. Fortunately, observational data from a number of BSRN ground sites (see Figure 4.4.1) and the satellite observational data provide information related to cloud cover for each observational period. Cloud parameters from the NASA ISCCP were used to infer the solar radiation in the GEWEX SRB 3.0 archive. Parameters within the ISCCP data provide a measure of the clearness for each satellite observation used in the SRB-inversion algorithms. Similarly, observations from upward viewing cameras at the 27 BSRN sites shown in Figure 4.4.1 provided a measure of cloud cover for each ground observational period. The

clear sky comparison data shown in this section utilized ground cameras and the ISCCP data to match clearness conditions. In particular, the comparison shown below uses clearness criteria defined such that clouds in the field of view of the upward viewing camera and the field of view from the ISCCP satellites must both be less than 10%.



[\(Return to Content\)](#)

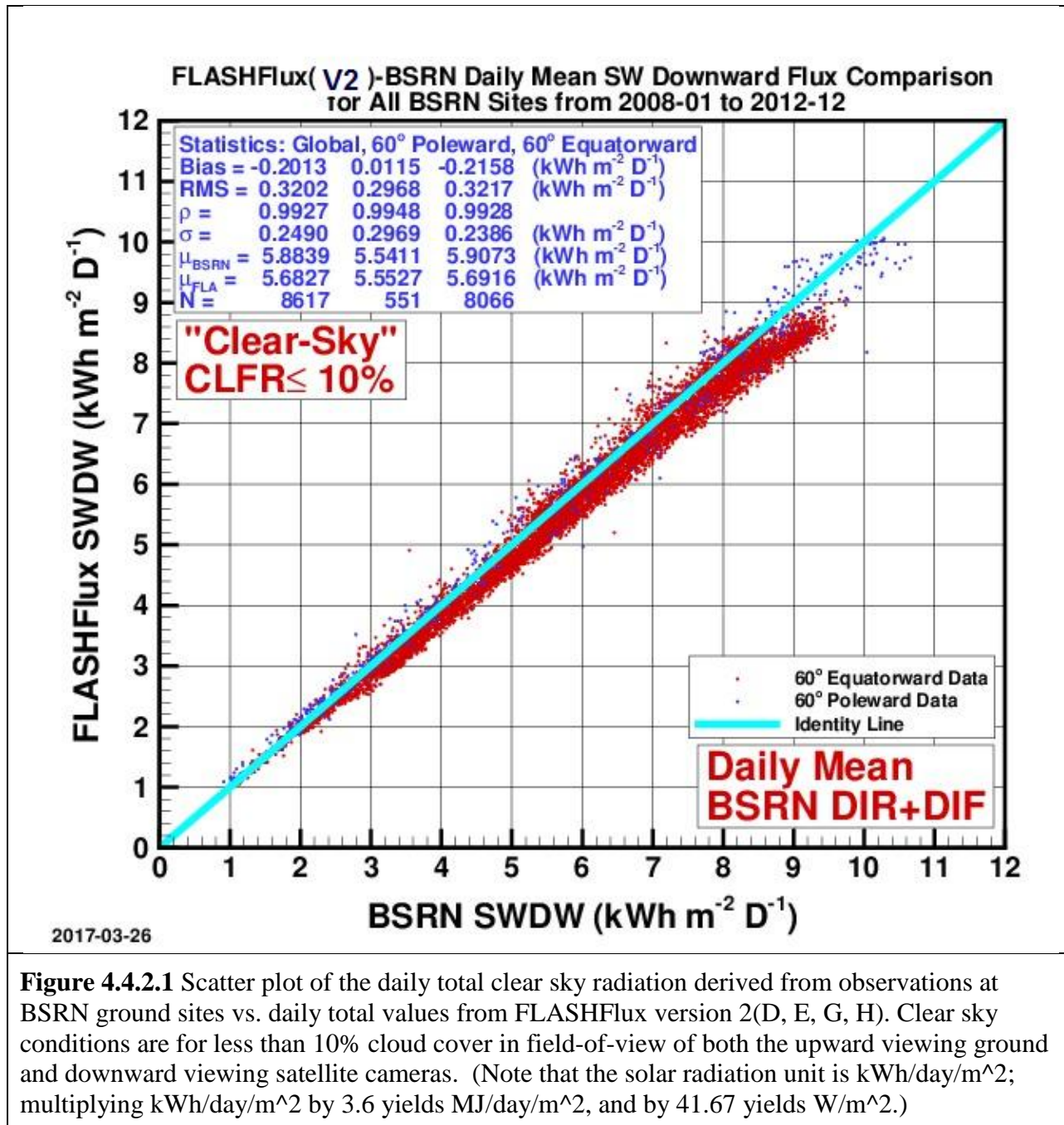
**4.4.1 SRB 3.0 Daily Mean SW Solar Insolation (Clear Sky Conditions):** A scatter plot of the total (i.e. diffuse plus direct) surface insolation observed at the BSRN ground sites versus the corresponding insolation values from the SRB release 3.0 archive is shown in Figure 4.4.1.1 for daily mean SW for clear sky conditions. The comparison covers the time period January 1, 1992, the earliest that data from BSRN is available, through December 31, 2007. The statistics given in the upper left box are for all BSRN sites (Globally), those located 60-degree poleward, and for those located 60-degree equatorward. The Bias is the difference between the mean ( $\mu$ ) of the respective solar radiation values for SRB and BSRN. RMS is the root mean square difference between the respective SRB and BSRN values. The correlation coefficient between the SRB and BSRN values is given by  $\rho$ , the variance in the SRB values is given by  $\sigma^2$ , and N is number of SRB:BSRN month pairs for each latitude region.

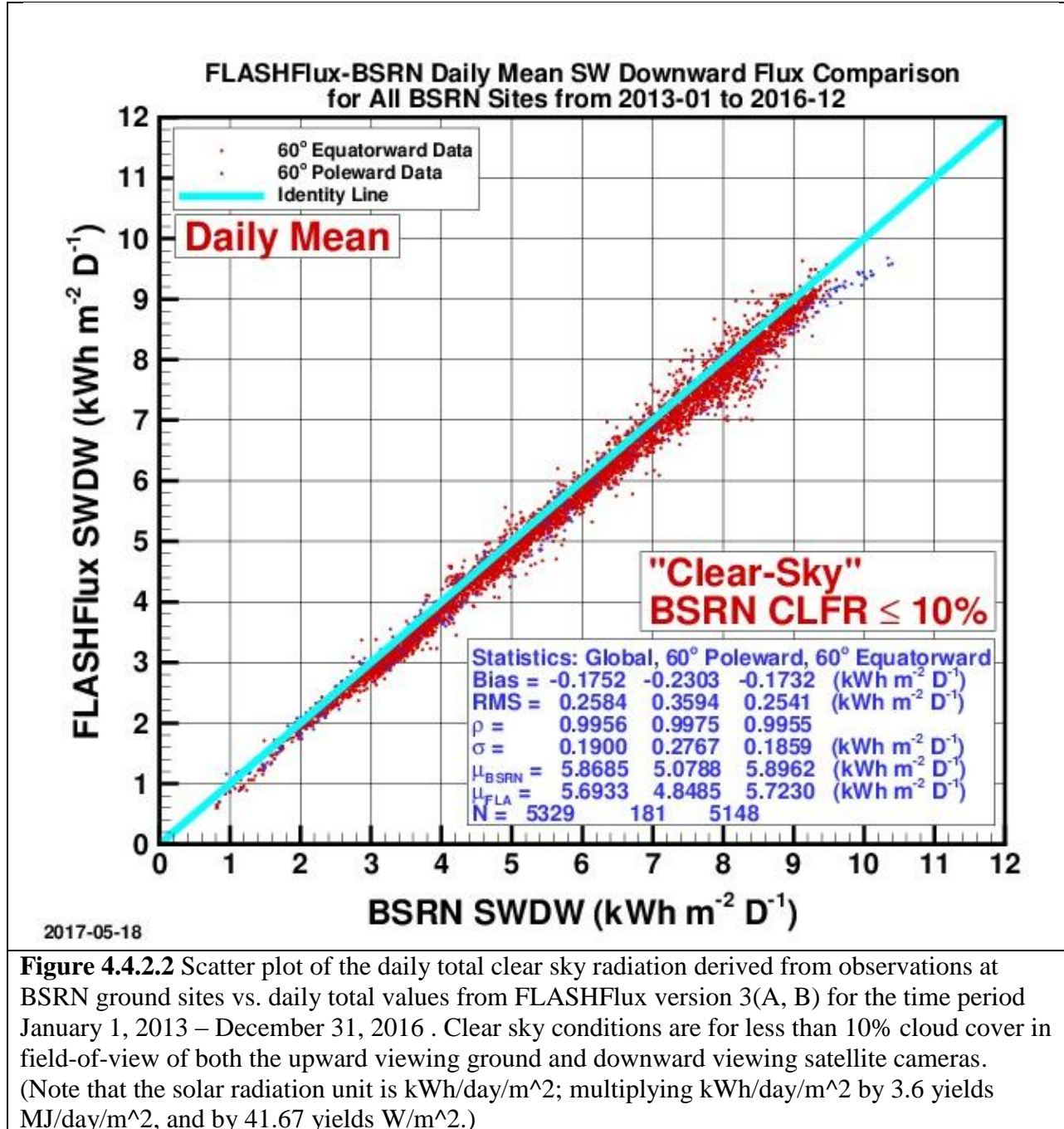


[\(Return to Content\)](#)

**4.4.2 FLASHFLux Daily Mean SW Solar Insolation (Clear Sky Conditions):** Scatter plots comparing the FLASHFlux SW clear sky solar insolation to the BSRN observations are shown in Figures 4.4.2.1, and 4.4.2.2 for FLASHFlux versions -2(D, E, F, G, H), and the ensemble of versions 2 + 3 in Figure 4.4.2.3. The statistics given in the upper left box are for all BSRN sites (Globally), those located 60-degree poleward, and for those located 60-degree equatorward. The Bias is the difference between the mean ( $\mu$ ) of the respective solar radiation values for FLASHFlux and BSRN. RMS is the root mean square difference between the respective

FLASHFlux and BSRN values. The correlation coefficient between the FLASHFlux and BSRN values is given by  $\rho$ , the variance in the FLASHFlux values is given by  $\sigma$ , and N is number of FLASHFlux:BSRN pairs for each latitude region.





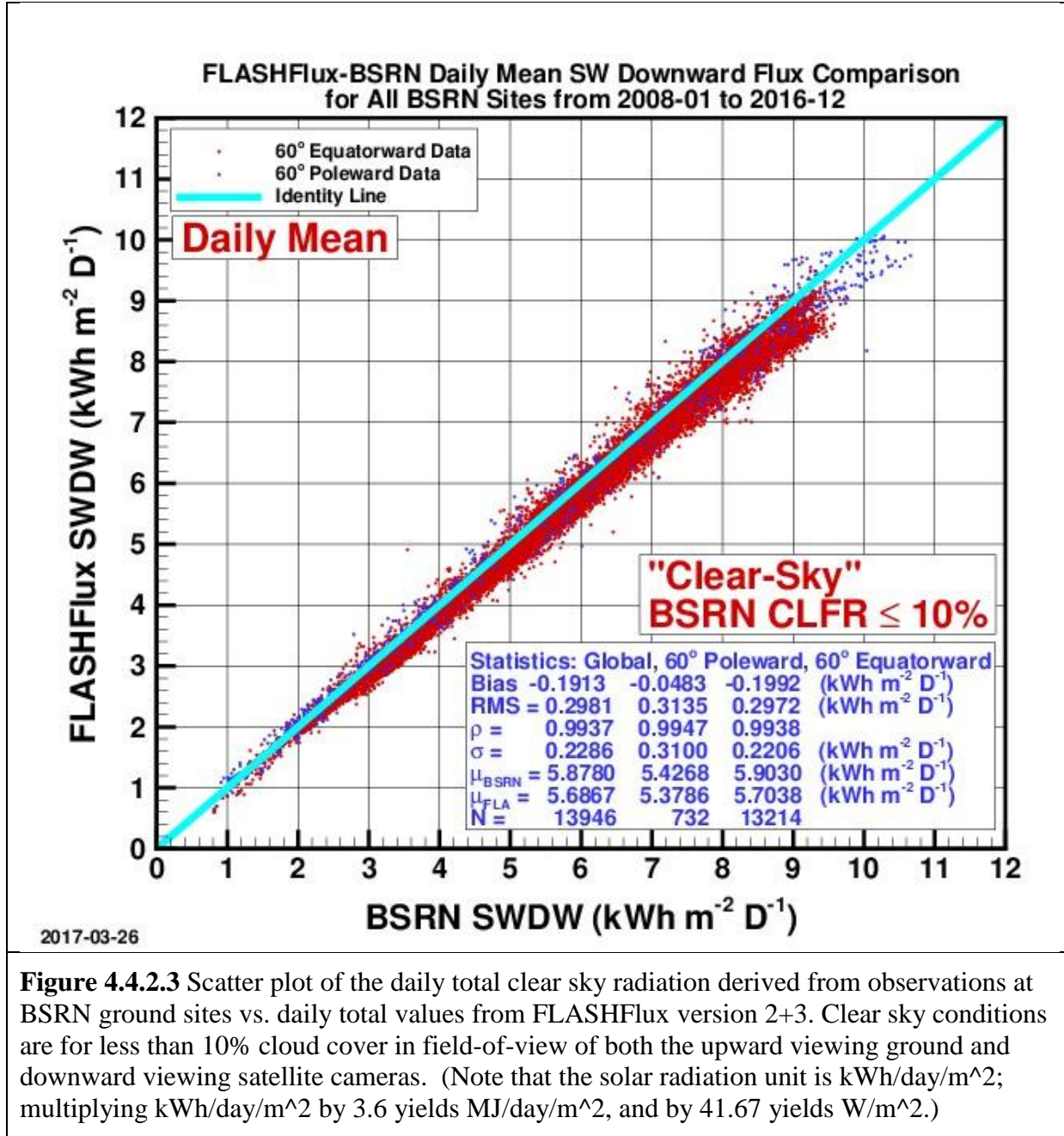


**Figure 4.4.2.3** Scatter plot of the daily total clear sky radiation derived from observations at BSRN ground sites vs. daily total values from FLASHFlux version 2+3. Clear sky conditions are for less than 10% cloud cover in field-of-view of both the upward viewing ground and downward viewing satellite cameras. (Note that the solar radiation unit is kWh/day/m<sup>2</sup>; multiplying kWh/day/m<sup>2</sup> by 3.6 yields MJ/day/m<sup>2</sup>, and by 41.67 yields W/m<sup>2</sup>.)

[\(Return to Content\)](#)

**5.0. Diffuse Horizontal and Direct Normal Irradiance:** The all sky (i.e. including the effect of clouds if present) total global solar radiation from the SRB archive discussed in Section VI is the sum of diffuse and direct radiation on the horizontal surface. However, estimates of all sky diffuse,  $(H^{\text{All}})_{\text{Diff}}$ , and direct normal radiation,  $(H^{\text{All}})_{\text{DNR}}$ , are often needed parameters for the design of hardware such as solar panels, solar concentrator size, day lighting, as well as agricultural and hydrology applications. From an observational perspective,  $(H^{\text{All}})_{\text{Diff}}$  on a horizontal surface is that radiation remaining with  $(H^{\text{All}})_{\text{DNR}}$  from the sun's beam blocked by a shadow band or tracking disk.  $(H^{\text{All}})_{\text{Diff}}$  is typically measured using a sun tracking pyrheliometer

with a shadow band or disk to block the direct radiation from the sun. Similarly, from an observational perspective,  $(H^{All})_{DNR}$  is the amount of the beam radiation impinging on a surface perpendicular to the beam, and is typically measured using a pyrheliometer tracking the sun throughout the day.

[\(Return to Content\)](#)

**5.1. SSE Method:** Measurements of  $(H^{All})_{Diff}$  and  $(H^{All})_{DNR}$  are difficult to make and consequently are generally only available at high quality observational sites such as those in the BSRN network. In order to use the global estimates of the total surface solar radiation,  $H^{All}$ , from SRB Release 3.0 to provide estimates of  $(H^{All})_{Diff}$  and  $(H^{All})_{DNR}$ , a set of polynomial equations have been developed relating the ratio of  $[(H^{All})_{Diff}]/[H^{All}]$  to the clearness index  $KT = [H^{All}]/[H^{TOA}]$  using ground based observations from the BSRN network. These relationships were developed by employing observations from the BSRN network to extend the methods employed by RETScreen (RETScreen, 2005) to estimate  $(H^{All})_{DNR}$ .

In this section we outline the techniques for estimating the  $[(H^{All})_{Diff}]$  and  $[(H^{All})_{DNR}]$  from the solar insolation values available in SRB Release 3.0. In the following section results of comparative studies with ground site observations are presented, which serve to validate the resulting  $[(H^{All})_{Diff}]$  and  $[(H^{All})_{DNR}]$  and provide a measure of the overall accuracy of our global results.

**All Sky Monthly Averaged Diffuse Radiation  $[(H^{All})_{Diff}]$  on a Horizontal Surface:** As just noted, measurements of  $(H^{All})_{Diff}$ ,  $(H^{All})_{DNR}$ , and  $H^{All}$  are made at the ground stations in the BSRN network. These observational data were used to develop the set of polynomial equations given below relating the ratio  $[(H^{All})_{Diff}]/[H^{All}]$  to the clearness index  $KT = [H^{All}]/[H^{TOA}]$ . We note that the top of atmosphere solar radiation,  $H^{TOA}$ , is known from satellite observations.

**For latitude,  $\phi$ , between 45°S and 45°N:**

$$\begin{aligned} [(H^{All})_{Diff}]/[H^{All}] &= \\ &0.96268 - (1.45200 * KT) + (0.27365 * KT^2) + (0.04279 * KT^3) + (0.000246 * SSHA) + \\ &(0.001189 * NHSA) \end{aligned}$$

**For latitude,  $\phi$ , between 90°S and 45°S and between 45°N and 90°N:**

If  $0^\circ \leq SSHA \leq 81.4^\circ$ :

$$\begin{aligned} [(H^{All})_{Diff}]/[H^{All}] &= 1.441 - (3.6839 * KT) + (6.4927 * KT^2) - (4.147 * KT^3) + (0.0008 * SSHA) - \\ &(0.008175 * NHSA) \end{aligned}$$

If  $81.4^\circ < SSHA \leq 100^\circ$ :

$$\begin{aligned} [(H^{All})_{Diff}]/[H^{All}] &= 1.6821 - (2.5866 * KT) + (2.373 * KT^2) - (0.5294 * KT^3) - (0.00277 * SSHA) - \\ &(0.004233 * NHSA) \end{aligned}$$

If  $100^\circ < SSHA \leq 125^\circ$ :

$$\begin{aligned} [(H^{All})_{Diff}]/[H^{All}] &= 0.3498 + (3.8035 * KT) - (11.765 * KT^2) + (9.1748 * KT^3) + (0.001575 * SSHA) - \\ &(0.002837 * NHSA) \end{aligned}$$

If  $125^\circ < \text{SSHA} \leq 150^\circ$ :

$$\frac{[(H^{\text{All}})_{\text{Diff}}]}{[H^{\text{All}}]} = 1.6586 - (4.412 * \text{KT}) + (5.8 * \text{KT}^2) - (3.1223 * \text{KT}^3) + (0.000144 * \text{SSHA}) - (0.000829 * \text{NHSA})$$

If  $150^\circ < \text{SSHA} \leq 180^\circ$ :

$$\frac{[(H^{\text{All}})_{\text{Diff}}]}{[H^{\text{All}}]} = 0.6563 - (2.893 * \text{KT}) + (4.594 * \text{KT}^2) - (3.23 * \text{KT}^3) + (0.004 * \text{SSHA}) - (0.0023 * \text{NHSA})$$

where:

$$\text{KT} = [H^{\text{All}}]/[H^{\text{TOA}}];$$

$\text{SSHA}$  = sunset hour angle in degrees on the “monthly average day” (Klein 1977);

$\text{NHSA}$  = noon solar angle from the horizon in degrees on the “monthly average day”.

The above set of polynomial equations relate the ratio of monthly averaged horizontal diffuse radiation for all sky conditions to the monthly averaged total solar radiation for all sky conditions  $\{ [(H^{\text{All}})_{\text{Diff}}]/[H^{\text{All}}] \}$  to the clearness index  $\text{KT} = [H^{\text{All}}]/[H^{\text{TOA}}]$ .

#### **All Sky Monthly Averaged Direct Normal Radiation:**

$$[(H^{\text{All}})_{\text{DNR}}] = ([H^{\text{All}}] - [(H^{\text{All}})_{\text{Diff}}]) / \text{COS}(\text{THMT})$$

where:

$\text{THMT}$  is the solar zenith angle at the mid-time between sunrise and solar noon for the “monthly average day” (Klein 1977; also see Table VI.1 below).

$$\text{COS}(\text{THMT}) = f + g [(g - f)/2g]^{1/2}$$

$H^{\text{All}}$  = Total of direct beam solar radiation and diffuse atmospheric radiation falling on a horizontal surface at the earth's surface

$(H^{\text{All}})_{\text{Diff}}$  = diffuse atmospheric radiation falling on a horizontal surface at the earth's surface

$$f = \sin(\phi) \sin(\delta)$$

$$g = \cos(\phi) \cos(\delta)$$

where:

$\phi$  is the latitude in radians;

$\delta$  is the solar declination in radians.

If  $\text{SSHA} = 180^\circ$ , then  $\text{COS}(\text{THMT}) = f$ .

[\(Return to Content\)](#)

**5.2 Validation:** : Figures V-1 and V-2 show respectively scatter plots for the monthly mean diffuse and monthly mean direct normal radiation for all sky conditions computed from measured values at the BSRN sites (designated as BSRN SWDF and BSRN SWDN) versus the corresponding SSE values (designated as SRB SWDF and SRB SWDN) derived from the expression discussed above. Figures V-3 and V-4 show similar scatter plots for clear sky conditions.

Correlation and accuracy parameters are given in the legend boxes. Note that for the all sky condition the correlation and accuracy parameters are given for all sites (i.e. Global), for the BSRN sites regions above 60° latitude, north and south, (i.e. 60° poleward) and for BSRN sites below 60° latitude, north and south (60° equatorward).

### 5.2.1. Monthly Mean Diffuse (All Sky Conditions)

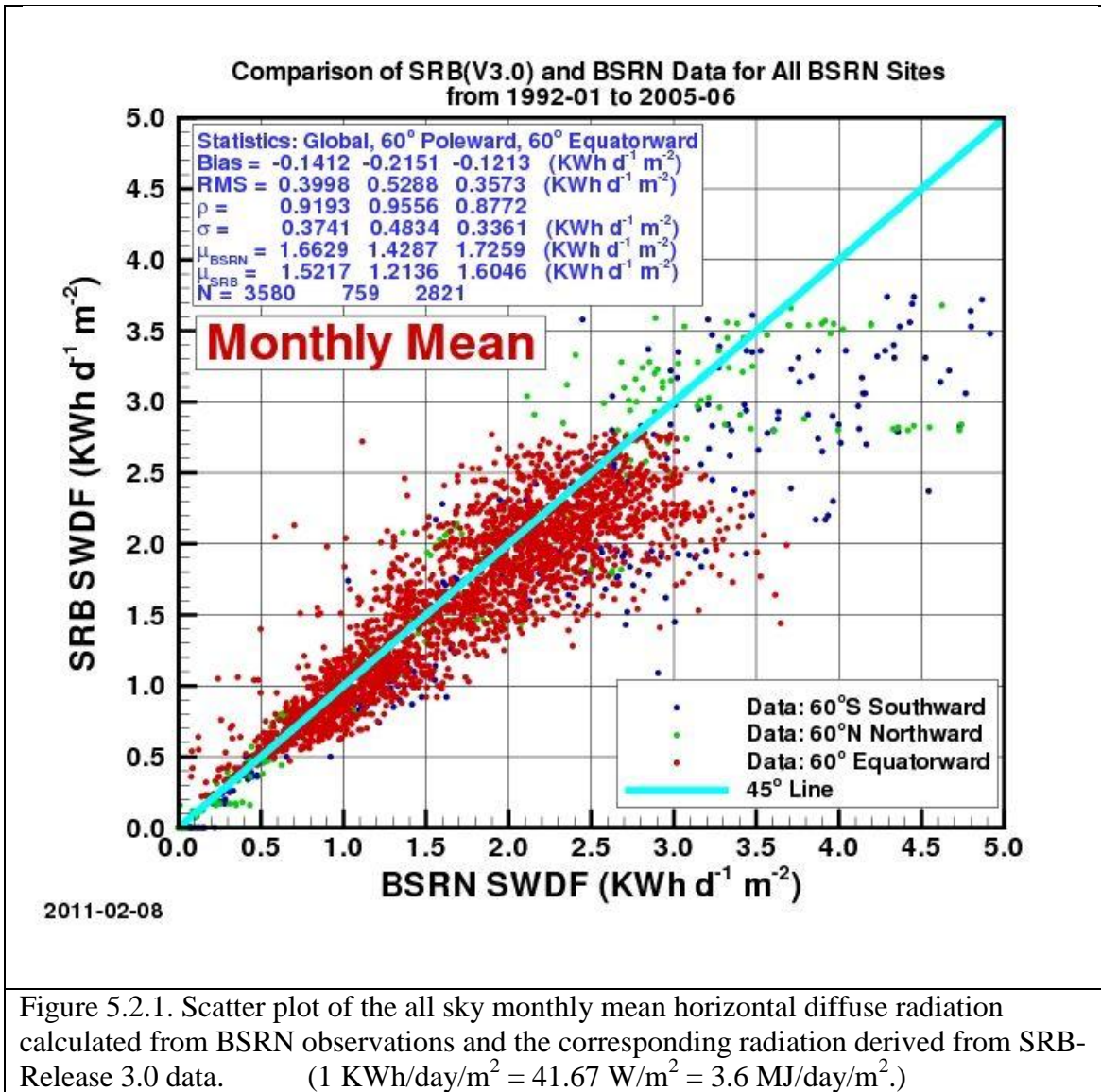


Figure 5.2.1. Scatter plot of the all sky monthly mean horizontal diffuse radiation calculated from BSRN observations and the corresponding radiation derived from SRB-Release 3.0 data. (1 KWh/day/m<sup>2</sup> = 41.67 W/m<sup>2</sup> = 3.6 MJ/day/m<sup>2</sup>.)

However, because of the scarcity of clear sky values only the global region is used for the statistics in Figures V-3 and V-4. The Bias is the difference between the mean ( $\mu$ ) of the respective solar radiation values for SRB and BSRN. RMS is the root mean square difference between the respective SRB and BSRN values. The correlation coefficient between the SRB and BSRN values is given by  $\rho$ , the variance in the SRB-BSRN difference is given by  $\sigma$ , and N is the number of SRB-BSRN comparable pairs for each latitudinal region.

[\(Return to Content\)](#)

### 5.2.2. Monthly Mean Direct Normal (All Sly Conditions)

Figure 5.2.2.1 compares the monthly averaged direct normal radiation for all sky conditions computed from BSRN ground observations (designated as BSRN SWDN) to monthly averaged ( $H^{All}_{DNR}$ ) calculated from SRB-R 3.0 (designated as SRB SWDN in Figure V-2) using the expressions discussed above.

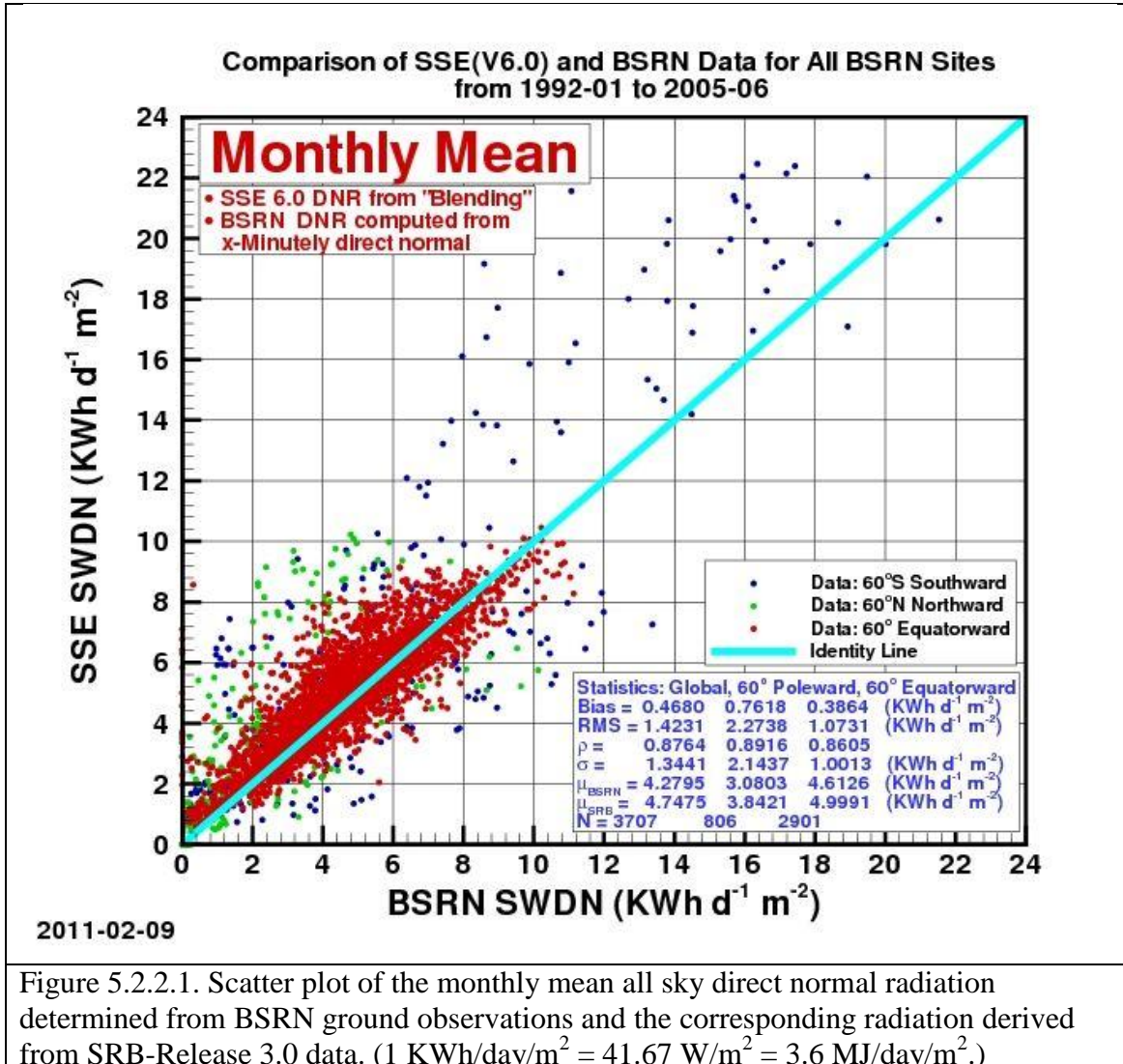


Figure 5.2.2.1. Scatter plot of the monthly mean all sky direct normal radiation determined from BSRN ground observations and the corresponding radiation derived from SRB-Release 3.0 data. (1 KWh/day/m<sup>2</sup> = 41.67 W/m<sup>2</sup> = 3.6 MJ/day/m<sup>2</sup>.)

[\(Return to Content\)](#)

### 5.2.3. Monthly Mean Diffuse (Clear Sky Conditions)

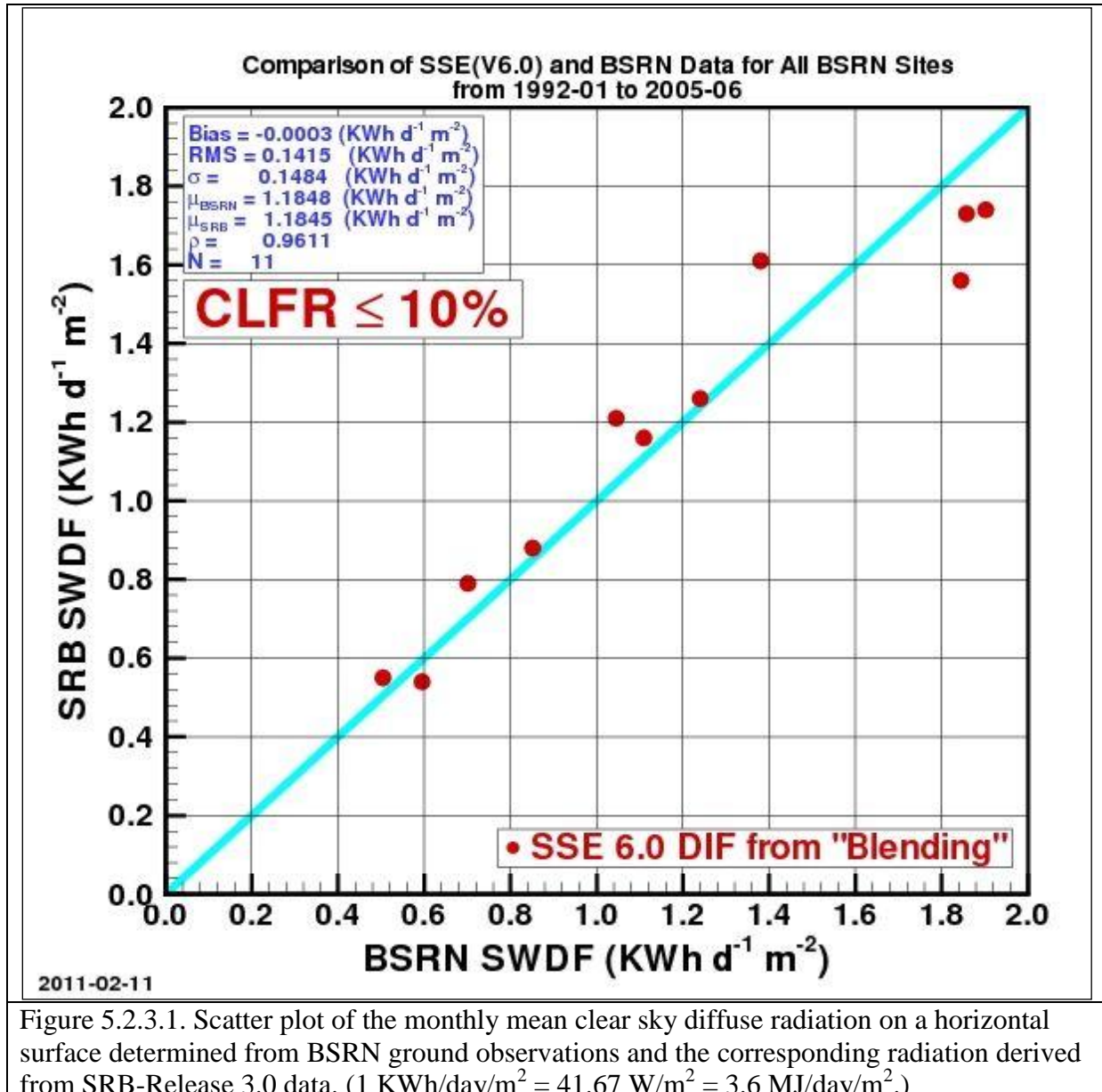
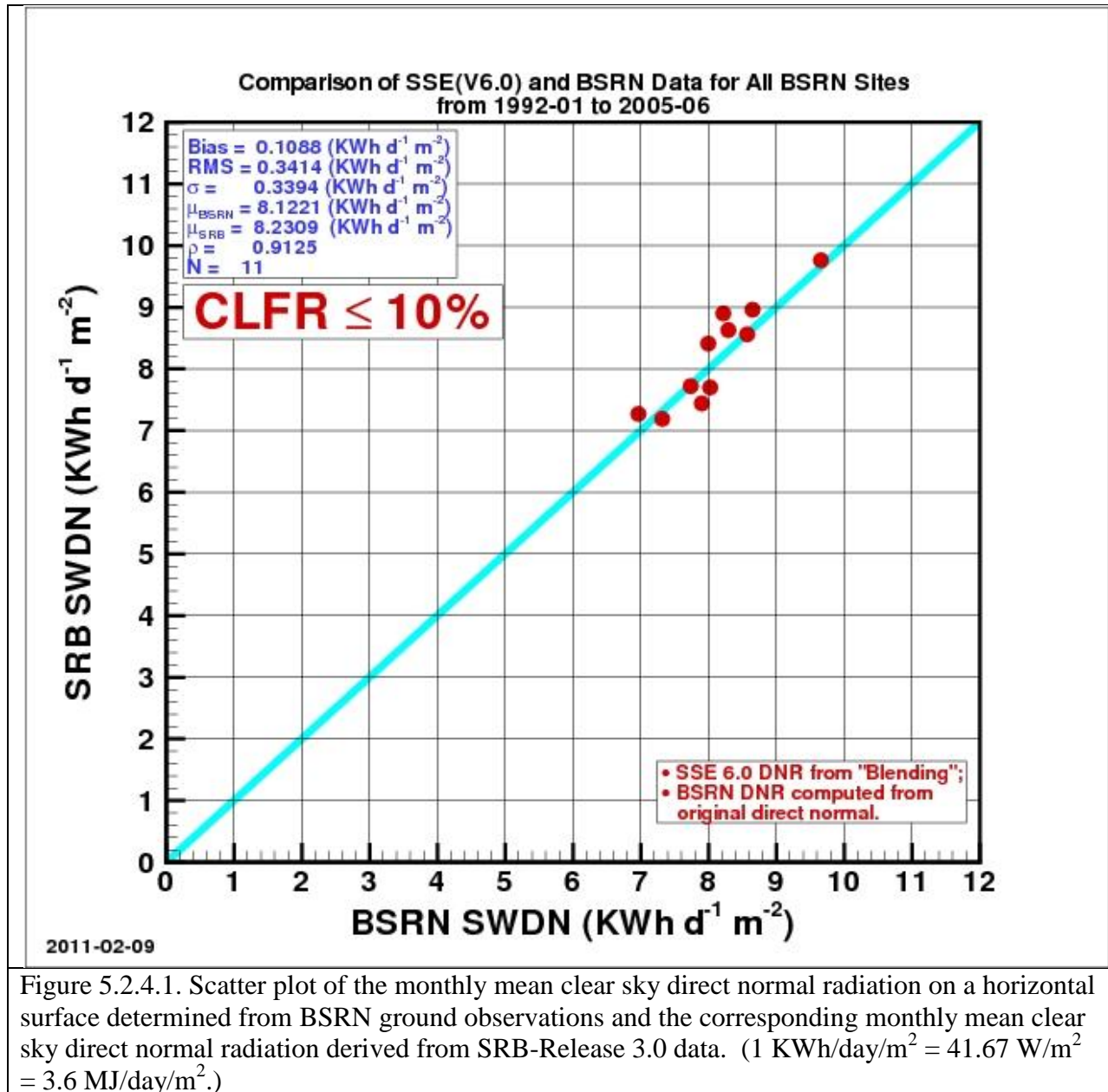


Figure 5.2.3.1. Scatter plot of the monthly mean clear sky diffuse radiation on a horizontal surface determined from BSRN ground observations and the corresponding radiation derived from SRB-Release 3.0 data. (1 KWh/day/m<sup>2</sup> = 41.67 W/m<sup>2</sup> = 3.6 MJ/day/m<sup>2</sup>.)

#### 5.2.4. Monthly Mean Direct Normal (Clear Sky Conditions)



[\(Return to Content\)](#)

## 6.0 Irradiance on a Tilted Surface

The calculation of the Irradiance impinging on a tilted surface in SSE Release 6.0 basically follows the method employed by RETScreen (RETScreen 2005). The major difference is that the diffuse radiation is derived from the equations described in Section 5.

[\(Return to Content\)](#)

**6.1. Overview of RETScreen Method:** In this section we briefly outline the RETScreen method. The RETScreen method uses the “monthly average day” hourly calculation procedures where the equations developed by Collares-Pereira and Rabl (1979) and Liu and Jordan (1960) are used respectively for the “monthly average day” hourly Irradiance and the “monthly average day” hourly diffuse radiation.

**Hourly Total and Diffuse Irradiance on a Horizontal Surface:** We first describe the method of estimating the hourly horizontal surface Irradiance ( $H_h$ ) and horizontal diffuse ( $H_{dh}$ ) for daylight hours between 30 minutes after sunrise to 30 minutes before sunset during the “monthly average day”. The “monthly average day” is the day in the month whose solar declination is closest to the average declination for that month (Klein 1977). Table 6.1.1 lists the date and average declination,  $\delta$ , for each month.

**Table 6.1.1. List of the day in the month whose solar declination,  $\delta$ , is closest to the average declination for that month**

Month	Date in month	$\delta$ (°)	Month	Date in month	$\delta$ (°)
January	17	-20.9	July	17	21.2
February	16	-13.0	August	16	13.5
March	16	-2.4	September	15	2.2
April	15	9.4	October	15	-9.6
May	15	18.8	November	14	-18.9
June	11	23.1	December	10	-23.0

$$H_h = r_t H$$

$$H_{dh} = r_d H_d$$

where:

$H$  is the monthly average Irradiance on a horizontal surface from the SRB 3.0 data set;

$H_d$  is the monthly average diffuse radiation on a horizontal surface from the method described in section 6;

$$r_t = (\pi/24)*(A + B*\cos\omega)*[(\cos\omega - \cos\omega_s)/(\sin\omega_s - \omega_s \cos\omega_s)]$$

(Collares-Pereira and Rabl; 1979)

$$r_d = (\pi/24)*[(\cos\omega - \cos\omega_s)/(\sin\omega_s - \omega_s \cos\omega_s)] \text{ (Liu and Jordan; 1960)}$$

where:

$$A = 0.409 + 0.5016 \sin[\omega_s - (\pi/3)]$$

$$B = 0.6609 - 0.4767 \sin[\omega_s - (\pi/3)]$$

where:

$\omega$  = solar hour angle for each daylight hour relative to solar noon between sunrise plus 30 minutes and sunset minus 30 minutes. The sun is displaced  $15^\circ$  from the local meridian for each hour from local solar noon;

$\omega_s$  = sunset hour angle;

$$\omega_s = \cos^{-1}[-\tan(\xi) * \tan(\phi)], \text{ (negative before solar noon)}$$

where:

$\phi$  = Latitude

$$\delta = 23.45 * \sin[6.303 * \{(284 + n)/365\}] = \text{declination angle}$$

n = day of year, 1 = January 1

**Hourly total radiation on a tilted surface:** Next, we describe the method of estimating hourly total radiation on a tilted surface ( $H_{th}$ ) as outlined in the RETScreen tilted surface method. The equation, in general terms, is:

$$H_{th} = \text{solar beam component} + \text{sky diffuse component} + \text{surface reflectance component}$$

The solution is as follows:

$$\cos\theta_{zh} = \cos\phi \cos\delta \cos\omega + \sin\phi \sin\delta$$

$$\cos\theta_h = \cos\theta_{zh} \cos\beta_h + (\sin\theta_{zh}) (\sin\beta_h) (\cos(\gamma_{sh} - \gamma_h))$$

where:

$\beta_h$  = hourly slope of the PV array relative to horizontal surface.  $\beta_h$  is constant for fixed panels or panels in a vertical-axis tracking system.  $\beta_h = \theta_z$  for panels in a two-axis tracking system. Values for other types of tracking systems are given in Braun and Mitchell (1983).

$$\gamma_{sh} = \sin^{-1}[(\sin\omega \cos(\text{solar declination})) / \sin\theta_{zh}]$$

= hourly solar azimuth angle; angle between the line of sight of the Sun into the horizontal surface and the local meridian. Azimuth is zero facing the equator, positive west, and negative east.

$\gamma_h$  = hourly surface azimuth of the tilted surface; angle between the projection of the normal to the surface into the horizontal surface and the local meridian. Azimuth is zero facing the equator, positive west, and negative east.  $\gamma_h$  is constant for fixed surfaces.  $\gamma_h = \gamma_{sh}$  for both vertical- and two-axis tracking systems. See Braun and Mitchell (1983) for other types of tracking systems.

$\theta_{zh}$  = the solar zenith angle relative to the horizontal

$\theta_h$  = solar zenith angle relative to the normal of the tilted solar panel

$$H_{th} = (H_h - H_{dh})(\cos\theta_h/\cos\theta_{zh}) + H_{dh}[(1+\cos\beta_h)/2] + H_h * \rho_s[(1-\cos\beta_h)/2]$$

where:

$\rho_s$  = surface reflectance or albedo is assumed to be 0.2 if temperature is above 0°C or 0.7 if temperature is below -5°C. Linear interpolation is used for temperatures between these values.

Finally, the monthly average tilted surface Irradiance ( $H_t$ ) is estimated by summing hourly values of  $H_{th}$  over the “monthly average day”. It was recognized that such a procedure would be less accurate than using quality “day-by-day” site measurements, but RETScreen validation studies indicate that the “monthly average day” hourly calculation procedures give tilted surface results ranging within 3.9% to 8.9% of “day-by-day” hourly methods.

[\(Return to Content\)](#)

**6.2.0 Old SSE Monthly Tilted Solar Irradiances Tables:** The old SSE data archive provides multi-year averaged monthly and annual values of solar Irradiance incident on a tilted surface for a user specified latitude and longitude. The irradiance incident on an equator facing panel is provided for a horizontal panel (tilt angle = 0°), and at angles equal to the latitude, and latitude ± 15 ° along with the optimum tilt angle for the given latitude/longitude. It should be emphasized that the optimum tilt angle of a solar panel at a given latitude and longitude is not simply based on solar geometry and the site latitude. The solar geometry relative to the Sun slowly changes over the period of a month because of the tilted axis of the Earth. There is also a small change in the distance from the Sun to Earth over the month because of the elliptical Earth orbit around the Sun. The distance variation may cause a change in the trend of the weather at the latitude/longitude location of the tilted solar panel. The weather trend over the month may be toward either clearer or more cloudy skies over that month for that particular year. Either cloudy-diffuse or clear-sky direct normal radiation may vary from year to year. As a result, the SSE project makes hourly calculations of tilted solar panel performance for a monthly-average day for all 1-degree cells over the globe for a 22-year period. Both the tilt angles and Irradiance values provided should be considered as average values over that 22-year period.

**6.2.1. Update to The SSE Tilted Solar Irradiances.** The solar irradiances incident on equatorial facing tilted surfaces are currently available (as of 11/7/2018) through the POWER DAV and API services. This new service provides updated irradiance values corresponding to the tilted solar data originally provided through the old SSE data archive. For example, the new service provides climatologically averaged monthly values of the average, maximum, and minimum solar irradiance incident on a horizontal surface, a surface tilted at an angle equal to the latitude of the requested site, and a surface tilted at an angle equal to the user requested

latitude  $\pm$  15-deg. The new POWER data has been updated through the use of satellite-estimated surface albedo. In tropical latitude zones ( $\pm$  23.5 degrees of the equator), the tilted equatorially facing surface is rotated 180 degrees as the sun passes overhead on the selected site. This rotation keeps the orientation of the surface facing the sun. Users of this new offering will note that POWER values are typically within a few percent of the old SSE data for all tilt angles except for a vertical surface in the tropic latitude zones where the difference may be as high as 10% for some months of the year. The Tables included in [Appendix D](#) give the ratio of the old SSE tilted surface values to the new DAV values for a range of latitudes.

Additionally, the monthly optimal tilt angle calculations now include a sign to indicate whether the surface should remain equator facing (+) or reversed for polar facing (-) depending upon the solar geometry and cloudiness. The annual average optimal calculations in these tropical regions now provide an estimate of whether the surface should face equatorward or poleward through this sign convention. We would appreciate your user comments on this approach, especially for computing the optimal tilt for the tropical surfaces ( $\pm$  23.5 degree North or South).

The expressions used for calculating the solar geometry are given in [Appendix C](#).  
[\(Return to Content\)](#)

**6.3. Validation of Monthly Mean Irradiance on a Tilted Surface:** In this section results from three approaches for validation of the SSE monthly mean irradiance on a tilted surface are presented. The first involves comparison of the tilted surface irradiance values from the SSE and RETScreen formulation. The remaining two approaches provide more definitive validation statistics in that the SSE tilted surface Irradiance values are compared to measured tilted surface Irradiance values and to values that were derived from measurements of the diffuse and direct normal components of radiation at BSRN sites.

[\(Return to Content\)](#)

**6.3.1. SSE vs RETScreen.** Table 6.3.1.1 summarizes the agreement between the SSE and RETScreen formulation in terms of the Bias and RMSE between the two methods, and the parameters (i.e. slope, intercept, and  $R^2$ ) characterizing the linear least square fit to the RETScreen values (x-axis) to SSE Release 6.0 values (y-axis) when both the RETScreen and SSE methods have the same horizontal irradiance as inputs. Recall that the major difference between the two methods involves the determination of the diffuse radiation, and note that the results from the two methods are in good agreement.

[\(Return to Content\)](#)

**Table 6.3.1.1**

<b>Location</b>	<b>Lat x Long</b>	<b>Tilt Angle</b>	<b>Titled-Bias</b>	<b>Titled-RMSE</b>	<b>Titled-Slope</b>	<b>Titled-In'cept</b>	<b>Titled-R2</b>
Ottawa Int'l Airport, Ontario, Canada	45.3N x 75.7W	45	0.47	0.56	1.17	-1.19	0.94
Berverlodge, Alberta, CN	55.2N x 119.4W	40	0.30	0.36	1.09	-0.65	0.99
Castlegar AP, British Cl, CN	49.3N x 117.6W	49	0.35	0.45	1.24	-1.43	0.99
Totonto Int'l AP, Ontario, CN	43.7N x 79.6W	43	0.06	0.09	1.02	-0.12	1.00
Burmingham, AL	33.6N x 86.8W	48	0.06	0.07	1.05	-0.29	1.00
Dodge City, KS	37.8N x 100.0W	37	0.04	0.07	1.01	-0.11	0.99
Covington, KY	39.1N x 84.7W	39	0.03	0.05	1.00	-0.03	1.00
San Francisco, CA	37.6N x 122.4W	37	0.03	0.05	1.00	-0.01	1.00
San Jose, Costa Rica	10.0N x 84.2W	25	-0.09	0.24	0.79	1.08	0.93
<hr/>							
Boulogne Sur Seine, France	50.7N x 1.6E	35	0.15	0.18	1.06	-0.36	1.00
Riyadh (Saud-AFB), Saudi Arabia	24.7N x 46.7E	39	0.09	0.11	1.07	-0.51	0.99
Tabuk (Saud-AFB), Saudi Arabia	28.4N x 36.6E	43	0.07	0.09	1.09	-0.59	0.97
Bisha (Civ/Mil), Saudi Arabia	20.0N x 42.6E	35	-0.16	0.45	0.53	2.99	0.26
Beer-Sheva/Teyman, Israel	31.2N x 34.8E	46	0.05	0.09	0.98	0.07	0.99
Jerusalem/Atarot, Israel	31.5N x 35.2E	46	0.10	0.12	0.99	-0.05	0.99
Naha (Civ/JASDF), Japan	26.2N x 127.7E	41	0.07	0.08	1.00	-0.08	1.00
<hr/>							
Brasila, Brasil	15.8S x 47.9W	30	-0.09	0.24	0.83	1.02	0.94
Antofagasta, Chile	23.4S x 70.5W	38	0.08	0.10	1.01	-0.13	1.00
Arica/Chacallute, Chile	18.4S x 70.5W	33	-0.20	0.49	1.14	-0.50	0.90
<hr/>							
Windhoek/Eros (SAAF), Namibia	22.6S x 17.1E	37	-0.05	0.32	0.89	0.74	0.74
Pretoria (Met), S. Africa	25.7S x 28.2E	40	0.06	0.09	1.02	-0.19	0.98
Pietersburg (SAAF), S. Africa	23.9S x 29.5E	38	0.07	0.09	0.99	-0.03	0.98
Johannesburg, S. Africa	26.1S x 28.2E	41	0.04	0.07	1.06	-0.38	0.99
Canberra, Australia	35.3S x 149.2E	35	0.04	0.06	0.99	0.00	1.00
			<b>AVE =</b>	<b>0.06</b>	<b>0.19</b>	<b>1.00</b>	<b>-0.03</b>
			<b>STD =</b>	<b>0.15</b>	<b>0.16</b>	<b>0.14</b>	<b>0.86</b>
							<b>0.15</b>

[\(Return to Content\)](#)

**6.3.2 SSE vs Direct Measurements of Tilted Surface Irradiance.** Figure 6.3.2.1 show the time series of the monthly mean solar irradiance derived from measurements and the corresponding values from SSE. Figure 6.3.2.1a gives the measured and SSE solar irradiance on a horizontal surface and Figure 6.3.2.1b gives the measured and SSE values on a South facing surface tilted at 45°. The measured values were taken from the University of Oregon Solar Radiation Monitoring Laboratory archive (<http://solardat.uoregon.edu/index.html>) for Chaney, WA. For comparison the RETScreen values have also been included.

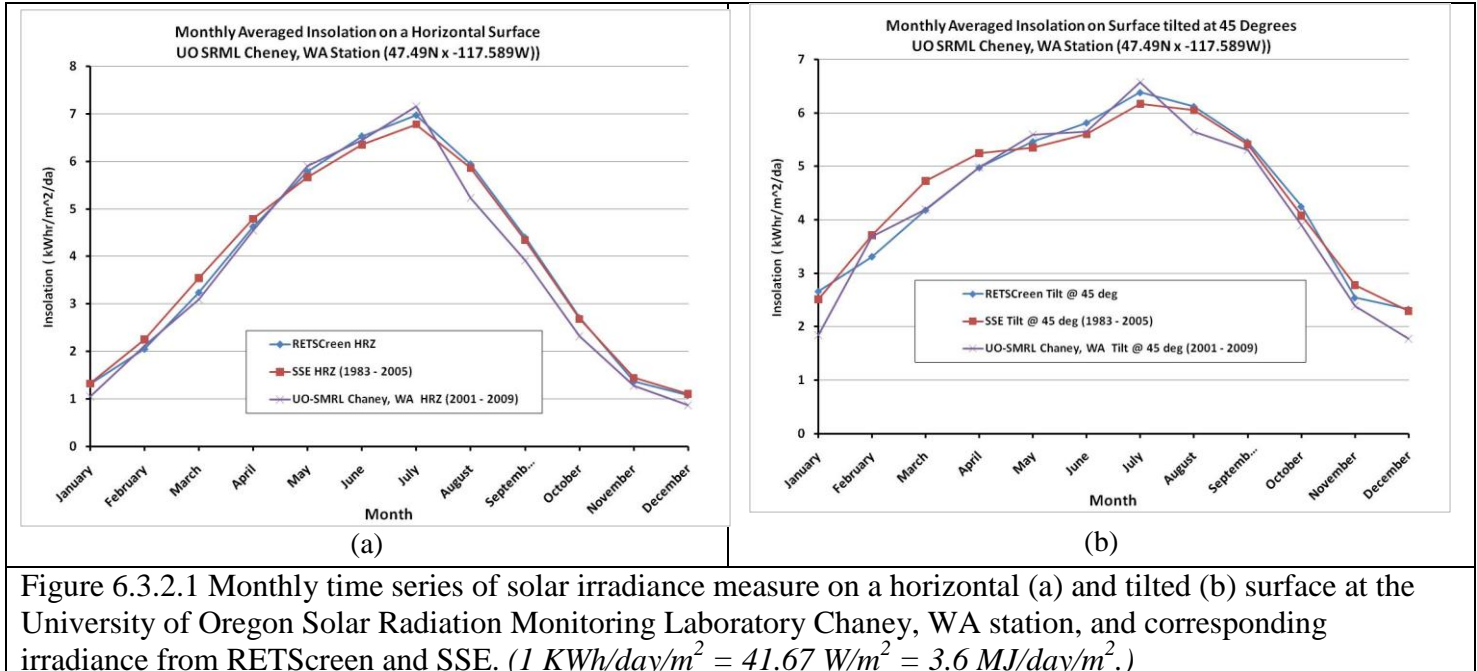


Figure 6.3.2.1 Monthly time series of solar irradiance measure on a horizontal (a) and tilted (b) surface at the University of Oregon Solar Radiation Monitoring Laboratory Chaney, WA station, and corresponding irradiance from RETScreen and SSE. ( $1 \text{ KWh/day/m}^2 = 41.67 \text{ W/m}^2 = 3.6 \text{ MJ/day/m}^2$ .)

[\(Return to Content\)](#)

**6.3.3 SSE vs BSRN Tilted Surface Irradiance.** Solar irradiance measurements at the most of the ground sites in the Base Line Surface Network include the diffuse and direct normal components as well as a direct measurement of the global, or total, irradiance on a horizontal surface. These measurements are typically made with at 1-, 2-, 3- or 5-minute intervals throughout the day. The diffuse and direct normal measurements, coupled with the solar zenith angle, provide the necessary components to estimate solar irradiance on a tilted surface as outlined below.

For any given BSRN site, consider a 3-D coordinate system with the origin at the BSRN site, X-axis pointing eastward, Y-axis northward, and Z-axis upward. For any given instant corresponding to a BSRN record, the unit vector pointing to the Sun is  $\{\sin(Z)\cos[(\pi/2)-A]\mathbf{i}, \sin(Z)\sin[(\pi/2)-A]\mathbf{j}, \cos(Z)\mathbf{k}\}$ , and the unit vector along the normal of a surface tilted toward the equator is  $[0\mathbf{i}, -\sin(T)\mathbf{j}, \cos(T)\mathbf{k}]$  for Northern Hemisphere, and  $[0\mathbf{i}, \sin(T)\mathbf{j}, \cos(T)\mathbf{k}]$  for Southern Hemisphere, where Z is the solar zenith angle, A is the azimuth angle of the Sun, and T is the tilt angle of the tilted surface. And the direct flux on the tilted surface is the direct normal flux times the dot product of the aforementioned two unit vectors which is  $-\sin(Z)\cos(A)\sin(T) + \cos(Z)\cos(T)$  for Northern Hemisphere and  $\sin(Z)\cos(A)\sin(T) + \cos(Z)\cos(T)$  for Southern Hemisphere. If the dot product of the two unit vectors is less than zero, which means the Sun is behind the tilted surface, the direct flux on the tilted surface is set to zero. After this conversion, the 3-hourly, daily and monthly means of the direct component on the tilted surface can then be derived. The diffuse component on a tilted surface is partly from the ground reflectance. For the scarcity of surface albedo measurement at the BSRN sites, we assume that the diffuse component on the tilted surface is the same as on the horizontal surface for a first estimate. This is equivalent to treating the surface albedo as 0.4 on average based on the available comparable

SRB-BSRN pairs of data points. The sum of the direct and diffuse components is the total flux on the tilted surface.

Figure 6.3.3.1 is a scatter plot of the climatological monthly mean irradiance on a tilted surface derived from the BSRN measurements of the diffuse and direct normal components versus the corresponding SSE tilted surface radiation values.

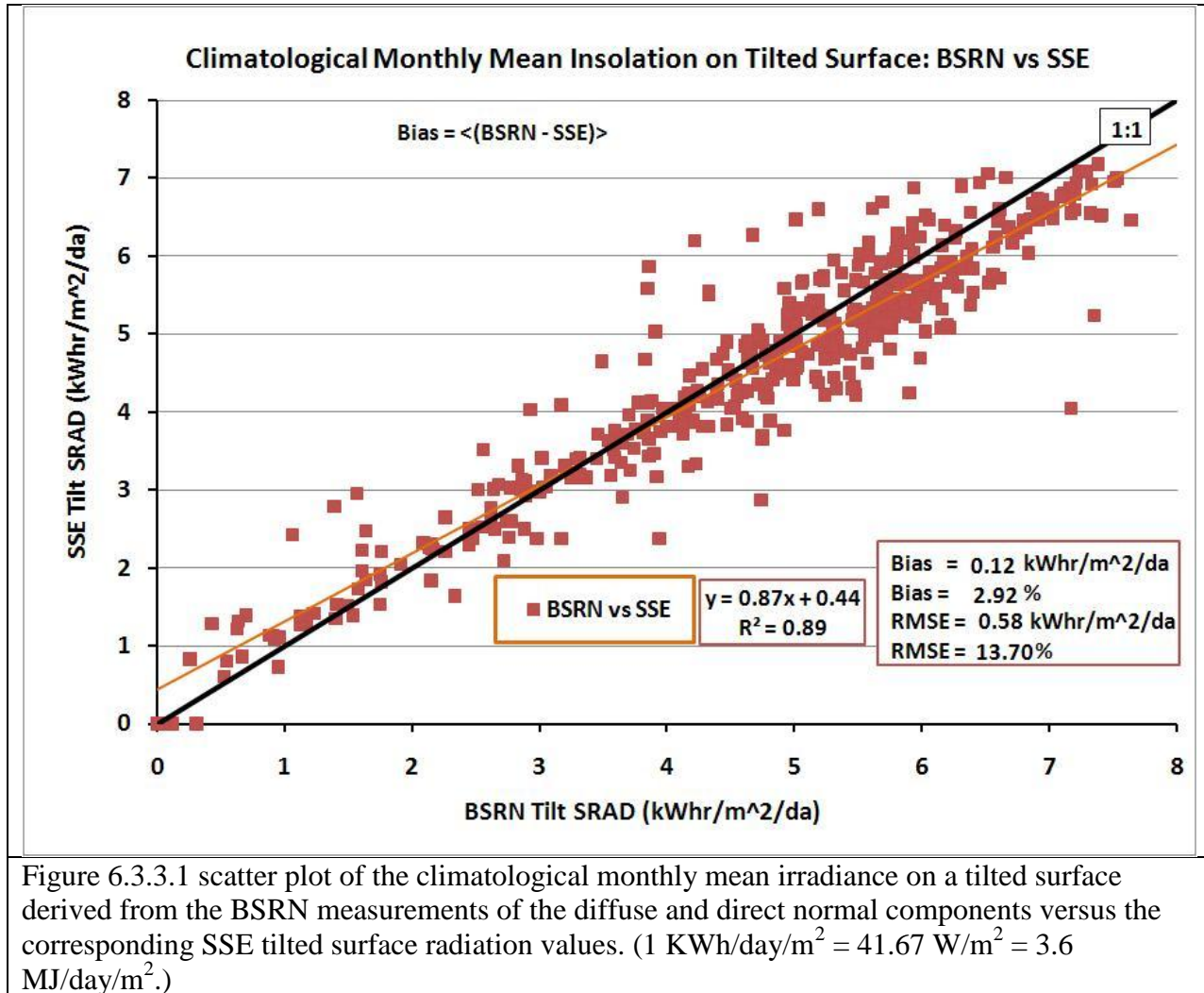


Figure 6.3.3.1 scatter plot of the climatological monthly mean irradiance on a tilted surface derived from the BSRN measurements of the diffuse and direct normal components versus the corresponding SSE tilted surface radiation values. ( $1 \text{ KWh/day/m}^2 = 41.67 \text{ W/m}^2 = 3.6 \text{ MJ/day/m}^2$ )

[\(Return to Content\)](#)

## 7. Parameters for Sizing Battery or Other Energy –Storage Systems

Solar energy systems that are not connected to an electrical grid system usually require back-up or storage equipment to provide energy during unusually cloudy days. Unusually cloudy conditions occurring over a number of consecutive days continually draw reserve power from batteries or other storage devices for solar systems not connected to an electrical grid. Storage devices must be designed to withstand continuous below-average conditions in various regions of the globe. Various industry organizations use different methods to size either battery or other

types of backup systems. One international organization has required that all stand-alone medical equipment that it purchases must operate for 6 BLACK or NO-SUN days in parts of the tropics. The methods used require different solar insolation parameters. Three types of parameters are provided in the SSE data set. They are listed in Table 7.1 and described in the subsequent text and in Whitlock et al (2005).

**Table 7.1. Parameters for Sizing Battery or other Energy-storage Systems:**

- Minimum available insolation as % of average values over consecutive-day period
- Solar Insolation deficits below expected values over consecutive-day period
- Equivalent number of NO-SUN days over consecutive-day period
- Available Surplus Insolation Over Consecutive –day period (%)

[\(Return to Content\)](#)

**7.1 Minimum percentage Insolation over a consecutive-day period (1, 3, 7, 14, or 21 days)** is the difference between the multi-year (Jul 1983 - Jun 2005) monthly averaged insolation and the multi-year monthly averaged minimum insolation over the indicated number of days (1, 3, ... days) within each month. The average is computed over the indicated days is a running average within each month. The defining equations are given below. (Note that a parameter enclosed by “< >” indicates the average value for the parameter.)

For month j, and year k the running average of the daily insolation over p days is given by

$$\langle SRAD \rangle_{jk}^p = [ \sum_{i=1}^p (\langle SRAD \rangle_{ijk}) ] / p$$

Where:

$\langle SRAD \rangle_{ijk}$ = Daily averaged surface insolation for day i, in month j, and year k

i = day in month for j

j = month of year

k = year in n-year time multi-year span (Jul 1983 - Jun 2005)

p = averaging period =1, 3, 7, 14, or 21 days

The multi-year monthly average of the running sum of insolation over the consecutive p-day average in month j is given by

$$\langle SRAD \rangle_j^p = \sum_{k=1}^n (\langle SRAD \rangle_{jk}^p) / n$$

Where:

n = 22 the number years in time span from Jul. 1983 – Jun 2005

The parameter Min/p-day for month j is the % difference between multi-year monthly average value,  $\langle SRAD \rangle_j^p$ , and the minimum value of  $\langle SRAD \rangle_j^p$  over the 1983 – 2005 time period and is given by

$$[Min/p-day]_j^p = 100 - (100 * [\langle SRAD \rangle_j^p - \langle SRADmin \rangle_j^p] / \langle SRAD \rangle_j^p)$$

$$\langle SRADmin \rangle_j^p = MIN(\langle SRAD \rangle_j^p)$$

[\(Return to Content\)](#)

**7.2 Solar radiation deficits below expected values incident on a horizontal surface over a consecutive-day period** is the multi-year monthly averaged deficit calculated as following

$$\langle \text{SRADdef} \rangle_j^p = \langle \text{SRADsum} \rangle_j^p - \langle \text{SRADsummin} \rangle_j^p$$

where

$$\langle \text{SRADsum} \rangle_j^p = \sum_{k=1}^n (\langle \text{SRADsum} \rangle_{jk}^p) / n$$

$$\langle \text{SRADsum} \rangle_j^p = \sum_{k=1}^n (\langle \text{SRADsum} \rangle_{jk}^p) / n$$

$$(\text{SRADsum})_{jk}^p = \sum_{i=1}^p (\langle \text{SRAD} \rangle_{ijk})$$

$\langle \text{SRAD} \rangle_{ijk}$  = Daily averaged surface insolation for day i, in month j, and year k

i = day in month for j

j = month of year

k = year in n-year time multi-year span (Jul 1983 - Jun 2005)

p = running average period = 1, 3, 7, 14, or 21 days

And

$$\langle \text{SRADsumMin} \rangle_j^p = \text{MIN}(\langle \text{SRADsum} \rangle_j^p)$$

[\(Return to Content\)](#)

**7.3 Equivalent number of NO-SUN or BLACK days** is based upon the deficit solar radiation below expected multi-year monthly averaged value and calculated as follows:

$$\langle \text{NoSunDa} \rangle_j^p = \langle \text{SRADdef} \rangle_j^p / \langle \text{SRAD} \rangle_j^p$$

Where:

$$\langle \text{SRADdef} \rangle_j^p = \langle \text{SRADsum} \rangle_j^p - \langle \text{SRADsumMin} \rangle_j^p$$

$$\langle \text{SRADsum} \rangle_j^p = \sum_{k=1}^n (\langle \text{SRADsum} \rangle_{jk}^p) / n$$

$$\langle \text{SRADsum} \rangle_j^p = \sum_{k=1}^n (\langle \text{SRADsum} \rangle_{jk}^p) / n$$

$$(\text{SRADsum})_{jk}^p = \sum_{i=1}^p (\langle \text{SRAD} \rangle_{ijk})$$

$$\langle \text{SRADsumMin} \rangle_j^p = \text{MIN}\{(\text{SRADsum})_{jk}^p\}$$

And

$$\langle \text{SRAD} \rangle_j = \sum_{k=1}^n (\langle \text{SRAD} \rangle_{jk}) / n = \text{multi-year monthly averaged for month } j$$

$$\langle \text{SRAD} \rangle_{jk} = \sum_{i=1}^m (\langle \text{SRAD} \rangle_{ijk}) / m = \text{monthly average SRAD for month } j \text{ in year } k$$

$$\langle \text{SRAD} \rangle_{ijk} = \text{daily averaged solar insolation for day } i, \text{ in month } j, \text{ in year } k.$$

i = day in month for j

j = month of year

k = 22 = number of years multi-year span (Jul 1983 - Jun 2005)

m = days in month j

[\(Return to Content\)](#)

**7.4 Available Surplus Insolation Over Consecutive –day period** (1, 3, 7, 14, or 21 days) is calculated for each month as the climatological average (i.e. multi-year monthly average ) over

the 22-year period (July 1983 – June 2005) as a percentage of the expected average insolation over the same consecutive day period. The parameter Max/p-day for month j is the % difference between multi-year monthly average value,  $\langle SRAD \rangle_j^p$ , and the maximum value of  $\langle SRAD \rangle_j^p$  over the 1983 – 2005 time period. The following summarizes the procedure for calculating the multi-year monthly average value of Max/p-day

$$[Max/p\text{-day}]_j^p = 100 - (100 * [\langle SRAD \rangle_j^p - \langle SRADmax \rangle_j^p] / \langle SRAD \rangle_j^p)$$

Where

$$\langle SRAD \rangle_j^p = \sum_{k=1}^n \langle SRAD \rangle_{jk}^p / n$$

= The multi-year monthly average of  $\langle SRAD \rangle_{jk}^p$  for month j

$\langle SRAD \rangle_{jk}^p = [\sum_{i=1}^p \langle SRAD \rangle_{ijk}] / p$  = The running average of the daily insolation over p days for month j & year k

$\langle SRAD \rangle_{ijk}$  = Daily averaged surface insolation for day i, in month j, and year k

i = day in month for j

j = month of year

k = year in n-year time multi-year span (Jul 1983 - Jun 2005)

p = averaging period = 1, 3, 7, 14, or 21 days

n = 22 the number years in time span from Jul. 1983 – Jun 2005

$\langle SRADmax \rangle_j^p = MAX(\langle SRAD \rangle_j^p)$

[\(Return to Content\)](#)

## 8. Solar Geometry.

Multi-year monthly averaged solar geometry parameters are available for any latitude/longitude via the “Data Tables for a particular location” web application. Table 8.1 lists the solar geometry

Table 8.1. Multi-year monthly averaged solar geometry parameters for each User provided latitude/longitude that are calculated based upon the “monthly average day”. These parameters provide guidance for solar panels.

### Solar Geometry:

- [Solar Noon](#)
- [Daylight Hours](#)
- [Daylight average of hourly cosine solar zenith angles](#)
- [Cosine solar zenith angle at mid-time between sunrise and solar noon](#)
- [Declination](#)
- [Sunset Hour Angle](#)
- [Maximum solar angle relative to the horizon](#)
- [Hourly solar angles relative to the horizon](#)
- [Hourly solar azimuth angles](#)

parameters provided to assistance users in setting up solar panels. [Appendix C](#) provides the equations for calculating each of the parameters, while [Appendix B](#) describes the methodology for calculating the multi-year monthly averages. Note that each of the solar geometry parameters

is calculated for the “monthly average day”; consequently each parameter is the monthly “averaged” value for the respective parameter for the given month. The “monthly average day” is the day in the month whose solar declination ( $\delta$ ) is closest to the average declination for that month (Klein 1977). Table 8.2 lists the date and average declination,  $\delta$ , for each month.

Table 8.2. List of the day in the month whose solar declination, $\delta$ , is closest to the average declination for that month					
Month	Date in month	$\delta$ (°)	Month	Date in month	$\delta$ (°)
January	17	-20.9	July	17	21.2
February	16	-13.0	August	16	13.5
March	16	-2.4	September	15	2.2
April	15	9.4	October	15	-9.6
May	15	18.8	November	14	-18.9
June	11	23.1	December	10	-23.0

[\(Return to Content\)](#)

**9.0 Overview of Underlying Meteorological Data:** The POWER-8 meteorological parameters listed above in Table 2.1, and repeated below, are based on Goddard’s Global Modeling and Assimilation Office (GMAO) assimilation model, the Modern Era Retrospective-Analysis for Research and Applications (MERRA-2; <https://gmao.gsfc.nasa.gov/reanalysis/MERRA-2/>), a new version of NASA’s Goddard Earth Observing System Data Assimilation System (Rienecker et al. (2008, 2011), Bosilovich, et. al. 2016, and Molod et al. (2011, 2015).

The meteorological parameters available through the POWER Release-8 archive include:

- (1) Daily mean temperature
- (2) Daily maximum and minimum temperatures
- (3) Earth skin temperature
- (4) Surface Pressure
- (5) Wind speed @ 2, 10 & 50m
- (6) Specific Humidity
- (7) Relative humidity
- (8) Dew/frost point temperatures
- (9) Precipitation
- (10) Heating degree-days below 18.3°C
- (11) Heating degree-days below 10°C
- (12) Heating degree-days below 0°C
- (13) Cooling degree-days above 18.3°C
- (14) Cooling degree-days above 10°C
- (15) Cooling degree-days above 0°C
- (16) Cloud cover

Each of the parameters is either obtained directly from or calculated using meteorological parameters taken from NASA’s Modern Era Retro-analysis for Research and Applications – (MERRA-2) assimilation model. The meteorological parameters emerging from the assimilation

model are estimated via “An atmospheric analysis performed within a data assimilation context [that] seeks to combine in some “optimal” fashion the information from irregularly distributed atmospheric observations with a model state obtained from a forecast initialized from a previous analysis” (Bloom, et al., 2005; Bosilovich, et. al. 2016). The model seeks to assimilate and optimize observational data and model estimates of atmospheric variables. Types of observations used in the analysis include (1) land surface observations of surface pressure; (2) ocean surface observations of sea level pressure and winds; (3) sea level winds inferred from backscatter returns from space-borne radars; (4) conventional upper-air data from rawinsondes (e.g., height, temperature, wind and moisture); (5) additional sources of upper-air data include drop sondes, pilot balloons, and aircraft winds; and (6) remotely sensed information from satellites (e.g., height and moisture profiles, total perceptible water, and single level cloud motion vector winds obtained from geostationary satellite images). Emerging from MERRA-2 are hourly global estimates of the vertical distribution of a range of atmospheric parameters.

Values from MERRA-2 are initially produced on a 1/2-degree by 2/3-degree global grid and regridded by the POWER project to a global  $0.5^{\circ}$  grid via bi-linear interpolation. The POWER archived data parameters are also transformed from Universal Time (UT) to solar local time (i.e., noon is defined to be solar noon without local time zone definitions taken into account). The MERRA-2 meteorological data available through POWER encompasses the time period from January 1, 1981 through a few month within near-real time. Each of the POWER MERRA-2 parameters is provided in a time series of daily mean values. All of the MERRA-2 parameters represent the average value over the half-degree spatial grid. The wind speed is at 2m, 10m, and 50m above the average elevation of the half-degree grid and precipitation surface value averaged over the grid. The remaining parameters are taken from the model at 2m above the average elevation of the grid box. As noted in the preceding paragraph the MERRA-2 parameters are calculated on hourly increments and converted by the POWER project to local time. The daily maximum and minimum temperatures are obtained from the 24 hourly temperature values. All other parameters are based upon averages or sums (i.e. HDD and CDD) of the hourly values.

The validation of the MERRA-2 meteorological parameters is based upon comparisons of the primary parameter to surface observations of the corresponding parameters. Statistics associated with the MERRA-2 vs. surface based values are reported to provide users with information necessary to assess the applicability of the MERRA-2 data to their particular project. Scatter plots of the MERRA-2 parameters vs. surface based values along with the correlation and accuracy parameters for each scatter plots are typically provided. The statistical parameters associated with a linear least squares fit to the respective scatter plots that are reported include: Pearson's correlation coefficient; the Bias between the mean of the respective MERRA-2 parameter and the surface observations; the root mean square error (RMSE) calculated as the root mean square difference between the respective MERRA-2 and observational values. Additional statistics typically provided are the variance in the MERRA-2 and observational data and the number of MERRA-2 / observational data pairs.

[Appendix A](#) provides the explicit equations used to calculate the statistical validation parameters.

[\(Return to Content\)](#)

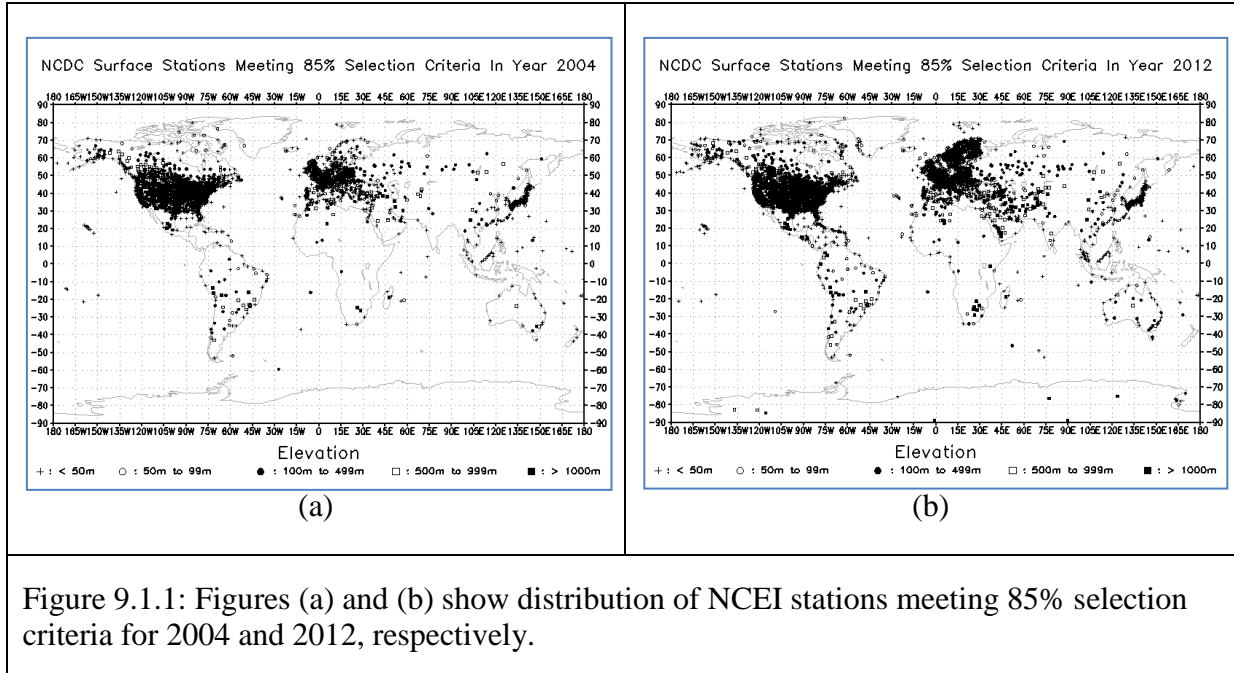
**9.1. Validation Methodology:** An assessment of the accuracy of the re-gridded MERRA-2 parameters is based upon comparison of the respective re-gridded MERRA-2 meteorological parameter with observations from the corresponding parameter reported in the National Center for Environmental Information (NCEI – formally National Climatic Data Center) Global “Summary of the Day” (GSOD -<http://www.ncdc.noaa.gov/oa/ncdc.html>) files. Comparison statistics (discussed below) are based upon comparisons of the given parameter for every third year beginning in 1981 through 2014, (e.g. 1981, 1984, 1987, etc.).

The daily observational data reported in the NCEI GSOD files are hourly observations from globally distributed ground stations with observations typically beginning at 0Z. For the analysis reported herein, the daily values were derived from the hourly observations filtered by an “85%” selection criteria applied to the observations reported for each station. Namely, only data from NCEI stations reporting 85% or greater of the possible 1-hourly observations per day and 85% or greater of the possible days per month were used to determine the daily average value of the given parameter.

Figure 9.1.1 shows the global distribution of the surface stations in the NCEI data files for 2004 and 2012 after applying our 85% selection criteria. There are 2704 surface stations in 2004 and 4731 in 2012 with the majority located in the northern hemisphere. As noted above, the MERRA-2 values represent the average value on a  $1/2^{\circ} \times 1/2^{\circ}$  latitude, longitude grid cell while the NCEI values are local observations.

In the following sections scatter plots associated with each meteorological parameter provide a visual indication of the agreement between the MERRA-2 values and surface observations. A more quantitative assessment of this agreement is given by the statistical parameters enumerated on each scatter plot. These include the slope, intercept and Pearson correlation coefficient associated with a linear least squares regression fit to the MERRA-2 vs. observational data, and the Mean Bias Error (MBE) and Root Mean Square Error (RMSE) between the model estimates and surface observations. See [Appendix A](#) for the expressions to calculate the statistical parameters.

Additionally, along the right side of each scatter plot is a color bar providing a measure of the distribution of the NCEI:MERRA-2 data pairs. The column on left side of the vertical color bar gives the number of data pairs per parameter bin associated with each color. The parameter bin size for the temperature values is  $1^{\circ}\text{C}$ ; for pressure 1mb; for precipitation rainfall accumulation 5mm; and for specific humidity 1g/kg. The column on the right side of color bar gives the percentage of total number of MERRA-2, ground site data pairs associated with each color.



[\(Return to Content\)](#)

**9.2. Temperatures:** In this section results from comparing the MERRA-2 mean air temperature (Tave) to observations reported in the National Center for Environmental Information (NCEI – formally National Climatic Data Center) Global “Summary of the Day” (GSOD - <http://www.ncdc.noaa.gov/oa/ncdc.html>) files are presented.

Figure 9.2.1 show respectively the scatter plot of the re-gridded MERRA-2 Tave temperature vs. the corresponding values from the NCEI GSOD files for every 3<sup>rd</sup> year from 1981 – 2014. The legend in the upper left corner of each scatter plot gives the associated mean Bias and RMSE ([eqs. A.5 & A.6](#)) along with the Slope, intercept, and Pearson correlation coefficient associated with the linear least squares fit to the plotted values (black line). The grey color line is the 1:1 line.

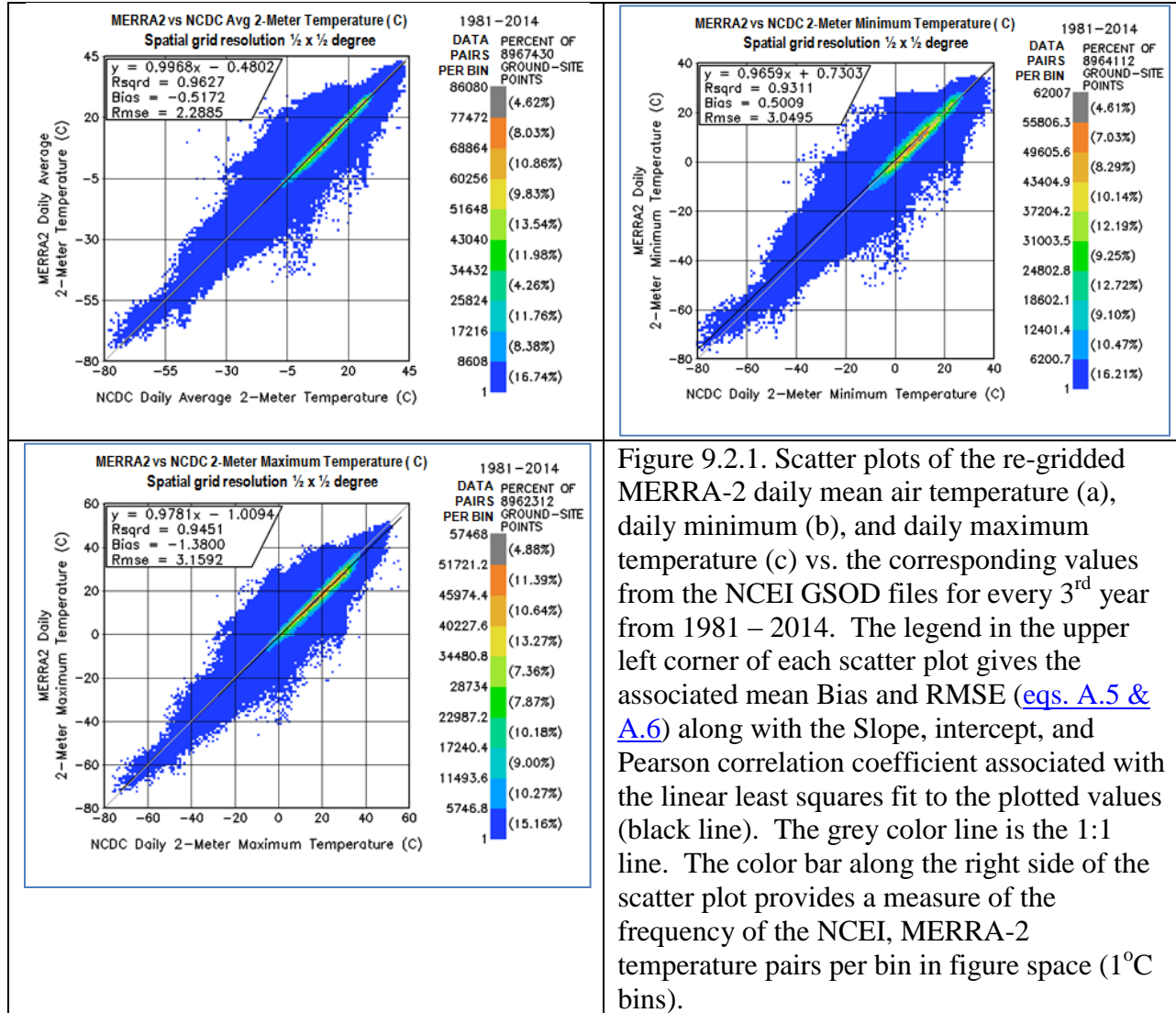


Figure 9.2.1. Scatter plots of the re-gridded MERRA-2 daily mean air temperature (a), daily minimum (b), and daily maximum temperature (c) vs. the corresponding values from the NCEI GSOD files for every 3<sup>rd</sup> year from 1981 – 2014. The legend in the upper left corner of each scatter plot gives the associated mean Bias and RMSE ([eqs. A.5 & A.6](#)) along with the Slope, intercept, and Pearson correlation coefficient associated with the linear least squares fit to the plotted values (black line). The grey color line is the 1:1 line. The color bar along the right side of the scatter plot provides a measure of the frequency of the NCEI, MERRA-2 temperature pairs per bin in figure space (1°C bins).

Recall that the spatial resolution of the MERRA-2 data in the POWER archive is  $\frac{1}{2}$ -degree latitude by longitude. The color bar along the right side of the scatter plot provides a measure of the frequency of the NCEI, MERRA-2 temperature pairs. For example, in Figure 9.2.1 (a) the left column along the vertical color bar shows that each data point in dark blue represents a 1°C temperature bin with 1 to 8,608 matching NCEI site temperature/ MERRA-2 data pairs ( $\leq 10\%$  of the maximum number of 86080 data pairs per bin). From the right hand column along the color bar it is seen that all of the points shown in dark blue contain 16.74% of the total number of ground site/MERRA-2 data pairs. Likewise, the darkest orange color represents regions with 68,864 to 77,472 matching temperature pairs (i.e., 80-90% of the maximum), and taken as a group all of the area represented by orange contain 8.03% of the total number of matching ground site/MERRA-2 data pairs. Thus, for the data shown in Figure 9.2.1 (a), approximately 83% of matching temperature pairs (i.e. excluding the data represented by the dark blue color) is “tightly” grouped along the 1:1 correlation line.

[\(Return to Content\)](#)

**9.3. Precipitation:** The precipitation data in POWER Release-8 Archive has been taken directly from the MERRA-2 assimilation model and represents an estimate of the daily mean value for the respective 0.5-degree grid cell. The MERRA-2 precipitation is an improvement in both time and global coverage over a previous precipitation data source (GPCP) used in former versions of the POWER website. For this reason, the GPCP precipitation data sources aren't available in this version of the POWER website.

### 9.3.1. Density Scatter Plot.

Figure 9.3.1 shows the scatter plots of the accumulation of the re-gridded MERRA-2 precipitation vs. the corresponding values from the NCEI GSOD data for every 3<sup>rd</sup> year from 1981 – 2014 (e.g. 1981, 1984, 1987, etc.) and Table 9.3.1 summarizes the statistics associated with the respective scatter plots

Table 9.3.1. Summary of statistics associated with the scatter plots in Fig. 9.3.1

Acc. Days	Slope	Intercept	R2	Bias	RMSE	% Along 1:1
1	0.36	2.06	0.15	0.80	7.96	N/A
5	0.57	6.12	0.45	2.15	15.12	81.44
15	0.53	16..86	0.53	6.35	31.35	75.3
30	0.63	32.98	0.54	12.68	53.52	72.38

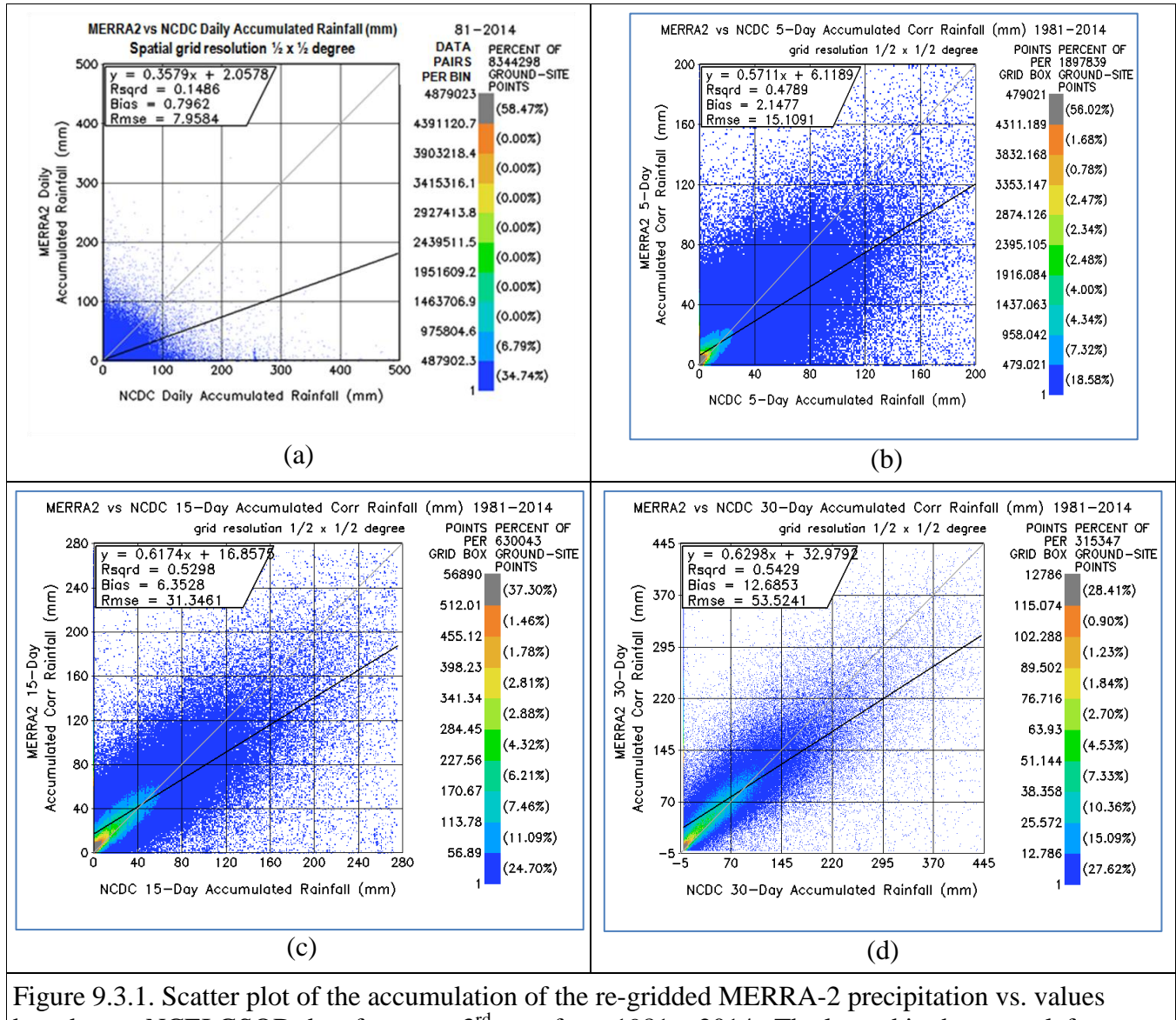


Figure 9.3.1. Scatter plot of the accumulation of the re-gridded MERRA-2 precipitation vs. values based upon NCEI GSOD data for every 3<sup>rd</sup> year from 1981 – 2014. The legend in the upper left corner of each scatter plot gives the associated mean Bias and RMSE ([eqs. A.5 & A.6](#)) along with the Slope, intercept, and Pearson correlation coefficient associated with the linear least squares fit to the plotted values (black line). The grey color line is the 1:1 line. The color bar along the right side of the scatter plot provides a measure of the frequency of the NCEI, MERRA-2 daily rain rate pairs per bin in figure space (1mm rainfall accumulation bins).

The legend in the upper left corner of each scatter plot gives the associated mean Bias and RMSE ([eqs. A.5 & A.6](#)) along with the Slope, intercept, and Pearson correlation coefficient associated with the linear least squares fit to the plotted values (black line). The grey color line is the 1:1 line. The color bar along the right side of the scatter plot provides a measure of the distribution of the NCEI, MERRA-2 rain rate pairs in bins of 1 mm of accumulated rain fall. For example, in Figure 9.3.1, the left column along the vertical color bar shows that each data point

in dark blue represents the number ground site/MERRA-2 data pairs within 10% (i.e., <487902) of the maximum number of data pairs within a 1x1 mm rain fall accumulation bins in the figure space (i.e., 4879023). Additionally, from the right side of the vertical color bar it can be seen that all the points shown in dark blue contain 34.74% of the total number of ground site, MERRA-2 data pairs (8,344,298).

Recall that the spatial resolution of the MERRA-2 data in the POWER archive is 0.5° latitude by 0.5° longitude. Accordingly, a high level of agreement with localized surface observations is not expected, particularly on a day to day comparison. The charts in Figures 9.3.1a -9.3.1d compares the MERRA-2 precipitation values to surface observations as the accumulation time is increased from 1-day, 5-days, 15-days, and 30-days respectively. Note that as the accumulation days increase the overall agreement between the MERRA-2 values and the surface observation improves, although the after 5-days the improvement is rather minimal.

### **9.3.2 Contingency Table.**

Many methods exist when it comes to the validation of precipitation (Yates, 2006; Ebert, 2007). Density scatter plots are a useful way to describe and display the validation statistics. However, the density scatter plots of the precipitation validation, due to the random nature of the daily precipitation, are dominated by days with little or no precipitation while days with heavy precipitation are less frequent. Categorical verification, in this case contingency tables, offer another way to examine the daily precipitation data. What the contingency table shows are the cases when the MERRA-2 daily precipitation and ground site daily precipitation (1) measured no precipitation on the same days (“correct negative”), (2) measured precipitation on the same days (“hits”; regardless of amount), (3) MERRA-2 measured precipitation while ground site does not (“false alarms”), and (4) MERRA-2 measured no precipitation while ground site did (“misses”).

For this contingency table analysis of the MERRA-2 daily precipitation, all the days when the ground site/MERRA-2 data pairs measured a valid precipitation amount, including days with no precipitation, were counted for every 3<sup>rd</sup> year during the 1981-2014 period. These “data days” total 8,958,351 days. The top table in Figure 9.3.2.1 shows a breakdown of the four categories mentioned previously, with the MERRA-2 data presented by the “rows” on the left side of the table and the NCEI ground site data presented by the “columns” on the top side of the table. Row 1 and Column 1 depict the “No Precipitation” category for the MERRA-2 and NCEI ground site data, respectively. Where Row 1 and Column 1 intersect shows the total number of data days (4,079,063) were both data sets measured no precipitation on the same days (“correct negative”). This represented 45.53% of the total data days counted.

Row 2 and Column 2 depict the “Precipitation” categories for the MERRA-2 and NCEI ground site data, respectively. Their intersection shows the total number of data days (1,858,936) where both data sets measured precipitation regardless of amount on the same days (“hits”). This represented 20.75% of the total data days counted. The “hits” category is broken down further in sub-categories, depicted in the lower table in Figure 9.3.2.1, along with statistics. The sub-categories consist of data days when the MERRA-2 precipitation is less than the NCEI ground site, when the MERRA-2 precipitation is greater than the NCEI ground site, and when the MERRA-2 precipitation is equal to the NCEI ground site. By “equal” means within the

measurement accuracy of the NCEI ground site instrumentations(0.508 mm). Out of the total number of data day “hits”, 248,069 (13.36%) data days occur when the MERRA-2 precipitation is equal to the NCEI ground site precipitation. Both the MERRA-2 precipitation and NCEI ground site precipitation share similar averages, standard deviations, and maximum values, though the minimum values differ by 0.50 mm. The MERRA-2 precipitation is less than the NCEI ground site precipitation on 903,183 (48.59%) data days out of the total number of data day “hits”. As expected, the MERRA-2 precipitation average and standard deviations are roughly 2.5 times less than the NCEI ground site precipitation average and standard deviations. The NCEI ground site precipitation maximum and minimum values are roughly 2 and 4 times greater than the MERRA-2 precipitation maximum and minimum values, respectively. The MERRA-2 precipitation is more than the NCEI ground site precipitation on 707,684 (38.07%) data days out of the total number of data day “hits”. As expected, the MERRA-2 precipitation average and standard deviations are roughly 2 times more than the NCEI ground site precipitation average and standard deviations. The MERRA-2 precipitation maximum and minimum values are roughly 1.5 times greater than the NCEI ground site precipitation maximum and minimum values.

MERRA-2 Corrected Precipitation Total number of data days: 8,958,351		NCEI	
		No Precipitation	Precipitation
MERRA-2	No Precipitation	4,079,063 (45.53%)	200,580 (2.24%)
	Precipitation	2,819,772 (31.48%)	1,858,936 (20.75%)

Total number of data days when both have precipitation: 1,858,936	Number of Data Days (% of Total)	Average		StdDev		Maximum		Minimum	
		MERRA-2	NCDC	MERRA-2	NCDC	MERRA-2	NCDC	MERRA-2	NCDC
MERRA-2 < NCEI	903,183 (48.59%)	5.39	13.64	7.52	17.76	215.52	497.08	0.26	1.02
MERRA-2 = NCEI +/- 0.508 mm	248,069 (13.36%)	2.94	2.98	3.92	3.90	129.29	129.03	0.26	0.76
MERRA-2 > NCEI	707,684 (38.07%)	10.4	4.75	10.11	6.01	330.78	215.9	1.28	0.76

Figure 9.3.2.1. Contingency table with focus on the ”Hits” category between the re-gridded MERRA-2 precipitation and values based upon NCEI GSOD data for every 3<sup>rd</sup> year from 1981 – 2014.

Row 1 and Column 2 depict the “No Precipitation” and “Precipitation” categories for the MERRA-2 and NCEI ground site data, respectively. Their intersection shows the total number of data days (200,580) where the MERRA-2 precipitation data measured no precipitation while

the NCEI ground site precipitation data measured precipitation, regardless of amount, on the same days (“misses”). This represented 2.24% of the total data days counted. The “misses” category is broken down further, depicted in the lower table in Figure 9.3.2.2, along with statistics. Shown are the data days when the MERRA-2 precipitation has no precipitation and the NCEI ground site has a precipitation amount greater than the measurement accuracy of the NCEI ground site instrumentations ( 0.508 mm). In these cases, the NCEI ground site precipitation has an average of 4.83 mm, a standard deviation of 9.83 mm, a maximum value of 410.97 mm, and a minimum value of 0.762 mm.

MERRA-2 Corrected Precipitation Total number of data days: 8,958,351		NCEI	
		No Precipitation	Precipitation
MERRA-2	No Precipitation	4,079,063 (45.53%)	200,580 (2.24%)
	Precipitation	2,819,772 (31.48%)	3,68,936 (0.75%)

Total number of data days when MERRA-2 has no precipitation and NCEI has precipitation: 200,580	Number of Data Days (% of Total)	Average		StdDev		Maximum		Minimum	
		MERRA-2	NCEI	MERRA-2	NCEI	MERRA-2	NCEI	MERRA-2	NCEI
MERRA-2 = 0 mm NCEI > 0.508 mm (uncertainty)	200,580 (2.24%)	0.0	4.83	0.0	9.83	0.0	410.97	0.0	0.762

Figure 9.3.2.2. Contingency table with focus on the ”Misses” category between the re-gridded MERRA-2 precipitation and values based upon NCEI GSOD data for every 3<sup>rd</sup> year from 1981 – 2014.

Row 2 and Column 1 depict the “Precipitation” and “No Precipitation” categories for the MERRA-2 and NCEI ground site data, respectively. Their intersection shows the total number of data days (2,819,772) where the MERRA-2 precipitation data measured precipitation while the NCEI ground site precipitation data measured no precipitation on the same days (“false alarms”). This represented 31.48% of the total data days counted. The “false alarm” category is broken down further, depicted in the lower table in Figure 9.3.2.3, along with statistics. Shown are the data days when the MERRA-2 precipitation measured precipitation and the NCEI ground site measured a precipitation amount less than and equal to the measurement accuracy of the NCEI ground site instrumentations, ( 0.508 mm). In these cases, the MERRA-2 precipitation has an average of 3.02 mm, a standard deviation of 5.02 mm, a maximum value of 213.31 mm, and a minimum value of 0.26 mm.

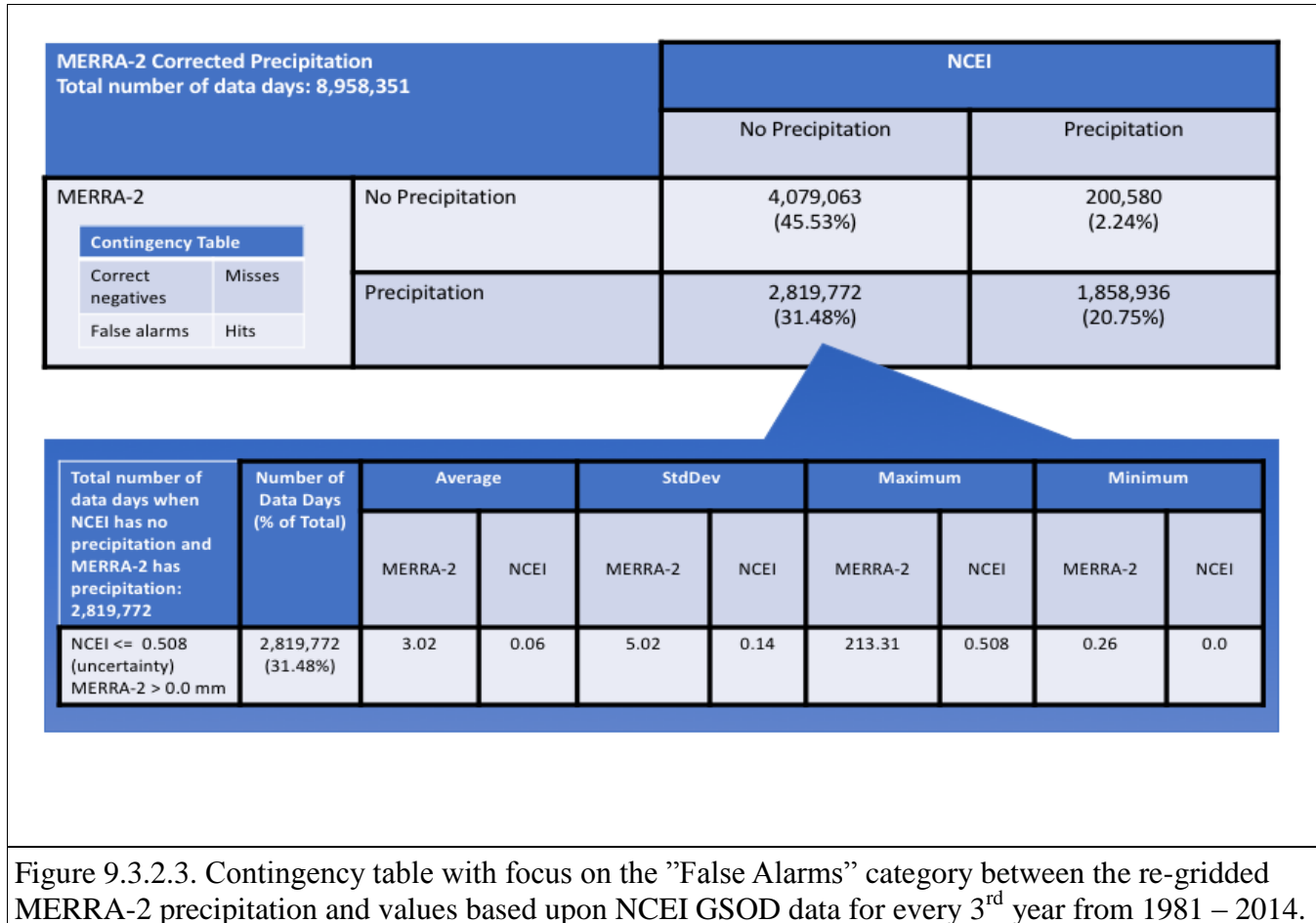
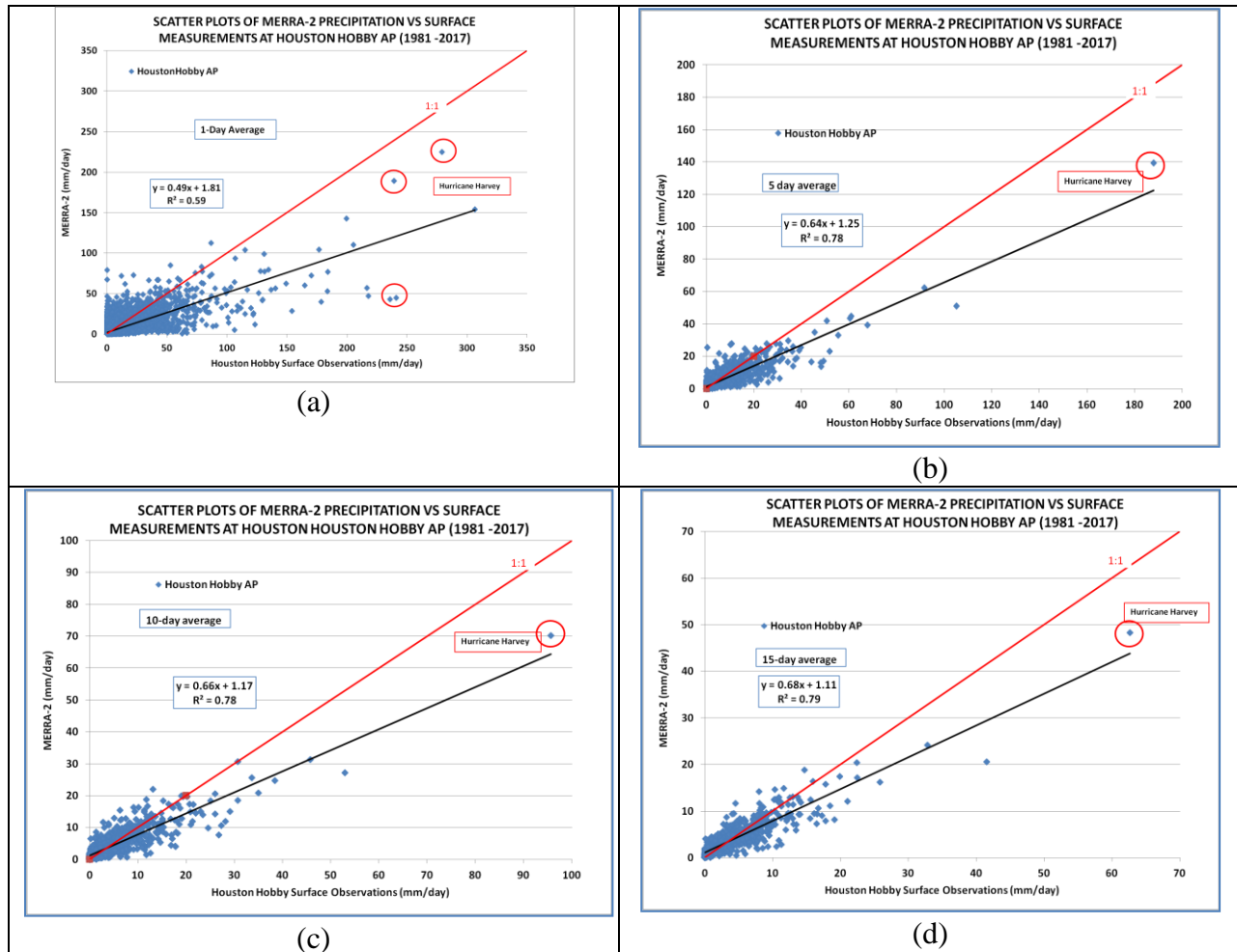


Figure 9.3.2.3. Contingency table with focus on the "False Alarms" category between the re-gridded MERRA-2 precipitation and values based upon NCEI GSOD data for every 3<sup>rd</sup> year from 1981 – 2014.

The findings from the contingency tables show additional information not easily seen in the density scatter plots in the Section 9.3.1. On data days when the MERRA-2 precipitation measured no precipitation, it agreed with the NCEI ground site precipitation 45.53% of the time ("correct negatives"), and only disagreed 2.24% of the time ("misses"). The percent of "misses" is relatively low compared to the other three categories in the table, with the NCEI ground site precipitation measurement average only being 4.83 mm or 0.19 inches. On data days when the MERRA-2 precipitation measured precipitation, the NCEI ground site also measured precipitation 20.75% of the time ("hits"), but disagreed 31.48% of the time ("false alarms"). On data days when the NCEI ground site measures precipitation, it's encouraging to note MERRA-2 predicts precipitation (20.75%) on the same data days more often than it doesn't (2.24%). In the "hits" category, however, only 2.77% of the total data days the MERRA-2 and NCEI ground site precipitation agree exactly within the accuracy of the ground site instrument (0.508mm). The percent of "false alarms" represents roughly one-third of data days in the table, with the MERRA-2 precipitation measurement average only being 3.02 mm or 0.12 inches. MERRA-2 is more likely to predict measured precipitation when none occurs at a ground site than predict no measured precipitation when it does occur at a ground site.

### 9.3.3. Localized Comparison.

The scatter plots in Figure 9.3.1 provide a global perspective covering a wide range of precipitation as well as ground station with varying levels of quality control. The ability of the MERRA-2 to provide precipitation data for local applications can be assessed in figures 9.3.3 where the daily averaged MERRA-2 precipitation associated with the half-degree cell covering the Houston, TX region is plotted against the corresponding daily averaged values from surface measurements at the Houston Hobby airport. Figures 9.3.3a – 9.3.3e cover the time period 1981 – 2017. Note, here again as in the data from a global perspective, the agreement improves as the averaging period increased from 1-day through 30-days, and as with the data in Figure 9.3.1 the improvement is marginal after 5-days. The data points circled in red are from the time period that Hurricane Harvey ([https://www.nhc.noaa.gov/data/tcr/AL092017\\_Harvey.pdf](https://www.nhc.noaa.gov/data/tcr/AL092017_Harvey.pdf)) passed over the Houston area. Figure 9.3.3g is a time series plot of the daily average precipitation from MERRA-2 and surface observations. Note the high correlation between MERRA-2 and the surface observations. Similar results to those in Figure 9.3.3 were also observed at other surface stations in Texas and in the Louisiana.



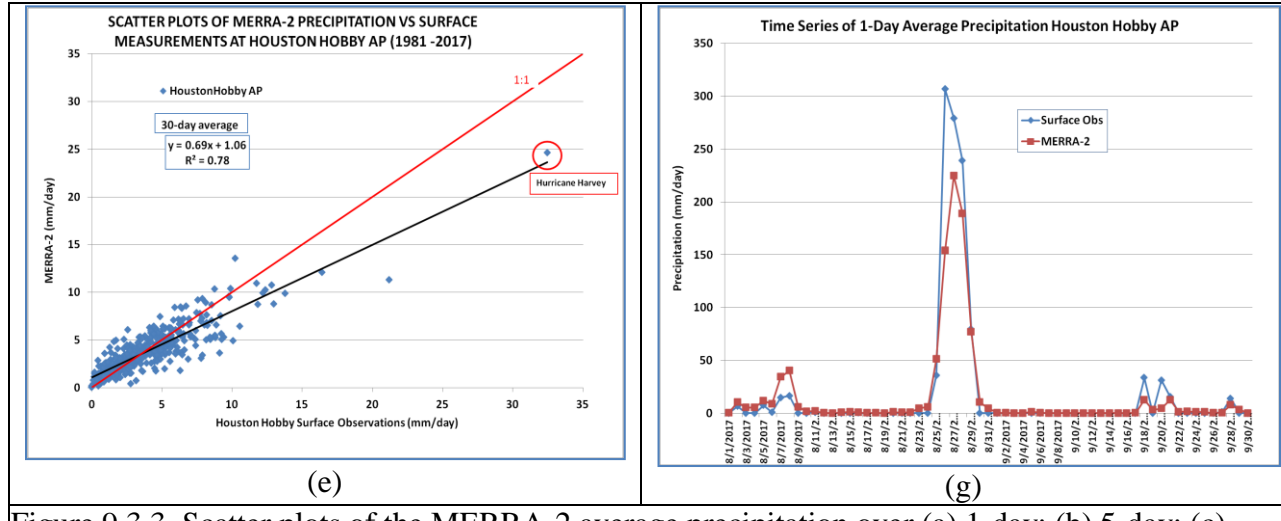
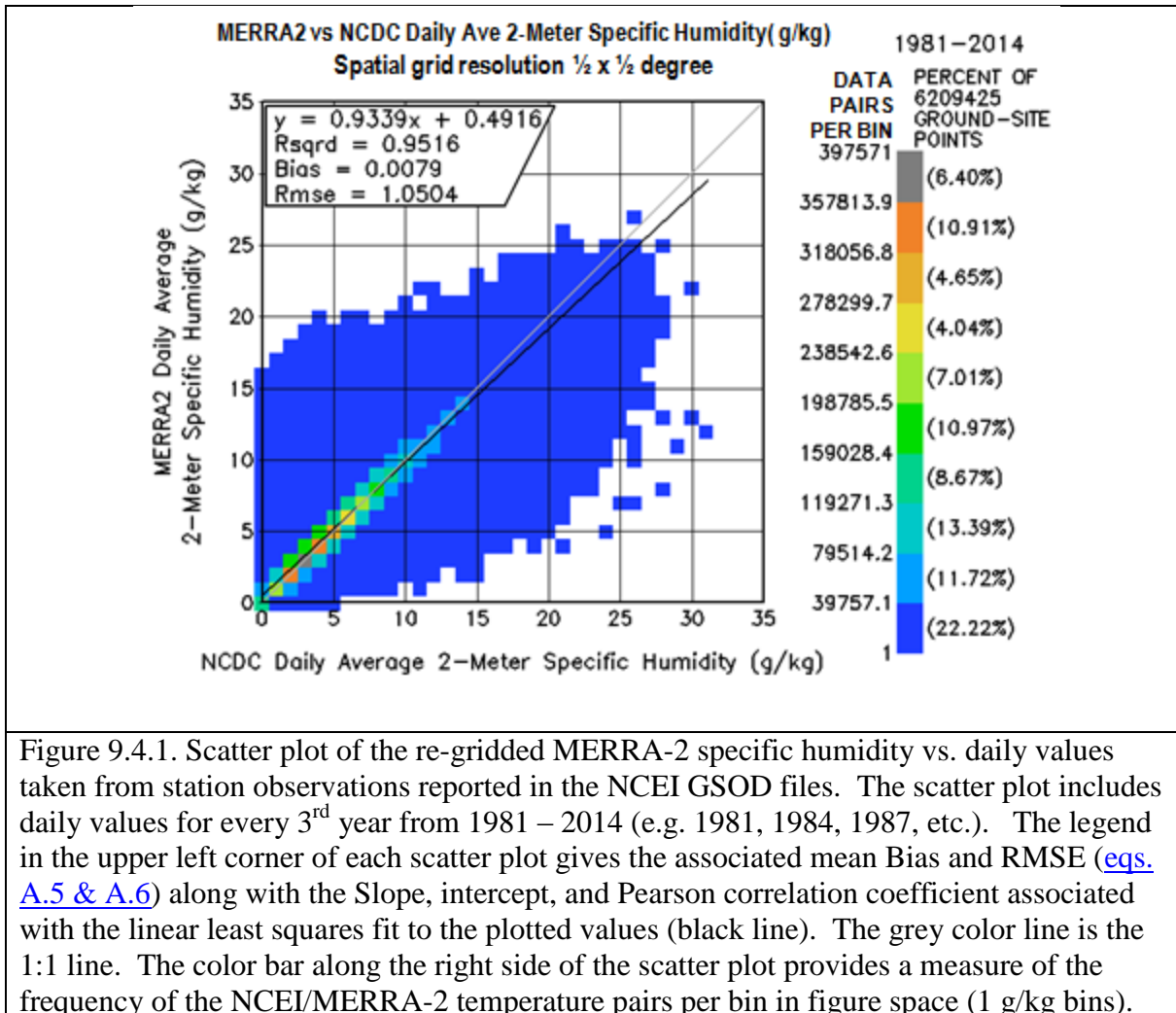


Figure 9.3.3. Scatter plots of the MERRA-2 average precipitation over (a) 1-day; (b) 5-day; (c) 10-day; (d) 15-day; and (e) 30-day periods over the time period January 1, 1981 – December 31, 2017. Figure (g) shows a time series plot of the 1-day average precipitation cover Hurricane Harvey (i.e. August 1, 2017 to September 30, 2017)

[\(Return to Content\)](#)

**9.4 Specific Humidity:** The daily mean specific humidity is taken directly from the re-gridded MERRA-2 and represents estimates at 2m above the local surface averaged over a  $0.5^\circ$  latitude x  $0.5^\circ$  longitude grid. Figure 9.4.1 shows the scatter plot of the MERRA-2 specific humidity vs. daily values taken from station observations reported in the NCEI GSOD files. The scatter plot includes daily values for every 3<sup>rd</sup> year from 1981 – 2014 (e.g. 1981, 1984, 1987, etc.). The legend in the upper left corner of each scatter plot gives the associated mean Bias and RMSE ([eqs. A.5 & A.6](#)) along with the Slope, intercept, and Pearson correlation coefficient associated with the linear least squares fit to the plotted values (black line). The grey color line is the 1:1 line.



The color bar along the right side of the scatter plot provides a measure of the distribution of the NCEI, MERRA-2 specific humidity pairs in bins of 1 g/kg. For example, in Figure 9.4.1, the left column along the vertical color bar shows that each data point in dark blue represents the number ground site/MERRA-2 data pairs within 10% (i.e.,  $\leq 39757$ ) of the maximum number of data pairs within a 1g/kg bins in the figure space (i.e., 397571). Additionally, from the right side of the vertical color bar it can be seen that all the points shown in dark blue contain 22.22% of the total number of ground site, MERRA-2 data pairs (6,209,425). The remaining 77.8% of the data pairs are concentrated along the 1:1 grey line.

[\(Return to Content\)](#)

**9.5 Relative Humidity:** The relative humidity (RH) values in the POWER archives are calculated from pressure ( $P_a$  in kPa), dry bulb temperature ( $T_a$  in  $^{\circ}\text{C}$ ), and mixing ratio (e.g. specific humidity,  $q$  in kg/kg), parameters that are available from the re-gridded MERRA-2 and represents estimates at 2m above the local surface averaged over a  $0.5^{\circ}$  latitude x  $0.5^{\circ}$  longitude grid. The following is a summary of the expressions used to calculate RH. The units are indicated in square brackets.

From Iribarne and Godson (1981) a fundamental definition of the Relative Humidity (Eq. 83, pg 75):

$$(9.5.1) \quad RH = (e_a/e_{sat}) \times 100\%$$

where

$e_a$  = the water vapor pressure and

$e_{sat}$  the saturation water vapor pressure at the ambient temperature  $T_a$ .

The 100% has been added to cast RH in terms of percent.

Since water vapor and dry air (a mixture of inert gases) can be treated as ideal gases, it can be shown that (Iribarne and Godson, pg 74, Eq. 76; Note that the symbol,  $r$ , use in Eq. 76 for the mixing ratio has been replaced by “w” and the factor of “10” has been added to convert the units to hPa.)

$$(9.5.2) \quad e_a = (10 \times P_a \times w) / (\epsilon + w) \text{ [hPa]}$$

where  $w$  is the mixing ratio define as the ratio of mass of water to dry air and

$$(9.5.3) \quad \epsilon = \frac{R'}{R_v} = \frac{287.05}{461.5} \simeq 0.622$$

where  $R'$  and  $R_v$  are the dry and water vapor gas constants respectively (note that there is no exact consensus for the gas constants past 3 significant digits, therefore the value of the ratio is kept to 3 significant digits). The mixing ratio is related to specific humidity by the relation (Jupp 2003, pg.37):

$$(9.5.4) \quad w = q / (1-q) \text{ [kg/kg]}$$

Combining (9.5.2) and (9.5.4) leads to the following expression for  $e$  in terms of  $q$ :

$$(9.5.5) \quad e_a = q \times 10 \times P_a / [\epsilon + q \times (1 - \epsilon)] \text{ [hPa]}$$

An eighth-order polynomial fit (Flatau, et. al. 1992) to measurements of vapor pressure over ice and over water provides an expression to calculate the saturated water vapor pressure over ice and over water. The eight-order fit for  $e_{wsat}$  is given by

$$(9.5.6) \quad e_{wsat} = A_{1w} + A_{2w} \times (T_a) + \dots + A_{(n-1)w} \times (T_a)^n$$

and

$$(9.5.7) \quad e_{isat} = A_{1i} + A_{2i} \times (T_a) + \dots + A_{(n-1)i} \times (T_a)^n ,$$

Where

$e_{wsat}$  = saturated vapor pressure over water in [hPa = mb]

$e_{isat}$  = saturated vapor pressure over ice [hPa=mb]

$T_a$  is the ambient dry bulb temperature in °C.

Table 9.5.1 gives the coefficients for  $e_{sat}$  over water and over ice and the temperature range over which the coefficient are applicable.

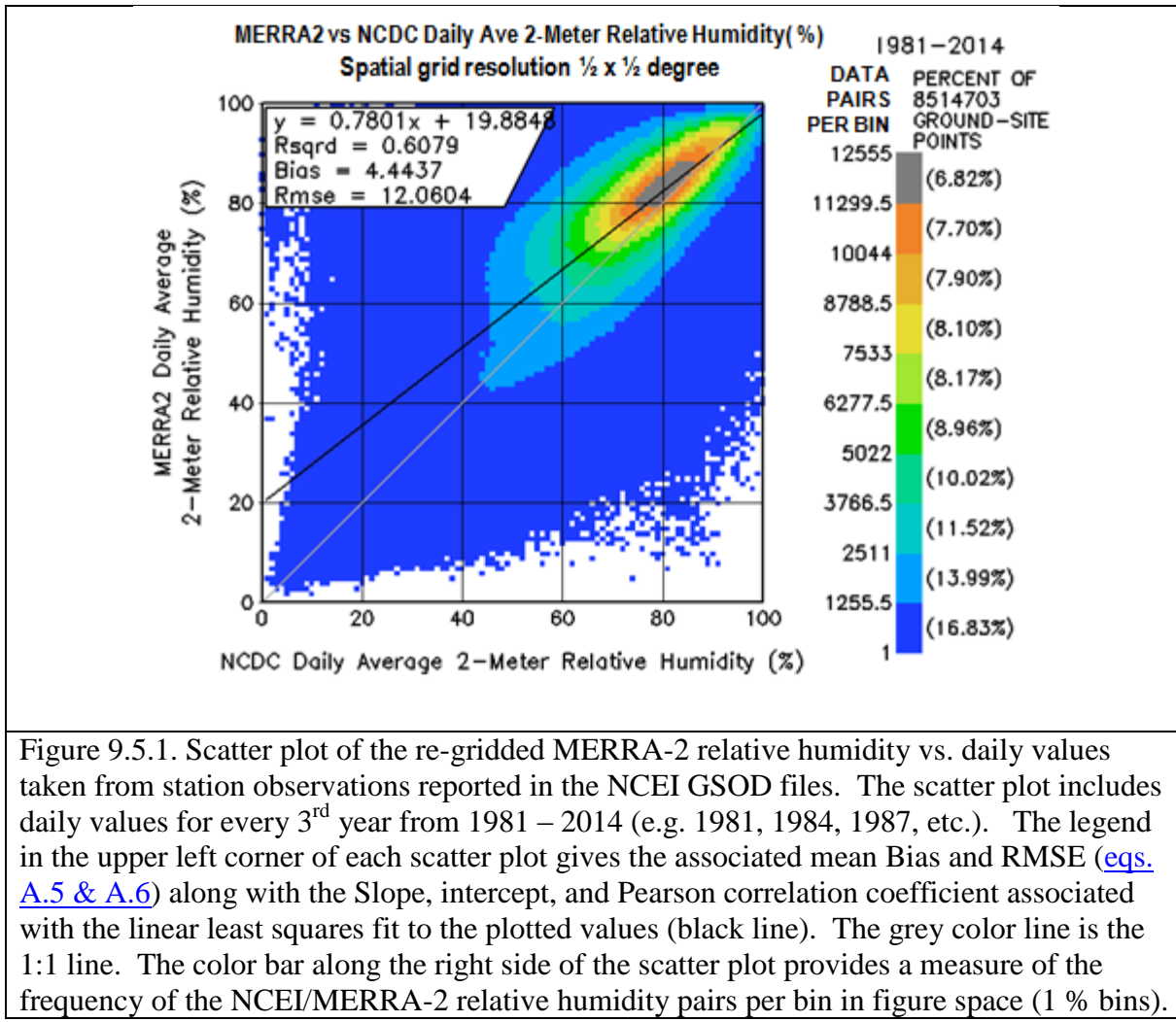
Table 9.5.1. Coefficients of the eight-order polynomial fit (Taken from Flatau, et. al. 1992 Table 4.) to measurements of saturated vapor pressure measurements,

Coefficients for $e_{sat}$ over water valid over the temperature range -85 °C to +70 °C	Coefficients for $e_{sat}$ over ice valid over the temperature range -90 °C to 0 °C
$A1w = 6.11583699$	$A1i = 6.09868993$
$A2w = 0.444606896$	$A2i = 0.499320233$
$A3w = 0.143177157E-1$	$A3i = 0.184672631E-1$
$A4w = 0.264224321E-3$	$A4i = 0.402737184E-3$
$A5w = 0.299291081E-5$	$A5i = 0.565392987E-5$
$A6w = 0.203154182E-7$	$A6i = 0.521693933E-7$
$A7w = 0.702620698E-10$	$A7i = 0.307839583E-9$
$A8w = 0.379534310E-13$	$A8i = 0.105758160E-11$
$A9w = -0.321582393E-15$	$A9i = 0.161444444E-14$

Note that only the relative humidity over water is calculated and provided in the POWER Archive consistent with the values reported by the National Weather Service.

Figure 9.5.1 shows the scatter plot of the MERRA-2 relative humidity vs. daily values taken from station observations reported in the NCEI GSOD files. The scatter plot includes daily values for every 3<sup>rd</sup> year from 1981 – 2014 (e.g. 1981, 1984, 1987, etc.). The legend in the upper left corner of each scatter plot gives the associated mean Bias and RMSE ([eqs. A.5 & A.6](#)) along with the Slope, intercept, and Pearson correlation coefficient associated with the linear least squares fit to the plotted values (black line). The grey color line is the 1:1 line.

The color bar along the right side of the scatter plot provides a measure of the distribution of the NCEI, MERRA-2 relative humidity pairs in bins of 1 %. For example, in Figure 9.5.1, the left column along the vertical color bar shows that each data point in dark blue represents the number ground site/MERRA-2 data pairs within 10% (i.e.,  $\leq 1255.5$ ) of the maximum number of data pairs within a 1g/kg bins in the figure space (i.e., 12555). Additionally, from the right side of the vertical color bar it can be seen that all the points shown in dark blue contain 16.83% of the total number of ground site, MERRA-2 data pairs (8514703). The remaining 83.2% of the data pairs are concentrated along the 1:1 grey line.



[\(Return to Content\)](#)

**9.6. Surface Pressure:** The daily mean surface pressure is taken directly from the re-gridded MERRA-2 and represents estimates of the atmospheric pressure at 2m above the local surface averaged over a 0.5° latitude x 0.5° longitude grid. Figure 9.6.1a shows the scatter plot of the MERRA-2 un-corrected pressure vs. daily values taken from station observations reported in the NCEI GSOD files. The scatter plot includes daily values for every 3<sup>rd</sup> year from 1981 – 2014 (e.g. 1981, 1984, 1987, etc.). The legend in the upper left corner of each scatter plot gives the mean Bias and RMSE ([eqs. A.5 & A.6](#)) along with the Slope, intercept, and Pearson correlation coefficient associated with the linear least squares fit to the plotted values (black line). The grey color line is the 1:1 line.

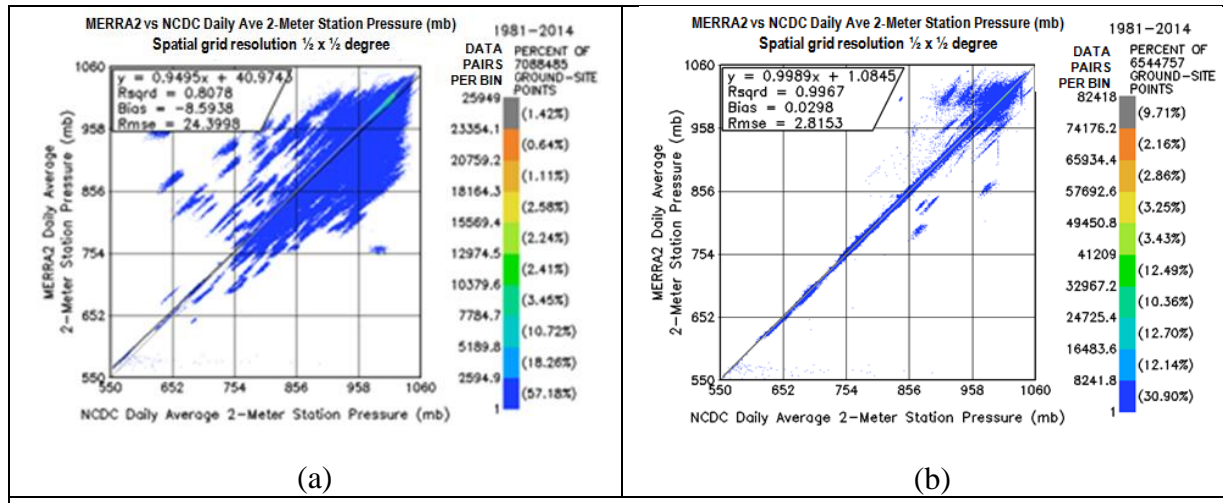


Figure 9.6.1a shows the scatter plot of the MERRA-2 un-corrected pressure vs. daily values taken from station observations reported in the NCEI GSOD files. Panel b shows the MERRA-2 corrected using the hypsometric equation to account for site grid box elevation differences (see text below). The scatter plot includes daily values for every 3<sup>rd</sup> year from 1981 – 2014 (e.g. 1981, 1984, 1987, etc.). The legend in the upper left corner of each scatter plot gives the mean Bias and RMSE ([eqs. A.5 & A.6](#)) along with the Slope, intercept, and Pearson correlation coefficient associated with the linear least squares fit to the plotted values (black line). The color bar along the right side of the scatter plot provides a measure of the frequency of the NCEI/MERRA-2 surface pressure pairs per bin in figure space (bins are 1 mb). The grey color line is the 1:1 line.

Recall that the elevation of the MERRA-2 grid box is the mean elevation of the earth's surface under the grid. In complex terrain one might expect to see a difference between the MERRA-2 elevation and that of the surface site resulting in a difference between the MERRA-2 pressure and that reported by the surface site. Figure 9.6.1b illustrates the improvements in the agreement between the MERRA-2 estimates of pressure and observational data by adjusting the MERRA-2 pressure using the hypsometric equation. The hypsometric equation (9.6.1), relates the thickness ( $h$ ) between two isobaric surfaces to the mean temperature ( $T$ ) of the layer as:

$$(9.6.1) \quad h = z_1 - z_2 = (RT/g)\ln(p_1/p_2)$$

where:

$z_1$  = elevation of the MERRA-2 grid

$z_2$  = elevation of the reporting surface site

$p_1$  = MERRA-2 pressure

$p_2$  = Station pressure

$R$  = gas constant for dry air, and

$g$  = gravitational constant

T = Temperature at Mid-point between  $z_1$  and  $z_2$

Solving equation 9.6.1 for  $p_2$  and substituting the known values for  $z_1$ ,  $z_2$ ,  $p_1$ ,  $R$ , and  $g$ , gives the adjusted MERRA-2 surface pressure ( $p_2$ ) at the elevation of the NCEI surface site. Comparing the unadjusted and adjusted surface pressure statistics in Figure 9.6.1, there is an increase in  $R_{sqrd}$  (0.8078 vs 0.9967) and decrease in Bias (-8.5938 vs 0.0298) and RMSE (24.3998 vs 2.8153). Also note the lowest 10% data pair per bin, which represents the largest part of the scatter (dark blue color), in the adjusted surface pressure Figure 9.6.1 (b) ranges from 0 to 8241.8 and represents 30.90% of the overall data pairs. The equivalent data pair per bins in the unadjusted surface pressure Figure 9.6.1 (a) covers the lowest 30% ranging from 0 to 7784.7 and representing 86.16% of the overall data pairs. Therefore, the pressure adjusting method decreased the largest part of the scatter (dark blue color) from 86.16% to 30.90%.

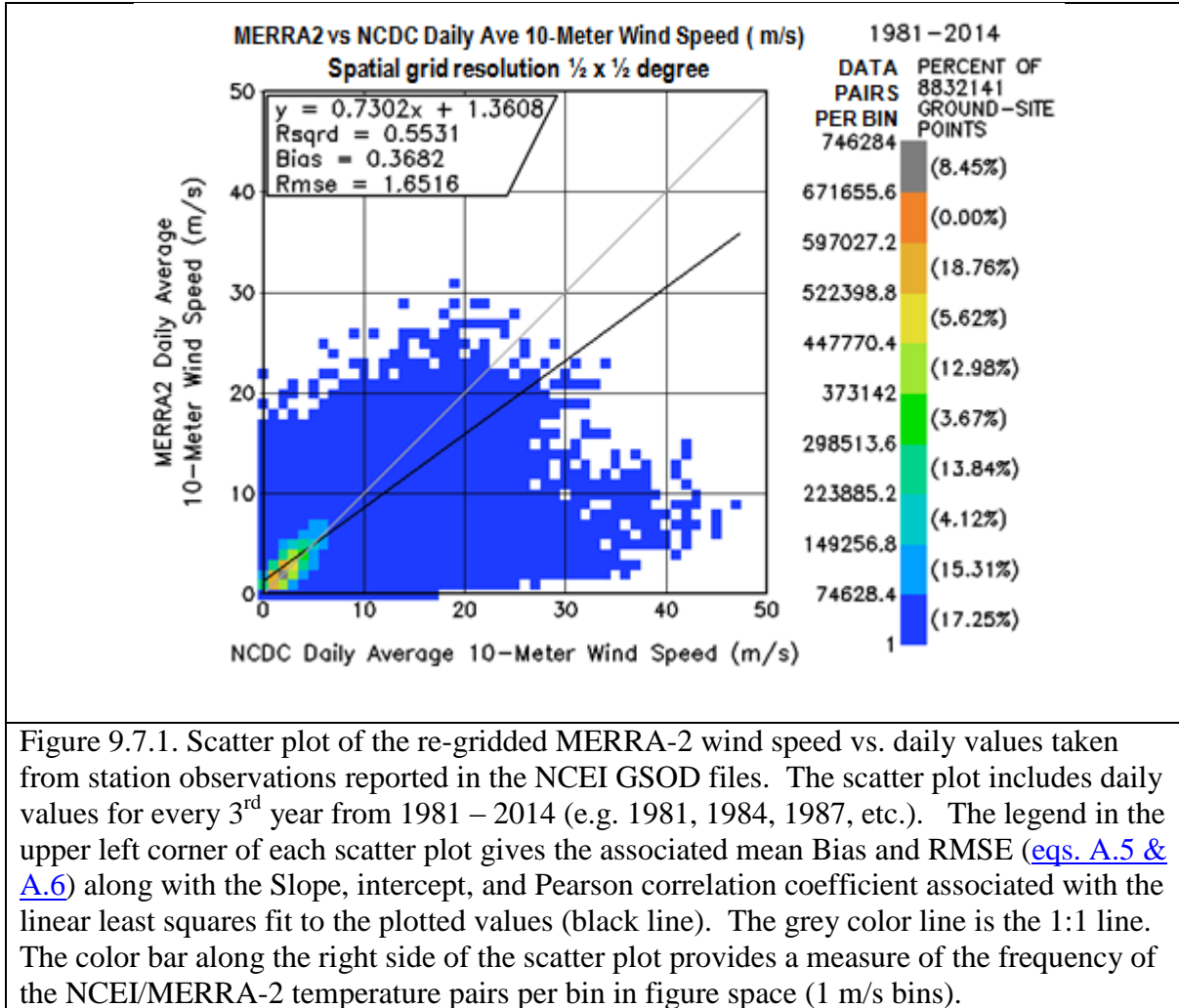
The color bar along the right side of the scatter plot provides a measure of the distribution of the NCEI, MERRA-2 specific humidity pairs in bins of 1 mb. For example, in Figure 9.6.1b, the left column along the vertical color bar shows that each data point in dark blue represents the number ground site/MERRA-2 data pairs within 10% (i.e.,  $\leq 8241.8$ ) of the maximum number of data pairs within a 1g/kg bins in the figure space (i.e., 82418). Additionally, from the right side of the vertical color bar it can be seen that all the points shown in dark blue contain 30.9% of the total number of ground site, MERRA-2 data pairs (6,209,425). The remaining 69.1% of the data pairs are concentrated along the 1:1 grey line.

It is noted here that POWER Release-8 provides the corrected pressure.

[\(Return to Content\)](#)

**9.7 Wind Speed:** The daily means winds are taken from MERRA-2 and represents estimates at 2m, 10m, and 50m above the local surface over a  $0.5^{\circ}$  latitude  $\times 0.5^{\circ}$  longitude grid. Figure 9.7.1 shows the scatter plot of the MERRA-2 wind speed at 10m vs. daily values taken from station observations reported in the NCEI GSOD files. The scatter plot includes daily values for every 3<sup>rd</sup> year from 1981 – 2014 (e.g. 1981, 1984, 1987, etc.). The legend in the upper left corner of each scatter plot gives the associated mean Bias and RMSE ([eqs. A.5 & A.6](#)) along with the Slope, intercept, and Pearson correlation coefficient associated with the linear least squares fit to the plotted values (black line). The grey color line is the 1:1 line.

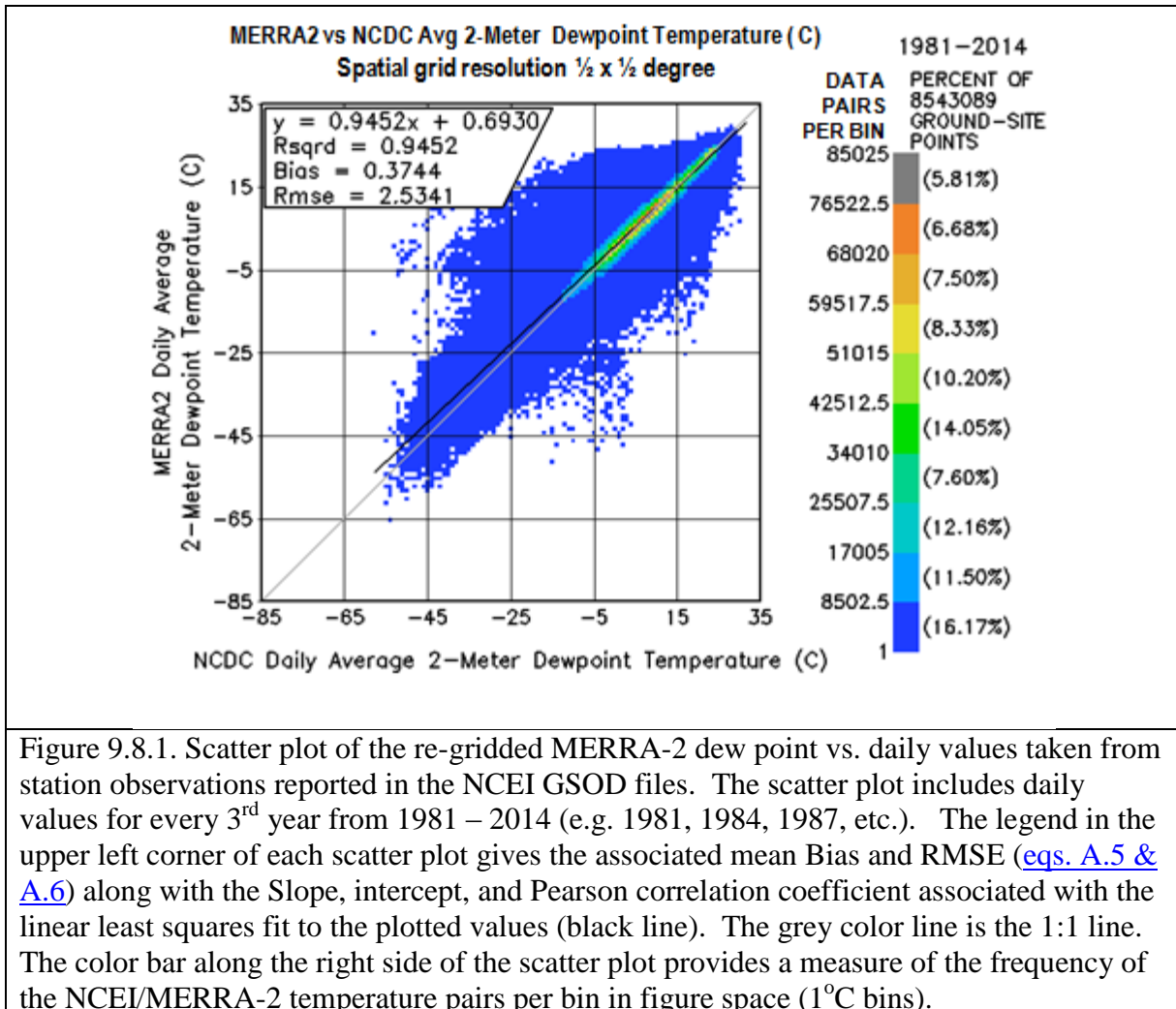
The color bar along the right side of the scatter plot provides a measure of the distribution of the NCEI, MERRA-2 wind speed pairs in bins of 1 m/s. For example, in Figure 9.7.1, the left column along the vertical color bar shows that each data point in dark blue represents the number ground site/MERRA-2 data pairs within 10% (i.e.,  $\leq 74628.4$ ) of the maximum number of data pairs within a 1m/s bins in the figure space (i.e., 746284). Additionally, from the right side of the vertical color bar it can be seen that all the points shown in dark blue contain 17.25% of the total number of ground site, MERRA-2 data pairs (8832141). The remaining 82.75% of the data pairs are concentrated along the 1:1 grey line in the lower left corner for wind speeds  $< 10$ m/s.



[\(Return to Content\)](#)

**9.8 Dew Point:** The daily mean dew point is taken directly from the re-gridded MERRA-2 and represents estimates at 2m above the local surface averaged over a 0.5° latitude x 0.5° longitude grid.

Figure 9.8.1 shows the scatter plot of the MERRA-2 daily averaged dew point temperature vs. the corresponding surface observations reported in the NCEI Global “Summary of the Day” (GSOD) files. The scatter plots are for all surface data meeting our 85% quality control criteria for every 3<sup>rd</sup> year from 1981 – 2014 (e.g. 1981, 1984, 1987, etc.). The legend in the upper left corner of each scatter plot gives the associated mean Bias and RMSE ([eqs. A.5 & A.6](#)) along with the Slope, intercept, and Pearson correlation coefficient associated with the linear least squares fit to the plotted values (black line). The grey color line is the 1:1 line.



The color bar along the right side of the scatter plot provides a measure of the distribution of the NCEI, MERRA-2 dew point pairs in bins of 1°C. For example, in Figure 9.8.1, the left column along the vertical color bar shows that each data point in dark blue represents the number ground site/MERRA-2 data pairs within 10% (i.e., <=8502.5) of the maximum number of data pairs within a 1m/s bins in the figure space (i.e., 85025). Additionally, from the right side of the vertical color bar it can be seen that all the points shown in dark blue contain 16.17% of the total number of ground site, MERRA-2 data pairs (8832141). The remaining 83.83% of the data pairs are concentrated along the 1:1 grey line.

[\(Return to Content\)](#)

**9.9. Heating/Cooling Degree Days:** An important application of historical temperature data is in the evaluation of Heating Degree Days (HDD) and Cooling Degree Days (CDD). The HDD and CDD are based upon the deviation of the daily averaged temperature, typically evaluated as  $(T_{max} + T_{min})/2$ , relative to reference temperature,  $T_{base}$ . The following expressions are used herein for calculating HDD and CDD (Chapter 14 of the ASHRAE 2013):

*Heating Degree Days:* For the days in a given time period (e.g. year, month, etc.)

$$9.9.1 \quad HDD = \bar{A} (T_{base} - \langle T_i \rangle)^+$$

and

*Cooling Degree Days:* For the days in a given time period (e.g. year, month, etc.)

$$9.9.2 \quad CDD = \bar{A} (\langle T_i \rangle - T_{base})^+$$

The “+” superscript in the above equations indicates that only the positive values of the bracketed quantity are taken into account in the sum. The sum is taken from  $i = 1$  to  $N$ , where  $N$  is number of days in the given time period. The POWER provides HDD and CDD values for  $T_{base} = 0^\circ\text{C}$ ,  $10^\circ\text{C}$ , and  $18.3^\circ\text{C}$ .

Figure 9.9.1 shows a scatter plot of the HDD  $T_{base} = 18.3^\circ\text{C}$  calculated via equation 9.9.1 using the MERRA-2 temperatures versus the corresponding HDD values taken from the ASHRAE Weather Data Viewer version 5.0 (WDV 5.0). The WDV values are based upon surface observations over the time period 1986 -2010; the MERRA-2 values correspond the temperature for the MERRA-2 half-degree grid cell over the given surface site. The scatter plot in Figure 9.9.1 encompasses 1,397 surface:grid pairs in the continental US (CONUS) and Alaska. While the overall agreement is good, note the cluster of data point circled in the middle and the upper right portion of the scatter plot. These data are associated with the surface sites shown on maps 1 and 2 in Figure 9.9.2, and are highlighted to call attention to two aspects of the MERRA-2 data that can be problematic depending on the application. Recall that the MERRA-2 values represent the average over a  $0.5^\circ$  latitude by  $0.5^\circ$  longitude grid. Accordingly, in mountainous regions (e.g. map 1) the average elevation of the MERRA-2 cell can be significantly different from the elevation of the local surface site. Similarly, in regions where the surface temperatures may have strong horizontal gradients, such as near coast lines (e.g. map 2) the average temperature of the MERRA-2 cell can be different than the local station. Figure 9.9.3 shows the scatter plot and associated statistics for the same stations used in Figure 9.9.1 when the elevation difference between the surface site and the MERRA-2 grid is less than 100 meters. Figures 9.9.4 (a) and (b) show the corresponding scatter plots for CDD with  $T_{base} = 10^\circ\text{C}$ .

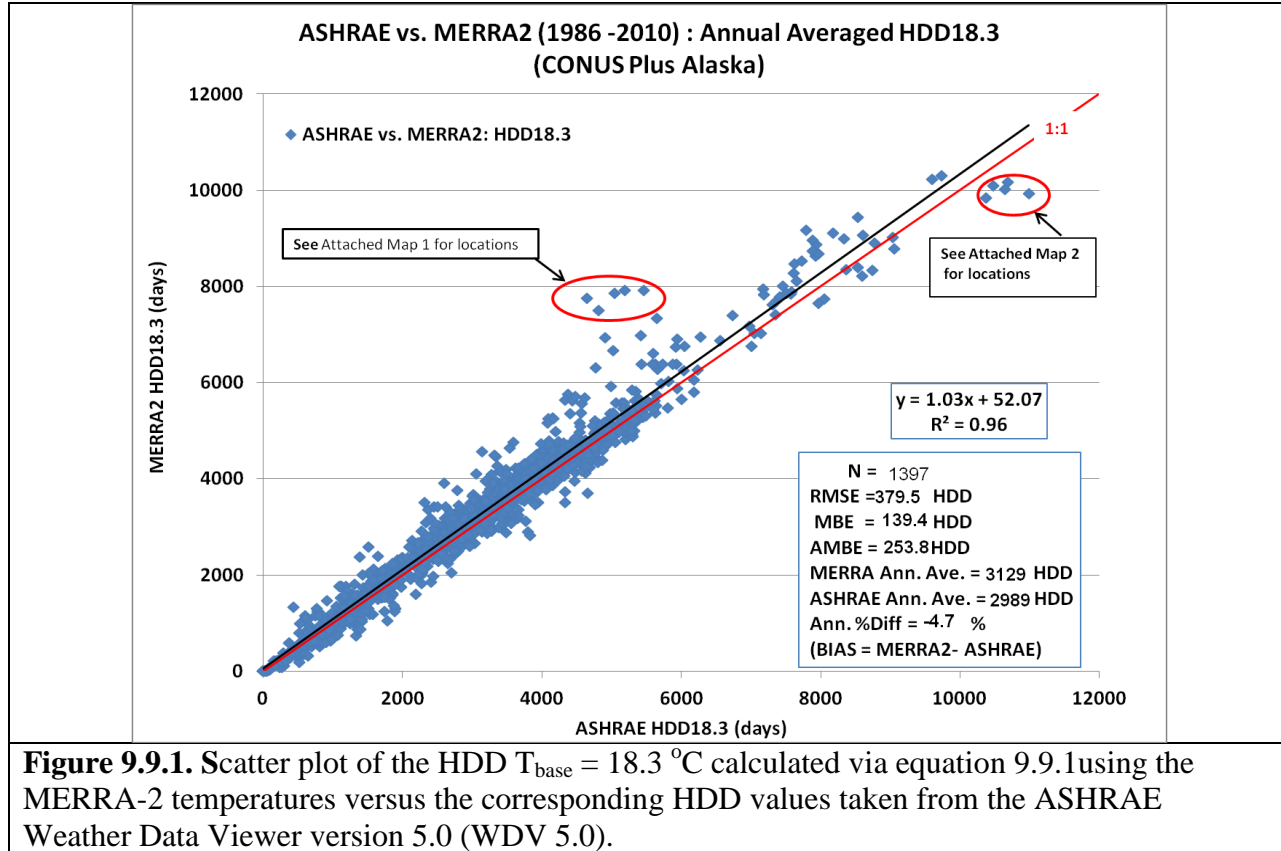


**Figure 9.9.1.** Scatter plot of the HDD  $T_{base} = 18.3^{\circ}\text{C}$  calculated via equation 9.9.1 using the MERRA-2 temperatures versus the corresponding HDD values taken from the ASHRAE Weather Data Viewer version 5.0 (WDV 5.0).

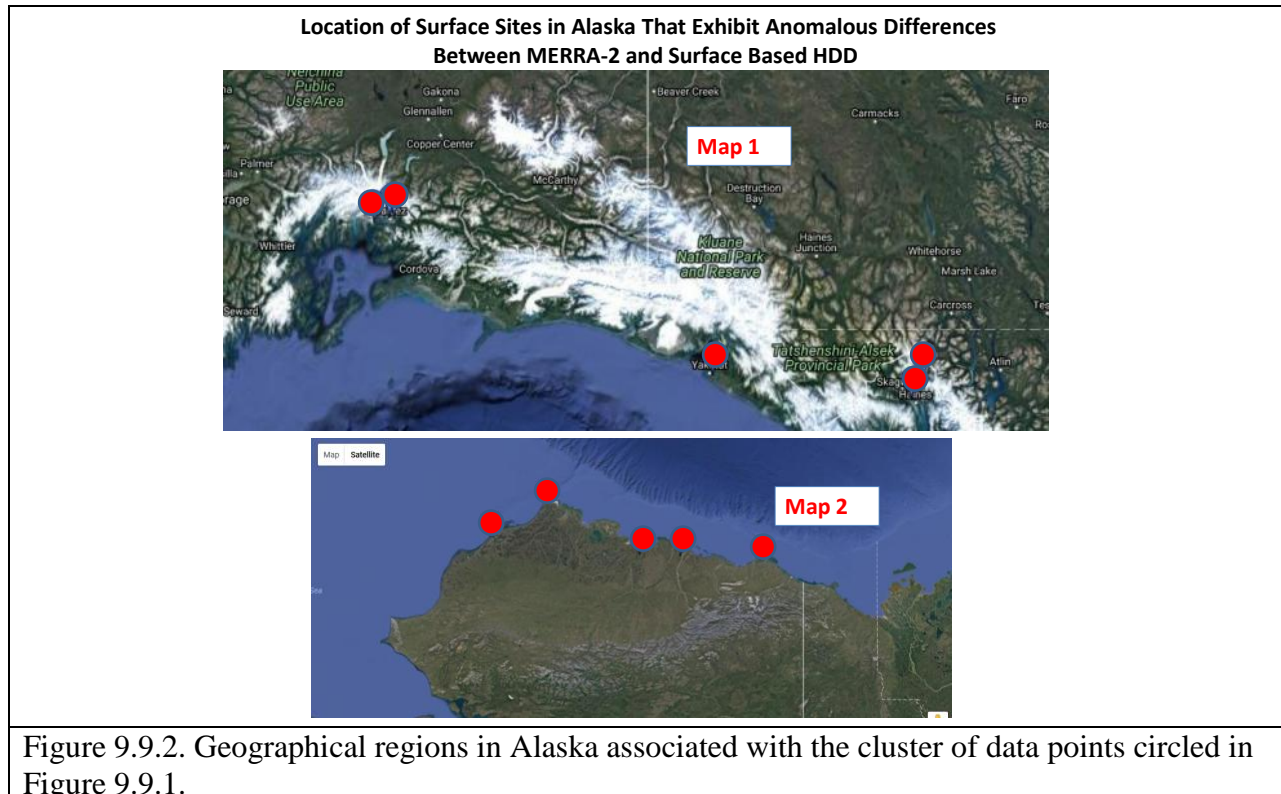


Figure 9.9.2. Geographical regions in Alaska associated with the cluster of data points circled in Figure 9.9.1.

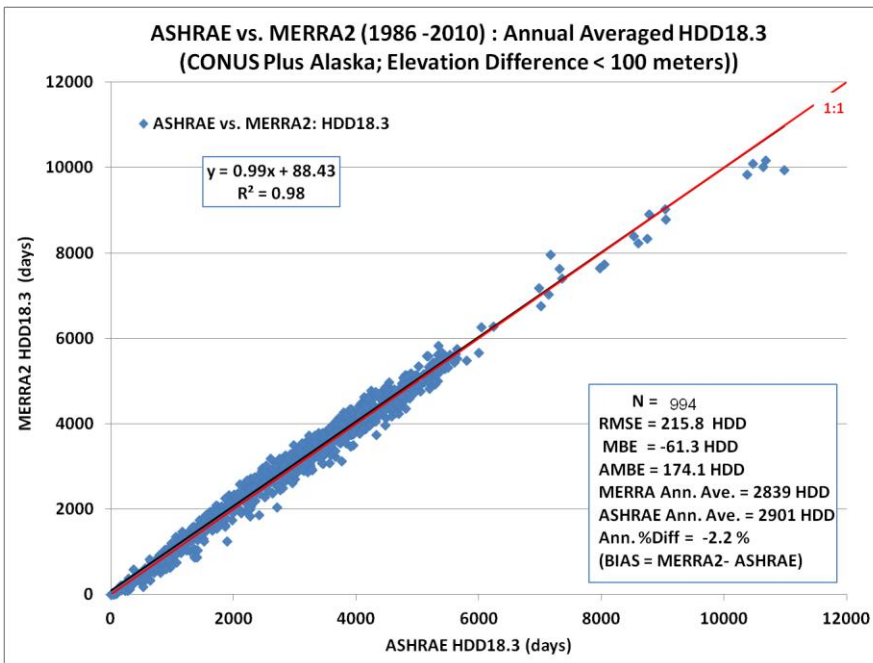
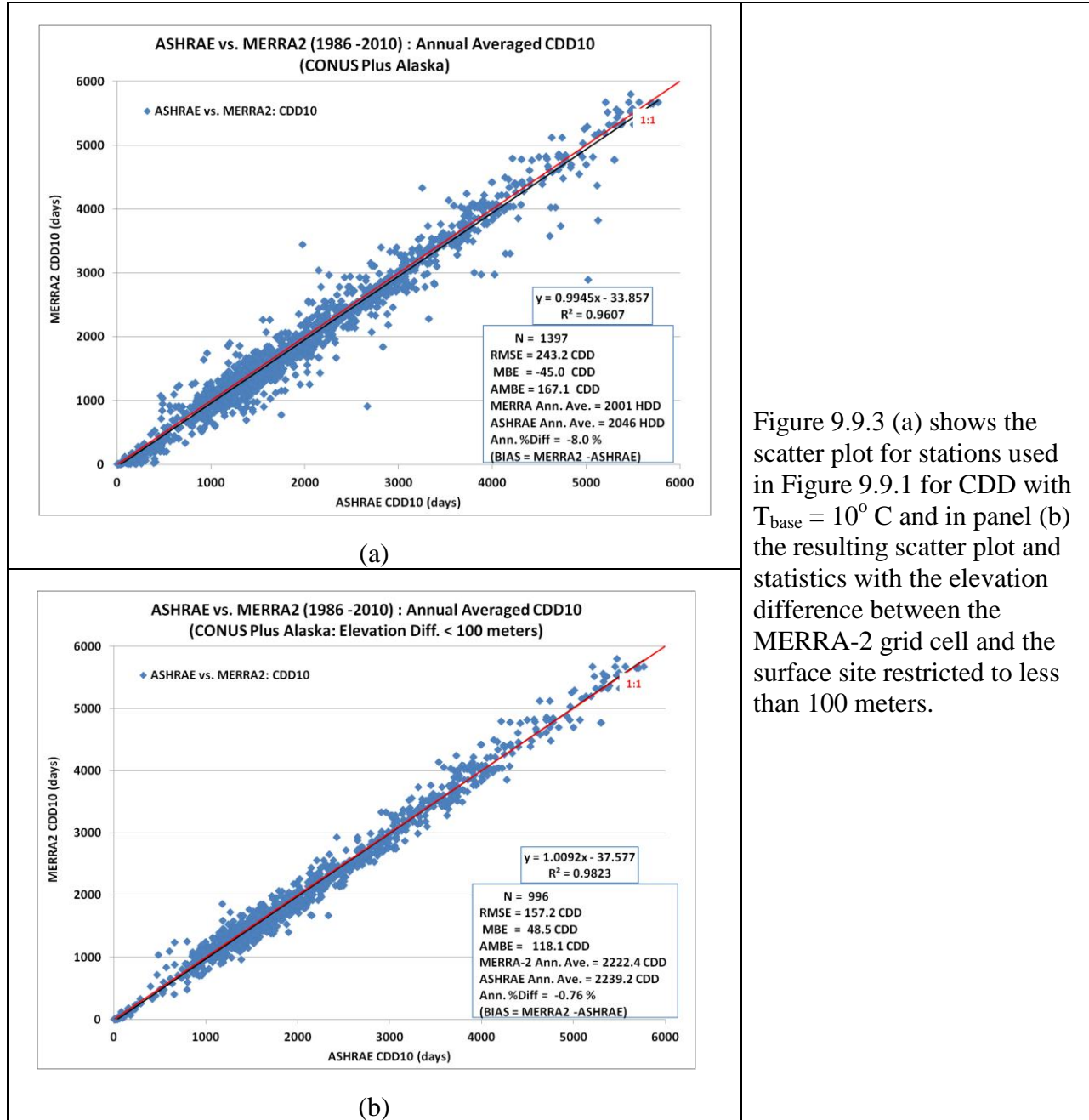


Figure 9.9.3. Scatter plot and associated statistics for the same stations used in Figure 9.9.1 when the elevation difference between the surface site and the MERRA-2 grid is less than 100 meters.

---



[\(Return to Content\)](#)

**9.10 Cloud Amount:** The cloud cover information enumerated below is produced using cloud information derived from International Satellite Cloud Climatology Project (ISCCP - <https://isccp.giss.nasa.gov/>) DX-pixel level cloud products. As with the solar data, the cloud cover information is initially generated by the Solar radiation Budget project on a global  $1^\circ \times 1^\circ$  latitude, longitude grid and then re-scaled  $0.5^\circ \times 0.5^\circ$  by replication of the  $1^\circ$  value to the four  $0.5^\circ$  grids within the  $1^\circ$ -grid. The percentage of cloud cover is computed as the number of pixels

in the  $1^{\circ}$ -grid containing clouds divided by the total number of pixels in the  $1^{\circ}$ -grid. The percentage of cloud cover is computed on 3-hourly time increments for a given month and then averaged over the climatological to yield the climatological averaged for each month.

The following monthly climatologically averaged cloud cover information is provided through the Renewable Energy (SSE) and Sustainable Building (SB) section of the POWER data portal for GMT times of 0, 3, 6, 9, 12, 15, 18, and 21 hours”

1. Monthly Averaged Daylight Cloud Amount
2. Monthly Averaged Cloud Amount
3. Monthly Averaged Frequency Of Clear Skies (i.e. cloud  $\leq 10\%$ )
4. Monthly Averaged Frequency Of Broken-cloud Skies (i.e. cloud cover 10 – 70%)
5. Monthly Averaged Frequency Of Near-overcast Skies (i.e. Cloud Cover  $\geq 70\%$ )

[\(Return to Content\)](#)

## 10. References

ASHRAE Handbook – Fundamentals 2013. Atlanta, GA: American Society of Heating, Refrigerating and Air-Conditioning Engineers, Inc

Bai, Jinshun, Xinpeng Chen, Achim Dobermann, Haishun Yang, Kenneth G Cassman, Fusuo Zhang- [Evaluation of NASA satellite-and model-derived weather data for simulation of maize yield potential in China](#) Agronomy Journal, 102, pp9-16, 2010

Bloom, S., A. da Silva, D. Dee, M. Bosilovich, J.-D. Chern, S. Pawson, S. Schubert, M. Sienkiewicz, I. Stajner, W.-W. Tan, M.-L. Wu, Documentation and Validation of the Goddard Earth Observing System (GEOS) Data Assimilation System - Version 4, Technical Report Series on Global Modeling and Data Assimilation, NASA/TM—2005-104606, Vol. 26, 2005

Braun, J. E. and J. C. Mitchell, Solar geometry for fixed and tracking surfaces, Solar Energy (ISSN 0038-092X), vol. 31, no. 5, 1983, p. 439-444.

**DOI:** [10.1016/0038-092X\(83\)90046-4](https://doi.org/10.1016/0038-092X(83)90046-4)

Bosilovich, M. G., F. R. Robertson, L. Takacs, A. Molod, and D. Mocko, 2016. Atmospheric Water Balance and Variability in the MERRA-2 Reanalysis. J. Clim. - Special MERRA-2 Collection. doi: [10.1175/jcli-d-16-0338.1](https://doi.org/10.1175/jcli-d-16-0338.1)

Collares-Pereira, M. and Rabl, A. (1979) The Average Distribution of Solar Radiation- Correlations between Diffuse and Hemispherical and between Daily and Hourly Insolation Values. Solar Energy, 22, 155-164. [http://dx.doi.org/10.1016/0038-092X\(79\)90100-2](http://dx.doi.org/10.1016/0038-092X(79)90100-2)

Cooper, P. I. (1969), The Absorption of solar radiation in solar stills. Solar Energy 12, 3 (1969)

Ebert, E.E., 2007, Methods for Verifying Satellite Precipitation Estimates. Measuring Precipitation from Space: EURAINSAT and the Future, Chapter 27, pp. 345-356, Copyright 2007 Springer.

Flatau, J. Piotr, Robert L. Walko, and William R. Cotton, 1992: *Polynomial Fits to Saturation Vapor Pressure*. Notes and Correspondence, Journal of Applied Meteorology. 1507-1513.

Fu, Q. and K. N. Liou, 1992; On the correlated k-distribution method for radiative transfer in nonhomogeneous atmospheres. Journal of the Atmospheric Sciences, **49**, 2139-2156.

Gupta, S. K., 1989: A Parameterization for Longwave Surface Radiation From Sun-Synchronous Satellite Data. J. Climate, 2 , 305-320.

Gupta, S. K., W. L. Darnell, and A. C. Wilber, 1992: A Parameterization of Longwave Surface Radiation From Satellite Data: Recent Improvements. J. Appl. Meteorol. , 31 , 1361-1367.

Gupta, S. K., D. P. Kratz, P. W. Stackhouse, Jr., and A. C. Wilber, 2001: The Langley Parameterized Shortwave Algorithm (LPSA) for Surface Radiation Budget Studies. NASA/TP-2001-211272, 31 pp. Available on-line at: <http://ntrs.nasa.gov/search.jsp>

Iribarne, J.V. and W.L. Godson, 1981: *Atmospheric Thermodynamics*. Geophysics and Astrophysics Monographs, D. Riedel Publishing Company, Dordrecht, Netherlands.

Jupp, D. L. B.; 2003, Calculating and converting between common water vapour measures in meteorological data and their use in support of earth observation validation, CSIRO Earth Observation Centre Technical Report, 2003/01.

Klein, S.A., 1977: Calculation of monthly average insolation on tilted surfaces. Solar Energy, Vol. 19, pp. 325-329.

Kratz, D. P., S. K. Gupta, A. C. Wilber, and V. E. Sothcott, 2010: Validation of the CERSEdition 2B surface-only flux algorithm. *J. Appl. Meteor. Climatol.*, **49**, 164–180,doi:10.1175/2009JAMC2246.1. (<https://doi.org/10.1175/2009JAMC2246.1>)

Kratz, David P. , Paul W. Stackhouse Jr., Shashi K. Gupta, Anne C. Wilber, Parnchai Sawaengphokhai, and Greg R. McGarragh, The Fast Longwave and Shortwave Flux (FLASHFlux) Data Product: Single-Scanner Footprint Fluxes, *Journal of Applied Meteorology and Climatology* April 2014, Vol. 53, No. 4

Liu, B. and Jordan, R. (1960) The Interrelationship and Characteristic Distribution of Direct, Diffuse and Total Solar Radiation. Solar Energy, 4, 1-19. [http://dx.doi.org/10.1016/0038-092X\(60\)90062-1](http://dx.doi.org/10.1016/0038-092X(60)90062-1)

Molod, A., L. Takacs, M.J. Suarez, J. Bacmeister, I.S. Song, A. Eichmann, Y. Chang, 2011: The GEOS-5 Atmospheric General Circulation Model: Mean Climate and Development from MERRA to Fortuna. Technical Report Series on Global Modeling

and Data Assimilation 104606 , v28.

Molod, A., L. Takacs, M.J. Suarez, J. Bacmeister, I.S. Song: Development of the GEOS-5 atmospheric general circulation model: evolution from MERRA to MERRA2; Geosci. Model Dev., 8, 1339-1356, 2015 (<https://doi.org/10.5194/gmd-8-1339-2015> )

Ohmura, A., E. Dutton, B. Forgan, C. Frohlich, H. Gilgen, H. Hegne, A. Heimo, G. Konig-Langlo, B. McArthur, G. Muller, R. Philipona, C. Whitlock, K. Dehne, and M. Wild, 1998: Baseline Surface Radiation Network (BSRN/WCRP): New precision radiometry for climate change research. Bull. Amer. Meteor. Soc. 79 No. 10, 2115-2136 ([doi:10.1175/1520-0477\(1998\)079<2115:bsrnbw>2.0.CO;2](https://doi.org/10.1175/1520-0477(1998)079<2115:bsrnbw>2.0.CO;2))

Pinker, R., and I. Laszlo, 1992: Modeling Surface Solar Irradiance for Satellite Applications on a Global Scale. *J. Appl. Meteor.*, 31, 194–211.

Rasch, P. J. N. M. Mahowald, B. E. Eaton , Representations of transport, convection, and the hydrologic cycle in chemical transport models: Implications for the modeling of short-lived and soluble species, Volume 102, Issue D23 20 December 1997 Pages 28127–28138

RETScreen: Clean Energy Project Analysis: RETScreen® Engineering & Cases Textbook, Third Edition, Minister of Natural Resources Canada, September 2005.  
[https://eclasse.teicrete.gr/modules/document/file.php/PEGA-FV105/RETSCREEN\\_Textbook\\_PV.pdf](https://eclasse.teicrete.gr/modules/document/file.php/PEGA-FV105/RETSCREEN_Textbook_PV.pdf) , Clean Energy Project Analysis: RETScreen Engineering & Cases Textbook, ISBN: 0-662-35672-1, Catalogue no.: M39-99/2003E-PDF).

Rienecker, M.M., M.J. Suarez, R. Todling, J. Bacmeister, L. Takacs, H. C. Liu, W. Gu, M. Sienkiewicz, R.D. Koster, R. Gelaro, I. Stajner, and E. Nielsen, 2008: The GEOS-5 Data Assimilation System -Documentation of Versions 5.0.1, 5.1.0, and 5.2.0. Technical Report Series on Global Modeling and Data Assimilation 104606, V27.

Rienecker, Michele M., Max J. Suarez, Ronald Gelaro, Ricardo Todling, Julio Bacmeister, Emily Liu, Michael G. Bosilovich, Siegfried D. Schubert, Lawrence Takacs, Gi-Kong Kim, Stephen Bloom, Junye Chen, Douglas Collins, Austin Conaty, Arlindo da Silva, Wei Gu, Joanna Joiner, Randal D. Koster, Robert Lucchesi, Andrea Molod, Tommy Owens, Steven Pawson, Philip Pegion, Christopher R. Redder, Rolf Reichle, Franklin R. Robertson, Albert G. Ruddick, Meta Sienkiewicz, and Jack Woollen, 2011: MERRA: NASA's Modern-Era Retrospective Analysis for Research and Applications. *J. Climate*, **24**, 3624–3648. (doi: <http://dx.doi.org/10.1175/JCLI-D-11-00015.1>)

Rossow, William B. and Robert A. Schiffer, 1999, Advances in Understanding Clouds from ISCCP, BAMS, 80, 2261-2287 ([https://doi.org/10.1175/1520-0477\(1999\)080<2261:AIUCFI>2.0.CO;2](https://doi.org/10.1175/1520-0477(1999)080<2261:AIUCFI>2.0.CO;2)).

Smith, G. L., R. N. Green, E. Raschke, L. M. Avis, B. A. Wielicki, and R. Davies, "Inversion Methods for Satellite Studies of the Earth's Radiation Budget: Development of Algorithms for the ERBE Missions." *Rev. of Geophys.* 24:407-421, 1986

Stackhouse, P. W., S. K. Gupta, S. J. Cox, T. Zhang, J. C. Mikovitz, and L. M. Hinkelmann, 2011: 24.5- Year SRB Data Set Released. GEWEX News, 21 , No. 1, 10-12.

White, Jeffery W., G. Hoogenboom, P.W. Stackhouse, J.M. Hoell, 2008: [Evaluation of NASA satellite- and assimilation model-derived long-term daily temperature data over the continental US](#). Agricultural and Forest Meteorology, Vol. 148, pp. 1574-1584, doi:10.1016/j.agrformet.2008.05.017

White, Jeffery W., G. Hoogenboom, P.W. Wilkens, P.W. Stackhouse, J.M. Hoell, 2011: [Evaluation of Satellite-Based, Modeled-Derived Daily Solar Radiation Data for the Continental United States](#). Agronomy Journal, Vol. 103(4), pp. 1242-1251

Wilber, A. C., D. P. Kratz, and S. K. Gupta, 1999: Surface emissivity maps for use in satellite retrievals of longwave radiation. NASA/TP -1999-209362 , 35 pp.

Whitlock, Charles H., W.S. Chandler, J.M. Hoell, T. Zhang, P.W. Stackhouse, Jr., 2005: [Parameters for Designing Back-Up Equipment for Solar Energy Systems](#). Proceedings of the International Solar Energy Society 2005 Solar World Congress, Orlando, Florida

Yates, E., A. Sandrine, V. Ducrocq, J.D. Creutin, D. Ricard, and K. Chancibault, 2006: Point and areal validation of forecast precipitation fields. Meteorol. Appl. Vol. 13, pp. 1-20

[\(Return to Content\)](#)

## Appendix A Validation Methodology

The validation of the SSE parameters available is based upon comparisons of the SSE primary parameters parameter to surface observations of the corresponding parameters and where possible comparisons of the SSE parameters calculated using the primary data to the corresponding parameters calculated using surface observations of the corresponding primary parameters. Examples of primary parameters comparisons include the SSE solar and temperature values compared to surface observations; while comparisons of relative humidity and heating-degree- days typify comparisons of calculated parameters using the SSE primary data and the corresponding ground based observational data.

Statistics associated with the SSE vs. surface based values are reported to provide users with information necessary to assess the applicability of the SSE data to their particular project. Scatter plots of the SSE parameter vs. surface based values along with the correlation and accuracy parameters for each scatter plots are typically provided. The statistical parameters associated with a linear least squares fit to the respective scatter plots that are reported include: Pearson's correlation coefficient; the Bias between the mean of the respective SSE parameter and the surface observations; the root mean square error (RMSE) calculated as the root mean square difference between the respective SSE and observational values. Additional parameters typically provided are the variance in the SSE and observational data and the number of SSE:observational data pairs.

The following are the expressions used to calculate the statistical parameters:

The Pearson's correlation coefficient is calculated using expressions taken from (REF)

$$(1) \quad r = r_{xy} = \frac{\sum x_i y_i - n \bar{x} \bar{y}}{(n - 1) s_x s_y}$$

where:

$n$  = number of data samples

$x_i$  and  $y_i$  represent the surface and SSE data respectively

$$\bar{x} = \frac{1}{n} \sum_{i=1}^n x_i$$

is the sample mean and analogously for  $\bar{y}$

$$s_x = \sqrt{\frac{1}{n-1} \sum_{i=1}^n (x_i - \bar{x})^2}$$

is the standard deviation of sample  $x_i$  and similarly for  $y_i$

The expression for the mean Bias between SSE *Parm* values and observations of *Parm* at a single surface site,  $j$ , is given as:

$$(1) (\text{Bias})^j = \left\{ \sum_i \{[(\text{Parm}_i^j)_{\text{SSE}} - (\text{Parm}_i^j)_{\text{Sur}}]\} \right\} / n$$

Where

$i$  = day within given time period

$j$  = site number

$n$  = number of data pairs within given time period

$\sum_i$  = sum over all data pairs at site  $j$

The expression for the mean Bias for multiple surface sites is given as:

$$(2) \text{Bias} = \left\{ \sum_i (\text{Bias})^j \right\} / N$$

Where the sum  $\sum_i$  is over all sites

$N$  = total number of sites

The expression for the RMSE between for SSE parameter, *Parm*, and surface observation of *Parm* at a single site  $j$  is given as

$$(1) (\text{RMSE})^j = \left\{ \left\{ \sum_i [(\text{Parm}_i^j)_{\text{SSE}} - (\text{Parm}_i^j)_{\text{Sur}}]^2 \right\} / n \right\}^{1/2},$$

And the RMSE for multiple sites'

$$(3) \text{RMSE} = \left\{ \sum_i (\text{RMSE})^j \right\} / N$$

Standard Deviation:

$$\sigma = \sqrt{\frac{1}{N} \sum_{i=1}^N (x_i - \mu)^2}$$

Where

$\mu$  = mean of sample

$x_i$  = individual values of SSE or observational values

[\(Return to Content\)](#)

## Appendix B Averaging Methodology

**Methodology for calculating monthly, annual & climatologically averaged parameters:** In general, daily averages were calculated for local solar time and stored using 3-hourly data from the Global Modeling and Assimilation Office (*GMAO*) data archive for the meteorological parameters and from the NASA/GEWEX Surface Radiation Budget Release-3.0 data sets for the solar parameters. Monthly averages by year were calculated from the dailies; annual averages, by year, were calculated from the monthly averages for the given year (i.e. the sum of the monthly averages divided by the number of months in the year, typically 12); climatologically (22-year) averages for a given month (e.g. multi-year monthly averages) were calculated as a sum of the monthly averages divided by the number of months (i.e. typically 22); climatologically annual averages were calculated as a sum of the climatologically averaged monthly averages divided by the number of months (typically 12).

The daily average of parameter *Parm* for day i, in month j, and year k is given by:

$$\langle \text{Parm} \rangle_{ijk} = \left( \sum_{h=1}^N \langle \text{Parm} \rangle_h \right) / N$$

Where

$$\langle \text{Parm} \rangle_h$$

Is the average values of *Parm* over the 3-hour period h and N = number of 3-hourly values for the given day.

The monthly average by year of parameter *Parm* for month j in year k is given by:

$$\langle \text{Parm} \rangle_{jk} = \left( \sum_{i=1}^d \langle \text{Parm} \rangle_{ijk} \right) / d$$

Where

$$\langle \text{Parm} \rangle_{ijk}$$

Is the daily average of parameter *Parm* for day i, in month j and year k and d = number of days in month j.

The annual average of Parameter *Parm* for year k is given by

$$\langle \text{Parm} \rangle_k = \left( \sum_{j=1}^m \langle \text{Parm} \rangle_{jk} \right) / m$$

Where

$$\langle \text{Parm} \rangle_{jk}$$

Is the monthly average of parameter *Parm*, for month j and in year k and m = number monthly averages in year k.

The climatologically monthly average (i.e. multi-year monthly average) of parameter *Parm* for month j over n years is given by:

$$\langle \text{Parm} \rangle_j = \left( \sum_{k=1}^n \langle \text{Parm} \rangle_{jk} \right) / n$$

Where

$$\langle \text{Parm} \rangle_{jk}$$

Is the monthly average of parameter *Parm* for month j, in year k and n = number of years in climate time period.

[\(Return to Content\)](#)

## APPENDIX C: Solar Geometry

The solar geometry parameters useful for designing and application of solar panels are available for each User defined Latitude/Longitude. These parameters and equations used to calculate each parameter are given below.

### C-1. Monthly Averaged Solar Noon (GMT time)

$$SN = 60 * hr + mn + 4 * (\text{lon} - \text{merid}) + 60 * \text{lon} / 15.0$$

SN= Solar Noon

lon = local longitude (user input); positive = East; negative West

merid = meridian through local time zone; positive = East; negative West

hr = hour

mn = minute

Return to [Solar Geometry](#) Section

### C-2. Monthly Averaged Daylight Hours (hours)

From John A. Duffie and William A. Beckman, Solar Engineering of Thermal Process 3<sup>rd</sup> Edition, Wiley, Aug 25, 2006 - [Technology & Engineering](#) - 928 pages

$$\text{daylight[mo]} = (\text{sMAM} - \text{rMAM}) / 60.0$$

Where:

daylight[mo] – daylight hours for given month

$$\text{sMAM} = \text{int}(12.0 * 60.0 + \text{RS} - (4.0 * (\text{lon} - \text{merid})) - \text{eotA});$$

$$\text{rMAM} = \text{int}(12.0 * 60.0 - \text{RS} - (4.0 * (\text{lon} - \text{merid})) - \text{eotA});$$

$$\text{eotA} = (\text{L} - \text{C} - \text{alpha}) / 15.0 * 60.0$$

$$\text{alpha} = L - 2.466 * \sin(2.0 * L) + 0.053 * \sin(4.0 * L)$$

$$\begin{aligned} L &= (280.460 + (36000.770 * t) + C) \\ &- \text{int}((280.460 + (36000.770 * t) + C) / 360.0) * 360.0 \end{aligned}$$

$$C = (1.915 * \sin(G)) + (0.020 * \sin(2.0 * G))$$

$$\begin{aligned} G &= (357.528 + 35999.05 * t) \\ &- \text{int}((357.528 + 35999.05 * t) / 360.0) * 360.0 \end{aligned}$$

$$\begin{aligned} t &= ((\text{MAM} / 60.0 / 24.0) + dy + \text{int}(30.6 * cM + 0.5) \\ &+ \text{int}(365.25 * (cY - 1976.0)) - 8707.5) / 36525.0 \end{aligned}$$

$$RS = -1 * (\sin(\Phi) * \sin(\xi) - \sin((-0.8333 - 0.0347 * (\text{El})^{1/2})) / \cos(\Phi) / \cos(\xi))$$

Where:

RS = Sunrise-to-Sunset Local Solar time (Minutes)

If  $|RS| \leq 1.0$   $RS = \text{acos}(RS) * 4$

If  $|RS| > 1.0$   $RS = 0.0$

Where

.  $\delta$  = Declination angle for the monthly averaged day

.  $\Phi$  = Latitude

. El = Elevation

. dy = monthly average day

. cy = calendar year

. merid = solar time based upon  $15^0$  of longitude per hour

Return to [Solar Geometry](#) Section

### C-3. Monthly Averaged Of Hourly Cosine Solar Zenith Angles (dimensionless)

$$\text{Average cos}(\Theta_Z) = \{f \cos^{-1}(-f/g) + g[1 - (f/g)^2]^{1/2}\} / \cos^{-1}(-f/g)$$

where:

$\Theta_Z$  = angle between the sun and directly overhead during daylight hours

f =  $\sin(\text{latitude}) * \sin(\text{solar declination})$

g =  $\cos(\text{latitude}) * \cos(\text{solar declination})$

Solar declination for each month is based upon the monthly average day (see [Table 7.2](#))

Gupta et al., 2001, *The Langley Parameterized Shortwave Algorithm (LPSA) for Surface Radiation Budget Studies*

Return to [\*\*Solar Geometry\*\*](#) Section

#### **C-4. Monthly Averaged Cosine Solar Zenith Angle At Mid-Time Between Sunrise And Solar Noon (dimensionless)**

$$\cos(\Theta_{ZMT}) = f + g[(g - f) / 2g]^{1/2}$$

where:

$\Theta_{ZMT}$  = Zenith angle at mid-time between sunrise and solar noon

$f = \sin(\text{latitude}) * \sin(\text{solar declination})$

$g = \cos(\text{latitude}) * \cos(\text{solar declination})$

Solar declination for each month is based upon the monthly average day (see [Table 7.2](#))

Gupta et al., 2001, *The Langley Parameterized Shortwave Algorithm (LPSA) for Surface Radiation Budget Studies*

Return to [\*\*Solar Geometry\*\*](#) Section

#### **C-5. Monthly Averaged Declination (degrees)**

$$\delta = 23.45 * \sin\{(360/365)*(284+JD + Hr/24)\}$$

Where

$\delta$  = Declination angle

JD = Julian day

Hr = hour

Reference: P. I. Cooper (1969), The Absorption of solar radiation in solar stills. Solar Energy 12, 3 (1969)

Return to [\*\*Solar Geometry\*\*](#) Section

#### **C-6. Monthly Averaged Sunset Hour Angle (degrees)**

$$\cos(\omega_s) = -\tan(\Phi)\tan(\xi)$$

Where all angles for each month are based upon the monthly average day ([Table 7.2](#))

$\omega_s$  = Sunset Hour angle

$\delta$  = Declination angle

$\Phi$  = Latitude

If  $\text{Cos}(\omega_s) < -1.0$  set  $\text{Cos}(\omega_s) = -1$   
 If  $\text{Cos}(\omega_s) > +1.0$  set  $\text{Cos}(\omega_s) = +1$   
 $\omega_s = \text{acos}\{\tan(\Phi)\tan(\xi)\}$

From John A. Duffie and William A. Beckman, Solar Engineering of Thermal Process 3<sup>nd</sup> Edition, Wiley, Aug 25, 2006 - [Technology & Engineering](#) - 928 pages

Return to [Solar Geometry](#) Section

### C-7. Monthly Averaged Maximum Solar Angle Relative To The Horizon (degrees)

$$\Theta_z = \text{acos}\{\sin(\xi)\sin(\Phi) + \cos(\xi)\cos(\Phi)\cos(\omega)\}$$

Where all angles for each month are based upon the monthly average day (see [Table 7.2](#))

$\Theta_z$  = Zenith angle

$\delta$  = Declination angle

$\Phi$  = Latitude

$\omega$  = Hour angle =  $\text{acos}(\cot(\Phi)\tan(\xi))$

$$\text{Max}(\Theta_z) = 90.0 - \Theta_z$$

J. E. Braun & J. C. Mitchell Solar Geometry for Fixed and Tracking Surfaces, Solar Energy 31, no. 5, pp 339-444 (1983)

Return to [Solar Geometry](#) Section

### C-8. Monthly Averaged Hourly Solar Angles Relative To The Horizon (degrees)

$$\text{ha} = ((\text{MAM} - 12.0 * 60.0) / 4.0)$$

Where all angles for each month are based upon the monthly average day (see [Table 7.2](#))

$\text{ha}$  = Hour Angle

$\text{MAM}$  = Solar Minutes After Midnight

$$\text{MAM} = (\text{iMAM} + (4.0 * (\text{lon} - \text{meridian}) + \text{eotA})) + 24.0 * 60.0$$

$$\text{iMAM} = 60 * \text{hr} + \text{mn};$$

$$\text{eotA} = (\text{L} - \text{C} - \text{alpha}) / 15.0 * 60.0$$

$$\text{alpha} = \text{L} - 2.466 * \sin(2.0 * \text{L}) + 0.053 * \sin(4.0 * \text{L})$$

$L = (280.460 + (36000.770 * t) + C)$   
 $- \text{int}((280.460 + (36000.770 * t) + C) / 360.0) * 360.0$

$G = (357.528 + 35999.05 * t)$   
 $- \text{int}((357.528 + 35999.05 * t) / 360.0) * 360.0$

$C = (1.915 * \sin(G)) + (0.020 * \sin(2.0 * G))$

$t = ((MAM / 60.0 / 24.0) + dy + \text{int}(30.6 * cM + 0.5)$   
 $+ \text{int}(365.25 * (cY - 1976.0)) - 8707.5) / 36525.0$

[Return to Solar Geometry Section](#)

### C-9. Monthly Averaged Hourly Solar Azimuth Angles (degrees)

#azimuthAngle = aziA in Degrees

aziA = RadToDeg \*  $\arccos\left(\frac{\sin(\text{lat}) * \cos(\text{Decl}) - \sin(\text{alt}) * \cos(\text{lat}) * \cos(\text{Decl})}{\cos(\text{alt}) * \cos(\text{lat})}\right)$

Where all angles for each month are based upon the monthly average day (see [Table 7.2](#))

$\Phi$  = Latitude in radians

$\delta$  = Declination angle in radians

ha = hour angle in radians

altA = altitude angle in

altA =  $(\pi/2.0 - \arccos((\cos(\Phi) * \cos(\delta)) * \cos(hA)))$   
 $+ (\sin(\Phi) * \sin(\delta)))$

[Return to Solar Geometry Section](#)

[\(Return to Content\)](#)

## APPENDIX D: Solar Radiation on a Tilted Surface: Old SSE vs New POWER

Below are tables showing the ratio of monthly average, monthly maximum and monthly minimum radiation incident on tilted surfaces calculated and available via the New POWER DAV and API to the values from the old SSE Tables. The ratios calculated for a range of latitudes and for horizontal and vertical surfaces and for surfaces tilted at angles equal to the latitude and latitude plus/minus 15°. With the exception of the vertical surface and the extreme latitude ( $\pm 70^\circ$ ) the values from New POWER are within a few percent to the values in SSE.

Parameter	Ratio of New POWER to SSE Table Values (10.2Nx100.1W)												
	JAN	FEB	MAR	APR	MAY	JUN	JUL	AUG	SEP	OCT	NOV	DEC	ANN
SI_EF_TILTED_SURFACE_NEG5													
SI_EF_TILTED_SURFACE_0	1.00	0.96	1.00	1.00	1.00	1.00	1.00	1.00	1.00	1.00	1.00	1.00	1.00
SI_EF_TILTED_SURFACE_10	1.00	0.95	1.00	1.00	1.00	1.00	1.00	1.00	1.00	1.00	1.00	1.00	1.00
SI_EF_TILTED_SURFACE_25	0.99	0.95	0.99	0.99	0.99	0.99	1.00	1.00	0.99	0.99	1.00	1.00	0.99
SI_EF_TILTED_SURFACE_90	0.91	0.84	0.82	0.71	0.86	0.89	0.88	0.84	0.83	0.87	0.91	0.92	0.87
SI_EF_OPTIMAL	0.99	0.95	1.00	1.00	1.00	1.00	1.00	1.00	1.00	0.99	0.99	0.99	0.99
SI_EF_OPTIMAL_ANG	0.92	0.89	0.92	1.00	-0.91	-0.92	-0.91	-1.00	0.83	0.90	0.91	0.93	0.55
Ratio of POWER/SSE: MAX SRAD;													
SI_EF_MAX_TILTED_SURFACE_NEG5													
SI_EF_MAX_TILTED_SURFACE_0	1.01	1.00	1.00	1.00	1.00	1.00	1.00	1.00	1.00	1.00	1.00	1.00	1.00
SI_EF_MAX_TILTED_SURFACE_10	1.00	1.00	1.00	1.00	1.00	1.00	1.00	1.00	1.00	1.00	1.00	1.00	1.00
SI_EF_MAX_TILTED_SURFACE_25	1.00	0.99	0.99	0.99	0.99	0.99	0.99	0.99	0.99	0.99	0.99	0.99	1.00
SI_EF_MAX_TILTED_SURFACE_90	0.91	0.88	0.82	0.67	0.86	0.90	0.89	0.82	0.81	0.87	0.91	0.92	0.88
SI_EF_MAX_OPTIMAL	0.99	0.99	1.00	1.00	1.00	1.00	1.00	1.00	1.00	1.00	0.99	0.99	1.00
SI_EF_MAX_OPTIMAL_ANG	0.95	0.93	0.93	1.00	0.92	0.87	0.85	0.83	1.00	0.91	0.94	0.93	0.58
Ratio of POWER/SSE: Min SRAD;													
SI_EF_MIN_TILTED_SURFACE_NEG5													
SI_EF_MIN_TILTED_SURFACE_0	1.00	1.00	0.95	1.00	1.00	1.00	0.98	1.00	1.00	1.00	1.00	0.93	0.99
SI_EF_MIN_TILTED_SURFACE_10	1.00	1.00	0.95	1.00	1.00	1.00	0.98	1.00	1.00	1.00	1.00	0.92	0.99
SI_EF_MIN_TILTED_SURFACE_25	0.99	0.99	0.94	0.99	0.99	0.99	0.98	0.99	0.99	0.99	0.99	0.92	0.98
SI_EF_MIN_TILTED_SURFACE_90	0.90	0.88	0.80	0.75	0.87	0.89	0.88	0.85	0.85	0.87	0.90	0.84	0.86
SI_EF_MIN_OPTIMAL	0.99	0.99	0.95	1.00	1.00	1.00	0.98	1.00	1.00	1.00	0.99	0.91	0.98
SI_EF_MIN_OPTIMAL_ANG	0.94	0.89	0.92	1.00	-0.89	-0.89	-0.89	-1.00	0.80	0.88	0.93	0.92	0.61

Parameter	Ratio of New POWER to SSE Table Values (10.2Sx100.1E)												
	JAN	FEB	MAR	APR	MAY	JUN	JUL	AUG	SEP	OCT	NOV	DEC	ANN
SI_EF_TILTED_SURFACE_NEG5													
SI_EF_TILTED_SURFACE_0	1.00	0.96	1.00	1.00	1.00	1.00	1.00	1.00	0.99	1.00	1.00	1.00	0.99
SI_EF_TILTED_SURFACE_10	1.00	0.96	1.00	1.00	1.00	1.00	1.01	1.00	1.00	0.99	0.99	1.00	0.99
SI_EF_TILTED_SURFACE_25	0.99	0.95	0.99	1.00	1.00	1.00	1.00	1.00	0.99	0.99	0.99	0.99	0.99
SI_EF_TILTED_SURFACE_90	0.85	0.77	0.82	0.88	0.92	0.94	0.93	0.91	0.84	0.72	0.83	0.87	0.87
SI_EF_OPTIMAL	1.00	0.96	1.00	1.00	1.00	1.00	1.00	1.00	1.00	0.99	0.99	1.00	0.99
SI_EF_OPTIMAL_ANG	0.85	0.80	1.00	0.95	0.97	0.95	0.94	0.96	1.00	1.00	0.91	0.87	0.56
Ratio of New POWER to SSE Table Values (10.2Sx100.1E)													
SI_EF_MAX_TILTED_SURFACE_NEG5													
SI_EF_MAX_TILTED_SURFACE_0	1.00	1.00	1.00	1.00	1.00	1.00	1.00	1.00	1.00	1.00	1.00	1.00	1.00
SI_EF_MAX_TILTED_SURFACE_10	1.00	1.00	1.00	1.00	1.00	1.00	1.00	1.00	1.00	1.00	1.00	1.00	1.00
SI_EF_MAX_TILTED_SURFACE_25	0.99	0.99	1.00	1.00	1.00	1.00	1.00	1.00	1.00	1.00	0.99	0.99	1.00
SI_EF_MAX_TILTED_SURFACE_90	0.84	0.75	0.80	0.89	0.93	0.94	0.93	0.91	0.84	0.66	0.82	0.87	0.87
SI_EF_MAX_OPTIMAL	0.99	1.00	1.00	1.00	1.00	1.00	1.00	1.00	1.00	1.00	1.00	0.99	1.00
SI_EF_MAX_OPTIMAL_ANG	0.87	0.83	1.00	0.91	0.94	0.95	0.95	0.96	1.00	1.00	0.85	0.88	0.51
Ratio of New POWER to SSE Table Values (10.2Sx100.1E)													
SI_EF_MIN_TILTED_SURFACE_NEG5													
SI_EF_MIN_TILTED_SURFACE_0	1.00	1.00	1.00	1.00	1.00	1.00	1.00	1.00	1.00	1.00	1.00	1.00	1.00
SI_EF_MIN_TILTED_SURFACE_10	1.00	0.99	1.00	1.00	1.00	1.00	1.00	1.00	1.00	1.00	1.00	1.00	1.00
SI_EF_MIN_TILTED_SURFACE_25	0.99	0.99	1.00	1.00	1.00	1.00	1.00	1.00	1.00	1.00	0.99	0.99	0.99
SI_EF_MIN_TILTED_SURFACE_90	0.85	0.82	0.83	0.88	0.92	0.93	0.92	0.90	0.85	0.77	0.84	0.87	0.87
SI_EF_MIN_OPTIMAL	1.00	1.00	1.00	1.00	1.00	1.00	1.00	1.00	1.00	1.00	1.00	1.00	1.00
SI_EF_MIN_OPTIMAL_ANG	0.91	0.75	1.00	0.95	0.94	0.94	0.94	0.96	1.00	1.00	0.80	0.85	0.55

Ratio of New POWER to SSE Table Values (Anlysis_38.96Nx77.1W)													
TiltAngle	JAN	FEB	MAR	APR	MAY	JUN	JUL	AUG	SEP	OCT	NOV	DEC	ANN
SI_EF_TILTED_SURFACE_0	1.00	0.96	1.00	1.00	1.00	1.00	1.00	1.00	1.01	0.99	1.00	1.00	0.99
SI_EF_TILTED_SURFACE_23	1.00	0.95	1.00	1.00	1.00	1.00	0.99	1.00	1.00	0.99	1.01	1.00	0.99
SI_EF_TILTED_SURFACE_38	1.00	0.94	0.99	0.99	0.99	0.99	0.99	0.99	1.00	0.99	1.00	1.00	0.99
SI_EF_TILTED_SURFACE_53	0.99	0.93	0.98	0.99	0.99	0.99	0.99	0.99	0.99	0.98	1.00	0.99	0.98
SI_EF_TILTED_SURFACE_90	0.98	0.91	0.94	0.93	0.92	0.90	0.92	0.91	0.95	0.95	0.98	0.97	0.94
SI_EF_OPTIMAL	0.99	0.94	0.99	1.00	1.00	1.00	1.00	1.00	1.00	0.98	1.00	0.99	0.99
SI_EF_OPTIMAL_ANG	0.98	0.96	0.95	0.91	0.90	1.00	1.00	0.94	0.97	0.96	0.97	0.97	0.94
Ratio of New POWER to SSE Table Values (Anlysis_38.96Nx77.1W)													
SI_EF_TILTED_SURFACE_0	1.00	1.00	1.00	1.00	1.00	1.00	1.04	1.00	1.01	1.00	1.00	1.00	1.00
SI_EF_TILTED_SURFACE_23	1.00	1.00	1.00	1.00	1.00	1.00	1.03	1.00	1.01	1.00	1.00	1.00	1.00
SI_EF_TILTED_SURFACE_38	1.00	1.00	0.99	0.99	0.99	0.99	1.03	0.99	1.01	1.00	1.00	1.00	1.00
SI_EF_TILTED_SURFACE_53	1.00	0.99	0.98	0.99	0.99	0.99	1.03	0.99	1.00	0.99	0.99	0.99	1.00
SI_EF_TILTED_SURFACE_90	0.98	0.97	0.95	0.93	0.91	0.90	0.94	0.92	0.96	0.96	0.97	0.98	0.95
SI_EF_OPTIMAL	0.99	0.99	0.99	1.00	1.00	1.00	1.04	1.00	1.01	0.99	0.99	0.99	1.00
SI_EF_OPTIMAL_ANG	0.98	0.96	0.95	0.96	1.00	1.00	1.00	0.94	0.97	0.98	0.97	0.98	0.96
Ratio of New POWER to SSE Table Values (Anlysis_38.96Nx77.1W)													
SI_EF_TILTED_SURFACE_0	1.00	1.00	1.00	1.00	1.00	1.00	1.00	1.00	1.00	0.99	1.01	1.00	1.00
SI_EF_TILTED_SURFACE_23	1.00	1.00	1.00	1.00	0.99	1.00	1.00	1.00	1.00	1.00	1.00	1.00	0.99
SI_EF_TILTED_SURFACE_38	1.00	0.99	0.99	0.99	0.99	0.99	0.99	0.99	0.99	0.99	1.00	1.00	0.99
SI_EF_TILTED_SURFACE_53	0.99	0.99	0.98	0.98	0.98	0.99	0.99	0.98	0.98	0.99	0.98	1.00	0.98
SI_EF_TILTED_SURFACE_90	0.98	0.96	0.94	0.93	0.92	0.91	0.92	0.92	0.94	0.96	0.96	0.97	0.94
SI_EF_OPTIMAL	0.99	0.99	0.99	1.00	1.00	1.00	1.00	1.00	1.00	0.99	0.99	1.00	0.99
SI_EF_OPTIMAL_ANG	0.98	0.95	0.94	0.95	0.89	0.80	0.86	0.93	0.97	0.98	0.96	0.97	0.95

Ratio of New POWER to SSE Table Values (45.96Nx77.1W)													
Parameter	JAN	FEB	MAR	APR	MAY	JUN	JUL	AUG	SEP	OCT	NOV	DEC	ANN
SI_EF_TILTED_SURFACE_0	1.00	0.96	1.00	1.00	1.00	1.00	1.00	1.00	1.01	1.00	1.01	1.00	1.00
SI_EF_TILTED_SURFACE_30	1.01	0.95	1.00	1.00	0.99	1.00	1.01	1.00	1.00	1.00	1.01	1.01	1.00
SI_EF_TILTED_SURFACE_45	1.01	0.95	1.01	0.99	0.99	1.00	1.00	0.99	1.00	0.99	1.01	1.01	0.99
SI_EF_TILTED_SURFACE_60	1.02	0.95	1.01	0.99	0.98	0.99	0.99	0.98	0.99	0.99	1.01	1.01	0.99
SI_EF_TILTED_SURFACE_90	1.03	0.96	1.02	0.96	0.91	0.90	0.91	0.92	0.95	0.96	1.00	1.02	0.96
SI_EF_OPTIMAL	1.02	0.95	1.01	1.00	1.00	1.00	1.00	1.00	1.00	0.99	1.01	1.01	1.00
SI_EF_OPTIMAL_ANG	1.02	1.02	1.02	0.96	0.93	0.88	0.90	0.91	0.97	0.94	1.00	1.00	0.98
SI_EF_MAX_TILTED_SURFACE_0	1.00	1.00	1.00	1.00	1.00	1.00	1.00	1.00	1.00	1.00	-999	0.99	-999
SI_EF_MAX_TILTED_SURFACE_30	1.01	1.01	1.01	1.00	0.99	1.00	1.00	0.99	0.99	1.00	-999	1.00	-999
SI_EF_MAX_TILTED_SURFACE_45	1.01	1.01	1.01	0.99	0.99	1.00	0.99	0.99	0.99	1.00	-999	1.01	-999
SI_EF_MAX_TILTED_SURFACE_60	1.02	1.02	1.02	0.99	0.98	1.00	0.99	0.98	0.98	0.99	-999	1.01	-999
SI_EF_MAX_TILTED_SURFACE_90	1.03	1.03	1.03	0.96	0.91	0.90	0.91	0.92	0.94	0.96	-999	1.01	-999
SI_EF_MAX_OPTIMAL	1.02	1.02	1.01	1.00	1.00	1.00	1.00	1.00	0.99	0.99	-999	1.01	-999
SI_EF_MAX_OPTIMAL_ANG	1.02	1.04	1.02	0.97	0.94	0.88	0.90	0.91	0.95	0.96	-999	1.00	-999
SI_EF_MIN_TILTED_SURFACE_0	1.00	1.00	1.00	1.00	1.00	1.00	1.00	1.00	1.00	1.01	-999	1.00	-999
SI_EF_MIN_TILTED_SURFACE_30	1.01	1.01	1.00	1.00	0.99	1.00	1.00	0.99	0.99	1.00	-999	1.01	-999
SI_EF_MIN_TILTED_SURFACE_45	1.01	1.01	1.01	0.99	0.98	1.00	1.00	0.99	0.99	1.00	-999	1.01	-999
SI_EF_MIN_TILTED_SURFACE_60	1.02	1.02	1.01	0.99	0.97	0.99	0.99	0.98	0.97	0.99	-999	1.02	-999
SI_EF_MIN_TILTED_SURFACE_90	1.03	1.03	1.02	0.96	0.91	0.91	0.91	0.92	0.94	0.96	-999	1.03	-999
SI_EF_MIN_OPTIMAL	1.02	1.02	1.00	1.00	1.00	1.00	1.00	1.00	0.99	1.00	-999	1.02	-999
SI_EF_MIN_OPTIMAL_ANG	1.03	1.02	1.02	0.96	0.92	0.88	0.90	0.95	0.94	0.96	-999	1.02	-999

Parameter	Ratio of New POWER to SSE Table Values (45.96Sx77.1W)												
	JAN	FEB	MAR	APR	MAY	JUN	JUL	AUG	SEP	OCT	NOV	DEC	ANN
SI_EF_TILTED_SURFACE_0	1.00	0.96	1.00	1.00	1.00	1.00	1.01	1.00	1.00	1.00	1.00	1.00	1.00
SI_EF_TILTED_SURFACE_30	1.00	0.94	0.99	1.00	1.00	1.01	1.01	1.00	0.99	1.00	1.00	1.00	0.99
SI_EF_TILTED_SURFACE_45	0.99	0.93	0.98	0.99	1.00	1.00	1.02	1.00	0.98	0.99	0.98	0.99	0.99
SI_EF_TILTED_SURFACE_60	0.97	0.92	0.97	0.98	0.99	0.99	1.01	0.99	0.97	0.98	0.97	0.98	0.97
SI_EF_TILTED_SURFACE_90	0.86	0.85	0.91	0.95	0.97	0.97	0.99	0.96	0.92	0.90	0.87	0.85	0.91
SI_EF_OPTIMAL	1.00	0.95	0.99	0.99	0.99	0.99	1.01	1.00	0.99	1.00	1.00	1.00	0.99
SI_EF_OPTIMAL_ANG	0.90	0.91	0.92	0.96	0.97	0.97	0.97	0.96	0.93	0.93	0.93	0.88	0.94
SI_EF_MAX_TILTED_SURFACE_0	1.00	1.00	1.00	1.00	1.04	1.00	1.03	1.00	1.00	1.00	1.00	1.00	1.01
SI_EF_MAX_TILTED_SURFACE_30	1.00	0.99	0.99	1.00	1.06	1.01	1.05	1.00	0.99	0.99	0.99	1.00	1.00
SI_EF_MAX_TILTED_SURFACE_45	0.99	0.98	0.98	0.99	1.06	1.00	1.05	0.99	0.99	0.99	0.98	0.99	0.99
SI_EF_MAX_TILTED_SURFACE_60	0.97	0.97	0.97	0.98	1.05	1.00	1.05	0.98	0.97	0.97	0.96	0.98	0.98
SI_EF_MAX_TILTED_SURFACE_90	0.86	0.89	0.92	0.95	1.04	0.98	1.03	0.95	0.93	0.90	0.86	0.85	0.92
SI_EF_MAX_OPTIMAL	1.00	1.00	0.99	0.99	1.05	1.00	1.05	0.99	0.99	1.00	1.00	1.00	1.00
SI_EF_MAX_OPTIMAL_ANG	0.90	0.91	0.92	0.94	0.98	0.98	0.98	0.96	0.93	0.93	0.88	0.88	0.94
SI_EF_MIN_TILTED_SURFACE_0	1.00	1.00	1.00	1.00	1.00	1.01	1.00	1.00	1.00	1.00	1.00	1.00	1.00
SI_EF_MIN_TILTED_SURFACE_30	1.00	0.99	0.99	1.00	1.01	1.00	1.00	1.00	0.99	1.01	0.99	1.00	1.00
SI_EF_MIN_TILTED_SURFACE_45	0.99	0.98	0.98	0.99	1.00	1.00	0.99	0.99	0.98	1.00	0.98	0.99	0.99
SI_EF_MIN_TILTED_SURFACE_60	0.97	0.96	0.97	0.98	1.00	0.99	0.99	0.98	0.97	0.99	0.97	0.98	0.98
SI_EF_MIN_TILTED_SURFACE_90	0.86	0.88	0.91	0.95	0.97	0.97	0.97	0.95	0.92	0.91	0.87	0.86	0.91
SI_EF_MIN_OPTIMAL	1.00	1.00	0.99	0.99	1.00	0.99	0.99	0.99	0.99	1.01	1.00	1.00	1.00
SI_EF_MIN_OPTIMAL_ANG	0.90	0.90	0.91	0.96	0.97	0.97	0.97	0.94	0.92	0.96	0.93	0.88	0.94

Ratio of New POWER to SSE Table Values (50.96Nx77.1W)													
Parameter	JAN	FEB	MAR	APR	MAY	JUN	JUL	AUG	SEP	OCT	NOV	DEC	ANN
SI_EF_TILTED_SURFACE_0	1.00	0.96	1.00	1.00	1.00	1.00	1.01	1.00	1.00	1.00	1.00	1.01	1.00
SI_EF_TILTED_SURFACE_35	1.01	0.94	1.01	1.01	1.00	1.00	1.00	0.99	1.00	1.00	1.00	1.02	1.00
SI_EF_TILTED_SURFACE_50	1.01	0.95	1.01	1.01	0.99	1.00	1.00	0.99	0.99	0.99	1.01	1.03	1.00
SI_EF_TILTED_SURFACE_65	1.02	0.95	1.02	1.02	0.98	0.97	0.99	0.97	0.98	0.98	1.02	1.03	0.99
SI_EF_TILTED_SURFACE_90	1.03	0.96	1.05	1.03	0.90	0.91	0.92	0.92	0.95	0.96	1.03	1.04	0.97
SI_EF_OPTIMAL	1.02	0.95	1.01	1.00	1.00	1.00	1.01	1.00	0.99	0.99	1.02	1.03	1.00
SI_EF_OPTIMAL_ANG	1.03	1.02	1.04	1.03	1.06	0.91	0.92	0.96	0.95	0.96	1.02	1.03	0.99
SI_EF_MAX_TILTED_SURFACE_0	1.00	1.00	1.00	1.00	1.00	1.00	1.00	1.00	1.00	1.00	1.00	1.01	1.00
SI_EF_MAX_TILTED_SURFACE_35	1.01	1.01	1.01	1.00	1.00	1.00	1.00	0.99	1.00	1.00	1.01	1.02	1.00
SI_EF_MAX_TILTED_SURFACE_50	1.02	1.01	1.02	1.01	0.99	0.99	0.99	0.98	0.99	0.99	1.02	1.03	1.00
SI_EF_MAX_TILTED_SURFACE_65	1.02	1.02	1.02	1.02	0.98	0.97	0.99	0.97	0.98	0.99	1.02	1.03	1.00
SI_EF_MAX_TILTED_SURFACE_90	1.03	1.04	1.05	1.04	0.90	0.90	0.91	0.92	0.95	0.97	1.03	1.04	0.98
SI_EF_MAX_OPTIMAL	1.02	1.02	1.02	1.00	1.00	1.00	1.00	0.99	0.99	0.99	1.02	1.03	1.00
SI_EF_MAX_OPTIMAL_ANG	1.01	1.03	1.04	1.03	1.12	1.00	0.93	0.96	0.95	0.96	1.02	1.01	0.99
SI_EF_MIN_TILTED_SURFACE_0	1.00	1.00	1.00	1.00	1.00	1.00	1.00	1.00	1.00	1.00	0.99	1.01	1.00
SI_EF_MIN_TILTED_SURFACE_35	1.01	1.01	1.01	1.01	0.99	1.00	1.00	0.99	0.99	0.99	1.01	1.02	1.00
SI_EF_MIN_TILTED_SURFACE_50	1.02	1.02	1.02	1.01	0.99	0.99	0.99	0.98	0.99	0.99	1.01	1.02	1.00
SI_EF_MIN_TILTED_SURFACE_65	1.02	1.03	1.03	1.02	0.98	0.97	0.99	0.96	0.98	0.98	1.02	1.02	1.00
SI_EF_MIN_TILTED_SURFACE_90	1.03	1.04	1.05	1.03	0.91	0.91	0.91	0.91	0.94	0.96	1.03	1.02	0.98
SI_EF_MIN_OPTIMAL	1.02	1.03	1.01	1.00	1.00	1.00	1.00	0.99	0.99	0.99	1.01	1.02	1.01
SI_EF_MIN_OPTIMAL_ANG	1.03	1.03	1.04	1.03	1.00	0.91	0.92	0.91	0.94	0.96	1.02	1.01	0.98

Parameter	Ratio of New POWER to SSE Table Values (50.96Sx77.1W)												
	JAN	FEB	MAR	APR	MAY	JUN	JUL	AUG	SEP	OCT	NOV	DEC	ANN
SI_EF_TILTED_SURFACE_0	1.00	0.96	1.00	1.01	1.00	1.01	1.00	1.01	1.00	1.00	1.00	1.00	1.00
SI_EF_TILTED_SURFACE_35	0.99	0.94	0.99	1.00	0.99	1.01	1.00	1.00	0.99	0.99	1.00	0.99	0.99
SI_EF_TILTED_SURFACE_50	0.98	0.93	0.98	0.99	0.99	1.01	0.99	1.00	0.98	0.98	0.98	0.98	0.98
SI_EF_TILTED_SURFACE_65	0.97	0.91	0.97	0.98	0.98	1.01	0.99	0.99	0.96	0.97	0.97	0.95	0.97
SI_EF_TILTED_SURFACE_90	0.87	0.85	0.92	0.96	0.96	0.99	0.97	0.97	0.93	0.91	0.88	0.87	0.92
SI_EF_OPTIMAL	1.00	0.95	0.99	0.99	0.98	1.01	0.99	0.99	0.98	1.00	1.00	1.00	0.99
SI_EF_OPTIMAL_ANG	0.92	0.92	0.92	0.96	0.97	0.97	0.97	0.97	0.93	0.93	1.00	0.91	0.94
SI_EF_MAX_TILTED_SURFACE_0	1.00	1.00	1.00	1.00	1.00	1.04	1.00	1.00	1.00	1.00	1.00	1.00	1.00
SI_EF_MAX_TILTED_SURFACE_35	1.00	0.99	0.99	0.99	1.00	1.08	1.01	1.00	0.99	0.99	1.00	1.00	1.00
SI_EF_MAX_TILTED_SURFACE_50	0.99	0.98	0.98	0.99	1.00	1.09	1.01	0.99	0.98	0.98	0.98	0.98	0.99
SI_EF_MAX_TILTED_SURFACE_65	0.97	0.96	0.97	0.98	0.99	1.08	0.99	0.98	0.97	0.96	0.97	0.96	0.98
SI_EF_MAX_TILTED_SURFACE_90	0.87	0.90	0.92	0.96	0.98	1.08	0.99	0.96	0.94	0.91	0.88	0.86	0.92
SI_EF_MAX_OPTIMAL	1.00	0.99	0.99	0.99	0.99	1.08	0.99	0.99	0.99	0.99	1.00	1.00	1.00
SI_EF_MAX_OPTIMAL_ANG	0.93	0.88	0.95	0.96	0.97	1.00	0.97	0.95	0.96	0.94	1.00	0.91	0.94
SI_EF_MIN_TILTED_SURFACE_0	1.00	1.00	1.00	1.00	0.99	1.00	1.00	0.97	1.00	1.00	1.00	1.00	1.00
SI_EF_MIN_TILTED_SURFACE_35	0.99	0.99	0.99	1.00	1.00	0.99	1.01	0.94	0.99	0.99	0.99	0.99	0.99
SI_EF_MIN_TILTED_SURFACE_50	0.98	0.97	0.98	1.00	0.99	0.98	1.00	0.94	0.98	0.98	0.98	0.98	0.98
SI_EF_MIN_TILTED_SURFACE_65	0.97	0.96	0.96	0.99	0.99	0.98	0.99	0.92	0.97	0.96	0.97	0.95	0.96
SI_EF_MIN_TILTED_SURFACE_90	0.87	0.89	0.91	0.96	0.97	0.97	0.98	0.90	0.93	0.90	0.88	0.87	0.91
SI_EF_MIN_OPTIMAL	1.00	0.99	0.99	1.00	0.99	0.98	0.99	0.93	0.99	0.99	1.00	1.00	0.99
SI_EF_MIN_OPTIMAL_ANG	0.85	0.91	0.92	0.94	0.97	0.97	0.97	0.95	0.93	0.89	0.87	0.82	0.92

Ratio of New POWER to SSE Table Values (70.96Nx77.1W)													
Parameter	JAN	FEB	MAR	APR	MAY	JUN	JUL	AUG	SEP	OCT	NOV	DEC	ANN
SI_EF_TILTED_SURFACE_0	-999	0.97	0.99	1.00	1.00	1.00	0.99	1.00	1.00	0.98	-999	-999	-999
SI_EF_TILTED_SURFACE_55	-999	0.97	1.05	1.08	1.14	1.06	1.00	1.01	1.00	1.03	-999	-999	-999
SI_EF_TILTED_SURFACE_70	-999	0.98	1.07	1.13	1.18	1.09	0.97	1.00	1.00	1.03	-999	-999	-999
SI_EF_TILTED_SURFACE_85	-999	0.98	1.11	1.18	1.29	1.15	0.96	0.97	1.00	1.04	-999	-999	-999
SI_EF_TILTED_SURFACE_90	-999	0.98	1.13	1.20	1.33	1.18	0.95	0.96	1.00	1.04	-999	-999	-999
SI_EF_OPTIMAL	-999	0.98	1.08	1.08	1.09	1.02	0.99	1.01	1.00	1.03	-999	-999	-999
SI_EF_OPTIMAL_ANG	-999	1.00	1.12	1.22	1.72	1.39	0.96	1.03	1.00	1.03	-999	-999	-999
SI_EF_MAX_TILTED_SURFACE_0	-999	1.00	-999	1.05	1.00	1.00	1.00	1.00	1.00	-999	-999	-999	-999
SI_EF_MAX_TILTED_SURFACE_55	-999	1.04	-999	1.15	1.14	1.06	1.01	1.01	0.99	-999	-999	-999	-999
SI_EF_MAX_TILTED_SURFACE_70	-999	1.05	-999	1.20	1.18	1.09	0.98	0.99	0.99	-999	-999	-999	-999
SI_EF_MAX_TILTED_SURFACE_85	-999	1.04	-999	1.26	1.28	1.15	0.97	0.97	0.99	-999	-999	-999	-999
SI_EF_MAX_TILTED_SURFACE_90	-999	1.04	-999	1.28	1.32	1.17	0.96	0.96	0.99	-999	-999	-999	-999
SI_EF_MAX_OPTIMAL	-999	1.04	-999	1.16	1.10	1.02	1.01	1.01	1.00	-999	-999	-999	-999
SI_EF_MAX_OPTIMAL_ANG	-999	1.00	-999	1.22	1.21	1.14	1.04	1.02	0.98	-999	-999	-999	-999
SI_EF_MIN_TILTED_SURFACE_0	-999	1.00	-999	1.00	1.00	1.00	0.97	1.00	0.99	-999	-999	-999	-999
SI_EF_MIN_TILTED_SURFACE_55	-999	1.12	-999	1.09	1.14	1.06	0.97	1.01	1.00	-999	-999	-999	-999
SI_EF_MIN_TILTED_SURFACE_70	-999	1.14	-999	1.13	1.19	1.09	0.95	1.00	1.00	-999	-999	-999	-999
SI_EF_MIN_TILTED_SURFACE_85	-999	1.13	-999	1.19	1.29	1.15	0.93	0.97	1.00	-999	-999	-999	-999
SI_EF_MIN_TILTED_SURFACE_90	-999	1.13	-999	1.22	1.34	1.18	0.93	0.96	1.00	-999	-999	-999	-999
SI_EF_MIN_OPTIMAL	-999	1.14	-999	1.08	1.08	1.02	0.97	1.01	1.00	-999	-999	-999	-999
SI_EF_MIN_OPTIMAL_ANG	-999	1.01	-999	1.31	1.66	1.35	1.00	1.03	1.00	-999	-999	-999	-999

Parameter	Ratio of New POWER to SSE Table Values (70.96Sx77.1W)												
	JAN	FEB	MAR	APR	MAY	JUN	JUL	AUG	SEP	OCT	NOV	DEC	ANN
SI_EF_TILTED_SURFACE_0	1.00	0.96	1.00	1.00	-999	-999	-999	-999	0.98	0.97	0.99	0.99	-999
SI_EF_TILTED_SURFACE_55	1.08	0.96	1.00	1.07	-999	-999	-999	-999	0.97	0.98	1.10	1.08	-999
SI_EF_TILTED_SURFACE_70	1.11	0.96	1.00	1.08	-999	-999	-999	-999	0.97	0.99	1.14	1.14	-999
SI_EF_TILTED_SURFACE_85	1.17	0.95	0.99	1.08	-999	-999	-999	-999	0.97	1.01	1.23	1.23	-999
SI_EF_TILTED_SURFACE_90	1.20	0.94	0.99	1.08	-999	-999	-999	-999	0.97	1.01	1.27	1.27	-999
SI_EF_OPTIMAL	1.03	0.96	1.00	1.08	-999	-999	-999	-999	0.97	0.97	1.04	1.02	-999
SI_EF_OPTIMAL_ANG	1.25	1.03	0.98	1.01	999	999	999	999	0.98	1.03	1.48	1.52	999
SI_EF_MAX_TILTED_SURFACE_0	1.00	1.00	-999	1.00	-999	-999	-999	-999	-999	-999	1.00	1.00	-999
SI_EF_MAX_TILTED_SURFACE_55	1.09	1.02	-999	1.01	-999	-999	-999	-999	-999	-999	1.09	1.09	-999
SI_EF_MAX_TILTED_SURFACE_70	1.10	1.02	-999	1.01	-999	-999	-999	-999	-999	-999	1.14	1.14	-999
SI_EF_MAX_TILTED_SURFACE_85	1.17	1.01	-999	1.00	-999	-999	-999	-999	-999	-999	1.23	1.23	-999
SI_EF_MAX_TILTED_SURFACE_90	1.19	1.00	-999	1.00	-999	-999	-999	-999	-999	-999	1.27	1.27	-999
SI_EF_MAX_OPTIMAL	1.03	1.02	-999	1.00	-999	-999	-999	-999	-999	-999	1.04	1.04	-999
SI_EF_MAX_OPTIMAL_ANG	1.39	1.07	999	0.99	999	999	999	999	999	999	1.50	1.50	999
SI_EF_MIN_TILTED_SURFACE_0	1.00	0.96	-999	1.00	-999	-999	-999	-999	-999	-999	1.00	1.00	-999
SI_EF_MIN_TILTED_SURFACE_55	1.07	0.96	-999	1.01	-999	-999	-999	-999	-999	-999	1.09	1.09	-999
SI_EF_MIN_TILTED_SURFACE_70	1.11	0.95	-999	1.02	-999	-999	-999	-999	-999	-999	1.15	1.15	-999
SI_EF_MIN_TILTED_SURFACE_85	1.18	0.94	-999	1.02	-999	-999	-999	-999	-999	-999	1.24	1.24	-999
SI_EF_MIN_TILTED_SURFACE_90	1.21	0.94	-999	1.02	-999	-999	-999	-999	-999	-999	1.28	1.28	-999
SI_EF_MIN_OPTIMAL	1.01	0.95	-999	1.02	-999	-999	-999	-999	-999	-999	1.02	1.02	-999
SI_EF_MIN_OPTIMAL_ANG	1.24	1.03	999	1.00	999	999	999	999	999	999	1.43	1.43	999

[\(Return to Content\)](#)

[\(Return to New Power Solar Tilt\)](#)